

**COMPARATIVE ANALYSIS OF VOLUME CALCULATIONS OF
ATTABAD LAKE IN HUNZA VALLEY USING VOID FILLED SRTM
DEM AND ASTER GDEM2**



BUSHRA AMIN

MPHIL (SPACE SCIENCE)

SS13-02



**Department of Space Science
University of the Punjab, Lahore**

**COMPARATIVE ANALYSIS OF VOLUME CALCULATIONS OF ATTABAD
LAKE IN HUNZA VALLEY USING VOID FILLED SRTM DEM AND ASTER
GDEM2**

BUSHRA AMIN

(SS13-02)



**A THESIS SUBMITTED IN THE PARTIAL FULFILMENT OF THE REQUIREMENT
FOR THE DEGREE**

OF

MASTER OF PHILOSPHY

IN

SPACE SCIENCE



UNIVERSITY OF THE PUNJAB, LAHORE, PAKISTAN

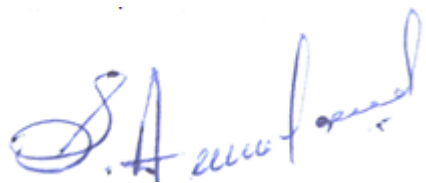
2015

CERTIFICATE OF APPROVAL

This thesis by Ms. Bushra Amin is here by approved for the submission to the University of the Punjab, Lahore in partial fulfillment of the requirements for the degree of MPhil in Space Science with specialization in Remote Sensing and GIS Degree.

SUPERVISORS

Dr. Syed Amer Mahmood
Associate Professor & Chairman
Department of Space Science
University of the Punjab



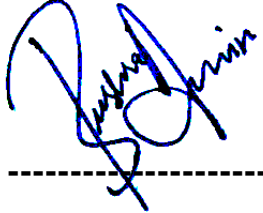
Mr. Tahir Mahmood Butt
Sr. Remote Sensing Analyst
GIS and WRD, Nespak
Lahore



Disclaimer

This document describes work undertaken as part of program of study in Department of Space Science at University of the Punjab. All views and opinions expressed therein remain the sole responsibility of the author, and do not necessarily represent those of institute.

This is certifying that present research work will not be used for any other purpose to obtain additional degree from other university.


BUSHRA AMIN -----

DEDICATION

I dedicate my dissertation work to my family and friends. A special feeling of gratitude to my loving parents whose words of encouragement and push for tenacity ring in my ears. My sisters have never left my side and are very special.

ACKNOWLEDGEMENT

Foremost, I am profoundly grateful to ALLAH for His blessing that continue to flow into my life, and because of You, I made this through against all odds.

I wish to thank my parents and my committee members who were more than generous with their expertise and precious time. A special thanks to Prof. Dr. Syed Amir Mehmood, my committee chairman and Sr. Tahir Mehmood Butt, senior remote sensing analyst in NESPAK for his countless hours of reflecting, reading, encouraging, and most of all patience throughout the entire process. I would like to acknowledge and thank my library staff for allowing me to conduct my research and providing any assistance requested. Special thanks go to Mr. Adil Latif (GIS and Remote Sensing Analyst in NESPAK) for their continued support. Finally I would like to thank the beginning teachers, mentor-teachers and administrators of our department that assisted me with thesis. Their excitement and willingness to provide feedback made the completion of this research an enjoyable experience.

I am profoundly grateful to my internal and external examiners for carefully reviewing the article and providing a valuable advice.

I am very thankful of those DEM data providers who made possible this comparison: (1) the National Geospatial-Intelligence Agency (NGA) and NASA for the SRTM, and CGIAR-CSI (2) The Ministry of Economy, Trade and Industry of Japan (METI) and the National Aeronautics and Space Administration (NASA) for the ASTER GDEM data set, NESPAK (National Engineering Service of Pakistan) for giving bathymetric field survey data, WAPDA for Lake Elevation Data, and NDMA for giving Attabad Lake depth data.

EXECUTIVE SUMMARY

Compared here are storage volumes determined for Attabad Lake in Hunza valley from 30-m Advance Space borne Thermal Emission and Reflection Radiometer (ASTER) Global Digital Elevation Models (GDEM2) and void filled Shuttle Radar Topographic Mission (SRTM) Digital Elevation Models (DEMs) of 90-m and 30-m in resolution. Results indicate that either DEM yields acceptable storage estimates for lake but SRTM3_1arcsec and SRTM4.1 provide the more accurate estimate. In this study we investigate the suitability of the SRTM and the ASTER GDEM2 for the storage volume of reservoir. All the volumetric calculations of proposed landslide-dammed lake are carried out by using two methods; one of them is contour interpolation method that focuses on the creation of contours to represent the lake levels and the other one is pixel by pixel method that uses digitized shorelines while the statistical approaches to obtain mean pool elevations on specific dates. DEMs were applied in two different resolutions and the approximated values of volumes were compared to values derived from the NESPAK bathymetric data based on field survey which used as the reference. Storage estimates are not significantly different between the datasets for proposed Lake. Besides artifacts, also changes due to different acquisition dates and techniques (optical, radar) also have an impact on the volumetric calculations. In evaluating these three sets of data, the ASTER GDEM2 values are constantly higher than the SRTM4.1 and SRTM3_1arcsec values in both area and volumes for a certain lake surface elevation; this difference grows larger with increasing pool height and lake volumes. Moreover, we achieved a more precise estimation of area and volume of Lake Gojal during filling, overtopping, and partial draining from pixel by pixel methodology that based on rigorous delimitation of the lake shoreline elevation; using combination of satellite imagery and digital topographic dataset. We analyzed that for the given lake shoreline, the number of counted grid cells for GDEM2 are greater as compare to SRTM3 (~90m,~30m). A 3D model of these DEMs revealed that ASTER DEM projects terrain features better than SRTM4.1 but not as much better as void filled SRTM3_1arcsec presents. We obtained the vertical accuracy of these two elevation datasets by comparing it to the actual official aeronautic data that tells us actual vertical elevation of runways in the Attabad region and found out RMSE with a small vertical difference of $\pm 3m$ for SRTM dataset while had a big absolute vertical difference of $\pm 13m$ for

GDEM2 overall runways. The results from both assessments showed their level of suitability for geometrics application for the concerned region. No matter whatever the method is used in calculating the volumes of impoundment but we concluded that higher accuracy is achieved with SRTM, recorded standard error of 0.1309 for SRTM3_1arcsec, 0.1966 for SRTM4.1, and 0.2961 for GDEM2. Our results indicate that a fusion of digital topographic data with high-resolution optical satellite imagery is very effective in producing key data on Attabad rockslide-dammed lake for geomorphic and hydrological analysis and engineering mitigation.

Index Terms - Digital Elevation Model (DEM), NESPAK, Attabad Lake, SRTM, ASTER, Storage capacity, RMSE

ACRONYMS

ALI	Advanced Land Imager
ASTER	Advanced Space borne Thermal Emission and Reflection Radiometer
CE	Circular error
CGIAR-	Consultative Group for International Agriculture Research Consortium for Spatial
CSI	Information
CIAT	Centro Internacional de Agricultura Tropical /International Center for Tropical Agriculture
DEM	Digital Elevation Model
EO	Earth Observing
EGM	Earth Gravitational Model
EROS	Earth Resource Observation and Science Center
ERSDAC	Earth Remote Sensing Data Analysis Center
ESRI	Environmental Systems Research Institute
FCC	False Color Composite
FWO	Frontier Works Organization
GDEM	Global Digital Elevation Model
GeoTIFF	Georeferenced Tagged Image File format
GIS	Geographic Information System
IFSAR	Interferometry Synthetic Aperture Radar
ISRIP	International Sedimentation Research Institute of Pakistan
JPL	Jet Propulsion Laboratory
KKH	Karakorum Highway
KML	Keyhole Markup Language
KMZ	Keyhole Markup Language Zipped
LE	Linear error
METI	Ministry of Economy, Trade and Industry
NASA	National Aeronautics and Space Administration
NDMA	National Disaster Management Authority

NED	National Elevation Dataset
NESPAK	National Engineering Service of Pakistan
NGA	National Geospatial-Intelligence Agency
NIMA	National Imagery and Mapping Agency
OLI	Operational Land Imager
RMSE	Root Mean Square Error
SOP	Survey of Pakistan
SRTM	Shuttle Radar Topographic Mission
UNITAR	United Nation Institute for Training and Research
UNOSAT	United Nation of Satellites
USGS	United States Geological Survey
UTM	Universal Transverse Mercator
VNIR	Visible Near Infrared
WAPDA	Water and Power Development Authority of Pakistan
WGS	World Geodetic System

TABLE OF CONTENTS

Serial No.	CHAPTERS	PAGE NO.
	DEDICATION.....	i
	ACKNOWLEDGEMENT.....	ii
	EXECUTIVE SUMMARY	iii
	ACRONYMS.....	v
	TABLE OF CONTENTS	vii
	LIST OF TABLES	x
	LIST OF FIGURES	xi
1	INTRODUCTION.....	1
1.1	Background.....	1
1.2	Rationale of Study	3
1.3	Research Objectives	4
1.4	Research Questions	5
1.5	Role of Digital Topographic Datasets in Present Study.....	6
1.5.1	Why you choose these DEMs	7
1.6	Evaluation of Vertical Elevation Error of Topography in Digital Terrain Data ...	10
1.7	Evaluation of Error of Area and Volume of River Impoundments in Digital Topography Data	11
1.8	Outline of the Chapters.....	12
2	LITERATURE REVIEW	14
2.1	History Behind the Formation of Landslide Dammed Lakes	14
2.2	Highlights of related studies in northwest Himalayas and Adjacent Areas	14
2.3	Historical Landslide Dams III – 2010 Upper Hunza at Attabad	15
2.4	Present Status of Atta bad Lake	20
2.5	Tracking and Quantification of Attabad Lake with NASA Imagery	21
2.5.1	March 16, 2010 (72 Days of Impoundment)	21
2.5.2	May 2, 2010 (116 Days of Impoundment).....	23

2.5.3	May 25, 2010 (139 Days of Impoundment).....	24
2.5.4	June 1, 2010 (146 Days of Impoundment)	25
2.5.5	July 2, 2010 (177 Days of Impoundment)	26
2.5.6	July 7, 2010 (182 Days of Impoundment)	27
2.5.7	August 23, 2010	29
2.5.8	October 3, 2010.....	31
2.5.9	August 3, 2011	32
2.6	Blasting of Attabad Lake Spillway on 15 MAY 2012	34
3	STUDY AREA.....	35
3.1	Location, Accessibility and Extend.....	35
3.2	Geology and Tectonics	36
3.2.1	Type of Landslide Strata	38
3.2.2	Huge Boulders	39
3.2.3	Network of Cracks	39
3.3	Topography and Geomorphology.....	42
3.4	Climate	44
3.5	Fruits	45
4	METHODOLOGY	46
4.1	Data Sources	46
4.1.1	Optical Satellite Imagery.....	47
4.2	Materials	48
4.3	General Validation Approach.....	49
4.4	Analysis of Contour Interpolation of DEMs for Estimating Lake Volumes	50
4.5	Interpreting Pixel-by-Pixel Shoreline Methodology for Quantifying Lake Volumes	55
4.6	Comparison of DEM Based Analysis and Pixel-by-Pixel Approach.....	68
5	RESULTS	72
5.1	Volume-Area and Volume-Elevation Relationship of Attabad Lake.....	72
5.2	Results of Accuracy Assessments.....	73
5.2.1	Trend Line Analysis.....	73
5.2.2	Percentage Difference (PD): A Method of Accuracy Assessment	77

5.2.3	Standard Error: A Way to Quantify Error.....	79
5.3	Statistical Analysis.....	81
5.3.1	Attribute (Contour) Analysis.....	82
5.3.2	Frequency Distribution of Attabad Lake	83
5.4	Visual Comparison.....	84
5.4.1	Hillshade Analysis.....	84
5.4.2	Profile Comparison.....	85
5.5	Implications of the Results	86
6	Discussion.....	88
6.1	Interpretations related to Accuracy Assessment.....	88
6.2	Interpretation of Statistical Results.....	88
6.3	Trustworthiness of Visual Comparisons.....	88
6.4	Validation Summary of the Results.....	89
7	CONCLUSION	90
7.1	Limitation.....	92
	Works Cited.....	94
	APPENDICES	I
	Appendix-A: Elevation Capacity Curves of Attabad Lake.....	I
	Appendix-B: Descriptions About Attabad Lake Level Reduction	IV
	Appendix C: Local GIS Data For Attabad Lake	V
	Appendix-D: Hunza Landslide Relief	VIII
	Appendix E: Detail Description of ASTGDENV2_0N36E074.....	IX

LIST OF TABLES

<u>TABLE NO.</u>	<u>TITLE</u>	<u>PAGE NO.</u>
	Table 1.1: Input Source Data Characteristics	9
	Table 1.2: Comparison of actual vertical elevation of runways in the Attabad region (data from World Official Aeronautical Database acquired via. http://worldaerodata.com/) with vertical elevation derived from SRTM and GDEM2 DEMs. RMSE for both DEMs is also stated.	11
	Table 3.1: Key Rock Units Renowned in Hunza Valley (Hussain & Awan, 2009)	38
	Table 3.2: Discovery of cracks in the affected area (Hussain & Awan, 2009).....	41
	Table 4.1: Remote Sensing data used for study	48
	Table 4.2: Software utilized for the current study.....	48
	Table 4.3: Table illustrates the first order geometric (area, volume) estimations of Attabad Lake extracted from contour interpolation of SRTM-3 and ASTER GDEM2 digital terrain data and compare it to the NESPAK data based on bathymetric field survey. Lake filling information is also given.....	52
	Table 4.4: Contrast between shoreline elevation data determined from NDMA Depths (Observed Data) or by Pixel Method and comparison of their associated volumes derived from Pixel by Pixel method or Contour Interpolation of DEMs (SRTM4.1, GDEM2 and SRTM3_1arcsec).....	70
	Table5.1: Percentage Difference among three datasets (SRTM4.1, GDEM2, and SSRTM3_1arcsec) reveals how much difference exists in their volumes.	77
	Table 5.2: Percentage Difference in Volumes -calculated from Contour Interpolation of DEMs- from Reference data based on field survey results of NESPAK	78
	Table 5.3: Polynomial fitted Volume (V) to Area (A) and Volume (V) to Elevation Relationship for actual Attabad Lake levels also showing the correlation coefficient (R²) and stand error (S) derived from SRTM4.1, GDEM2, SRTM3_1arcsec and NESPAK data 80	
	Table 5.4: Statistical Parameters for Attabad Lake derived from SRTM4.1, GDEM2, and SRTM3_1arcsec	81

LIST OF FIGURES

<u>FIGURE NO.</u>	<u>TITLE</u>	<u>PAGE NO.</u>
	Figure 2.1: Aerial view of Attabad landslide (Viewing downstream) on January 17, 2010 (Day 13 of impoundment) and natural debris dam features also highlighted that blocked the Hunza River forming Attabad Lake, filling in lower foreground [Pamir Times photograph]	16
	Figure 2.2: Aerial upstream view of 2010 Hunza landslide-dammed lake in northern Pakistan. This Pamir Times Photograph was taken on May 13, 2010 (127 day of impoundment) when lake waters constantly rising and filling the Hunza valley with pool height to be 2432 m.a.s.l. Another 12m increase was seen in lake prior to overtopping on May 29, 2010.....	17
	Figure 2.3: This photo of Focus Humanitarian Assistance depicts that the large boulder is falling into the water on the right hand image, presumably showing that channel widening is occurring. This pair indicates the downslope side of the channel where slow evolution of spillway is taking place (major change in between two images).....	19
	Figure 2.4: Photograph of Focus Humanitarian Assistance is taken on June 10, 2010 (12 days after overtopping), reveals flow along the spillway is prominently increased that controlled by the large boulder in the middle of the channel, also the deepening and the widening of the lower part of the channel with the formation of rapid is evident.....	20
	Figure 2.5: EO-1 satellite image acquired from http://earthobservatory.nasa.gov/ on March 16th 2010 displaying the Attabad landslide in Northwest Pakistan and debris dam and the extent of landslide-dammed Lake Attabad, 72 days after impoundment. The image has been rotated so that north is to the right.	22
	Figure: 2.6: This landslide lake false color image taken by ASTER on the Terra satellite on May2, 2010 representing water in blue, vegetation in red and bare rock in shades of beige and gray. North is on the right.	23
	Figure: 2.7: ASTER on NASA's Terra satellite obtained this landslide lake image in false color on May 25, 2010 indicating water with blue or vegetation with red color and bare rocks in tones of beige and gray. North is to the right so that river flowing southward to the image.	24
	Figure 2.8: False color image of Landslide Lake was captured on June1, 2010, demonstrating the water in varying tones of blue, vegetation in red and bare rocks in tones of brown and gray, also illustrating the previous lake levels past by Gulmit and Hussaini settlements. North is at right in this image.	25

Figure 2.9: In this EO-1 satellite true color image, the lake appears to have overtopped the rocky dam on July 2, 2010 which backing up the waters of the river past the settlements of Shishkat, Gulmit, and Hussaini. Hunza River flows towards south in this rotated image in which north is at right.	26
Figure: 2.10: This natural color image of Landslide Lake (blue-green) and of newly operational spillway was obtained on July7, 2010 by ALI on NASA’s EO-1 satellite. North is to the right and no considerable rise in lake level at that time.	27
Figure: 2.11: Detailed view of Landslide Lake on Hunza River Overflows into Spillway acquired July 7, 2010. Water pouring out the spillway looks white because of its rapid flow while rest of the lake looks blue-green in color.	28
Figure: 2.12: Stabilized water channel was observed on July 7, 2010 in this natural color image, showing the channel that filled with water nearly 1.5 to 2 km upstream from the settlement.	29
Figure: 2.13: Comparatively empty channel was noted on Aug 23, 2010, a few weeks later from July 7, 2010. An obvious reduction in water level is seen to NE of Hussaini.	30
Figure: 2.14: NASA’s EO-1 satellite acquired this natural color image on Oct.3, 2010 by ALI , suggesting the decline in water level at upstream margin of lake since July, 2010and river also returning to its former bed whereas long shadow describing the change in season in this scene.....	31
Figure 2.15: Lake (blue-green) lingering behind the earthen dam in this true color image, acquired on Aug.3, 2011 by ALI on NASA’s Terra satellite. Dam crest changed slightly between July 2010 and August 2011, also spillway revealed into the box area. North arrow is at right due to rotation of image.	33
Figure 2.16: Close-up view depicting the white water rushing through the spillway from the SW side of the lake.....	33
Figure 2.17: Snapshot provided by FWO on 15 MAY 2012 at the time of blasting of Attabad Lake Spillway.	34
Figure 3.1: Location map of Attabad landslide	35
Figure 3.2: Geology of the Attabad region in northern Pakistan. The rockslide overlying the two major geologic formations is shown in black polygon, (Red: Hunza Plutonic Unit; Light Green: Dumordu Unit) and a thrust fault reviewed (Searle, 1991).	37
Figure 3.3: Geological map of landslide area	37
Figure 3.4: Distribution of landslide material based on visual observation.....	39
Figure 3.5: Boulders lying at high degree backslope directly hit Attabad (Hussain & Awan, 2009)	39
Figure 3.6: Types of cracks lying at different locations	40
Figure 3.7: House damaged due to failure of slope at terraces (Hussain & Awan, 2009)....	42
Figure 3.8 Topographic Survey of landslide by NESPAK Engineers	43
Figure 3.9: Topographic map of Attabad and surroundings provided by Survey of Pakistan	43

Figure 3.10: Ariel view of Attabad village and surroundings (Hussain & Awan, 2009).....	44
Figure 3.11: Estimated monthly average flows at landslide location.....	45
Figure 4.1: Data about filling curve of lake depths and water surface elevations of Attabad Lake during landslide-dammed lake development and was derived from the National Disaster Management Authority (NDMA) Pakistan.	51
Figure 4.2: Plot of lake level elevations (m.a.s.l) and their volumes determined from the contour interpolation of SRTM4.1 (circles), GDEM2 (squares) and SRTM-3_1arcsec (diamond) DEMs and the NESPAK bathymetric data depend on field survey (stars). Datum is taken as 2322m.a.s.l. Dark black horizontal dashed line marks the approximated maximum lake elevation reached by Attabad Lake after stable overtopping started (2434m.a.s.l.).....	54
Figure 4.3: EO-1 ALI satellite imagery taken on 16th March 2010 indicating the Lake boundary in white color. NDMA provided the Lake Level Elevation 2389.3 at this time while datum assumed to be 2322 m.a.s.l.	56
Figure 4.4: Attabad Lake imaged on 02nd May 2010 by the ASTER satellite at the time of filling, digitized shoreline shown in white. The shoreline elevation measurements are determined from the pixel-by-pixel method.....	57
Figure 4.5: Digitized shoreline placed on ASTER satellite imagery showing the Attabad Lake extent of 25th May 2010. Lake level progressively reached to the overtopping level. .	58
Figure 4.6: ASTER image taken on 01st June 2010 two days after overtopping of Attabad Lake; shoreline displayed in white presenting larger extend of it. NDMA recorded the Lake depth of 112.2 m on that date.....	60
Figure 4.7: EO-1 ALI satellite image of Attabad Lake was captured on 07th July 2010 (182 days of impoundment), one day before on 06th July 2010. the lake level had been stabilized and at that time NDMA showed the lake depth of ~ 116.7 m in their report.....	61
Figure 4.8: Post-overtopping image of Attabad Lake was taken on 04th August 2011 by EO-1 ALI satellite. Lake portion highlighted in white. A significantly decreased in volume was observed at that time as obvious from figure. ISRIP-WAPDA measured the lake level elevation on 31st July 2011 by considering the datum to be 2,322 m a.s.l.....	63
Figure 4.9: Digitized shoreline represented in white is overlaid on Google earth imagery. During the course of 2012, no other satellite imagery of Attabad was available. Attabad Lake edge elevation determined at the given date was 08th November 2012. Darkness in figure indicates the long shadows of winter.....	64
Figure 4.10: LANDSAT8 image of Attabad Lake taken on 02nd May 2013, displaying the delineated lake boundary in white. The lake edge elevation picked from Google earth was 2403 m a.s.l.....	65
Figure 4.11: LANDSAT8 image of Attabad Lake acquired on 23rd April 2014, showing the delimited shoreline in white. Google earth displayed Lake edge elevation 2399 m a.s.l.	66

Figure 4.12: The most recent image of Attabad Lake is taken on 08th May 2015 by Landsat8 OLI satellite, depicting the delimited Lake boundary in white; also reduction in Lake Area is clearly visible. 67

Figure 4.13: Plots showing the comparison between volumes of landslide-dammed Lake Attabad approximated by contour interpolation method for nine shorelines and the Lake Volumes calculated by the pixel-by-pixel approach for the same shorelines. It is observed that pixel by pixel method gives lower values of volumes relative to contour interpolated approach that overestimates volumes. Horizontal dashed line with fill represents a series of values of the greatest volume of Attabad Lake stated in the literature (refer text below) while the horizontal solid line showing the Volumes of Attabad Lake that are calculated by utilizing pixel based approach. 69

Figure 5.1: Scatter plot demonstrating the relationship between Volume-Area (indicated by diamond box) and Volume-Elevation (depicted by square box) of Attabad Lake determined from the geometric calculations of a) SRTM4.1, b) GDEM2, c) SRTM3_1arcsec and d) NESPAK Field Survey Data that correspondingly represented by red, blue, green and black color..... 72

Figure 5.2: Polynomials of order 3 are fitted to the data by utilizing Excel’s TRENDLINE function while the R-squared (R^2) value on chart visually displaying the trend in the data. 75

Figure 5.3: Red, green, and blue bars correspondingly representing the Percentage Difference (PD) in contour interpolated volumes of STRM4.1, GDEM2, and SRTM3_1arcsec from the reference NESPAK data based on field survey. 79

Figure 5.4: Graphical Representation of Contours for Attabad Lake derived from SRTM4.1, GDEM2, and SRTM3_1arcsec and statistical parameters associated with them are found out using ArcGIS® geospatial analysis..... 82

Figure 5.5: Graphical comparison of Attabad Lake DEM generated from SRTM4.1, GDEM2, and SRTM3_1arcsec elevation data..... 83

Figure 5.6: Comparison of Frequency Distribution of SRTM4.1, GDEM2, and SRTM3_1arcsec for Attabad Lake..... 84

Figure 5.7: Shaded Relief map of SRTM4.1, GDEM2 and SRTM3_1arcsec representing Attabad Lake, clearly demonstrates the 3D effect of DEMs, also providing proper visualization of terrain features..... 85

Figure 5.8: Topographic Profile Comparison of SRTM4.1, GDEM2, and SRTM3_1arcsec 86

Figure 5.9: Ratio of volume (V) to area (A) determined from volume and area calculations ext racted from SRTM4.1, GDEM2, and SRTM3_1arcsec 87

1 INTRODUCTION

1.1 Background

Volume of the lake is defined as the maximum amount of water subjected to sudden drainage. The height of the lake is needs to be known for the calculation of highest surface area and volume of lake (Leblanc, et al., 2006). The water volume of lake and its changes over time are essential properties because they disturb the chemical, biological and physical processes of lake ecosystems. Water volumes in water bodies reveal the equilibrium between evaporation and rainfall and interactions between grounds and surface water systems (Brooks & Hayashi, 2002); (Medina, Gomez, Alonso, & Villares, 2010). Depending on the availability of areal and morphometric data, the water bodies' volume at specific periods can be found out by various methods. The most frequently adopted procedure is to establish mathematical equations relating area and volume to depth and water level using morphometric data (Hayashi & van der Kamp, 2000); (Brooks & Hayashi, 2002); (Gamble, Grody, Micacchion, & Mack, 2007); (Gleason, M.K., B.A., K.E., & J.N.H., 2007). Usually area, depth (h), and volume relationships are extracted from fine-resolution elevation maps that rely on detailed survey data (Hayashi & van der Kamp, 2000). A mathematical model is established in these methods from an original underwater topographic map. With passage of time the exactness of such models gradually reduces because these simulations cannot depict variations of the underwater terrain (Lu, Ouyang, Wu, Wei, & Tesemma, 2013).

One of the most recent developments in the landslide literature is the utilization of digital datasets comprising of both digital topographic models (i.e. ASTER GDEM2, SRTM-3, state/province datasets, and LIDAR data) (Chen, et al., 2006); (Evans, et al., 2009a); (Evans, et al., 2009b); (Lipovsky, et al., 2008), and a high resolution digital satellite imagery (e.g. LANDSAT1-8, ASTER, EO-1, Pleiades, and SPOT) (Wang & Lu, 2002) ; (Evans, et al., 2009a) ; (Evans, et al., 2009b) ; (Kargel, Leonard, Crippen, Delaney, Evans, & Schneider, 2010); (Kargel, Leonard, Crippen, Delaney, Evans, & Schneider, 2010) ; (Harp, Keefer, Sato, & Yagi, 2011). Mostly scientists with the help of these digital topographic datasets compute values for the geometrics and magnitudes of large events (e.g. length and width of path,

elevations, slope angles and slope orientations; landslide dammed lake extents, areas, and volumes), and through satellite imaging their temporal occurrence can be achieved (**Wang & Lu, 2002**); (**Evans, et al., 2009a**); (**Evans, et al., 2009b**); (**Kargel, Leonard, Crippen, Delaney, Evans, & Schneider, 2010**); (**Evans, Delaney, Hermanns, Storm, & Scarascia-Mugnozza, 2011**). There has also been wide ranging inter-comparisons and validation of digital topographic datasets to real world altitudes, with favorable results (**Farr, et al., 2007**); (**Becek, 2008**); (**Huggel, Schneider, D., J., & H. and Kääh, 2008**); (**Li, et al., 2012**); (**Suwandana E. , Kawamura, Sakuno, Y., & Raharjo, 2012**); (**Jing, Shortridge, Lins, & Wu, 2013**); (**Mashimbye, de Clercq, Van Niekerk, & A.V., 2014**).

Using a laser transit survey data and global positioning system receiver (**Wilcox & M., 2005**) developed the bathymetric surface maps of lake bottoms. This type of method is based on '3S' (RS, GPS, GIS) techniques. (**Gleason, M.K., B.A., K.E., & J.N.H., 2007**) made analytical models of surface area-volume with GPS data based on field survey. (**Minke, 2009**) determined time-effective water volumes at several scales and spaces by assimilating a lidar (light detection and ranging) DEM (digital elevation model) and the observed deepest and lowest water elevations. (**Lane & D'Amico, 2010**) estimated the isolated wetlands water volume in North Central Florida with the integration of lidar data and the triangulated irregular network (TIN) polygon volume model in ArcGIS®. Even though variations in water volumes of lakes and underwater terrain can be appropriately and precisely identified with these procedures but they are usually expensive and it is labor intensive to acquire and process the original data (**Flencer, Lotsari, Alho, & Kaayhko, 2012**); (**Furnans & B., 2008**).

The contour lines on a topographic map are easily interpreted as a series of lake water surface boundaries at various water levels and can be used to reproduce the underwater topography of that lake, and that all lakes will exhibit wet-dry phases, annually or a period of years. The underwater terrain of the lake can be rebuild, if the information on the variations in area of the lake water surface at various times can be obtained, combined with field-survey water level data (**Feng, Hu, Chen, Li, Tian, & Much, 2011**). In the last half century, the advancement in satellite remote-sensing imagery makes it possible to get temporal information on the changes of water surface areas (**Lu, Wu, Wang, & Yan, 2011**). Multi-spectral remote-sensing images have been used widely for observing surface water over the last 20 years, and several mapping

methods have been suggested according to the characteristics of the water bodies' responsiveness to different spectral ranges. (McFeeters, 1996) established the normalized difference water index (NDWI) to delineate open water bodies using visible green light and reflective near-infrared radiation, (Xu, 2006) improved the NDWI with short-wave infrared radiation and gave a new name MNDWI to the modified index. (Ouma & Tateishi, 2006) proposed a water index (WI) for delimiting coastal boundary by combining the NDWI with the Tasseled Cap Wetness (TCW) index. (Ahmet İRVEM, 2010) in 2010 used Ripple method for reservoir volume estimations. In the above mentioned methods, MODIS (Moderate Resolution Imaging Spectroradiometer) (Rogers & Kearney, 2004); (Xiao, et al., 2005), SPOT (Système Pour l'Observation de la Terre) (Bastawesy, Khalaf, & Arafat, 2008), ASTER (Advanced Spaceborne Thermal Emission and Reflection Radiometer) (Sivanpillai & Miller, 2010), Landsat TM/ETM+ (Thematic Mapper/Enhanced Thematic Mapper Plus) (Lu, et al., 2008); (Zhang, Wu, Zhu, Wang, Li, & Chen, 2011), HJ-1A/B (Lu, Wu, Wang, & Yan, 2011) and georeferenced Landsat8/Earth Observing (EO-1) data (Delaney K. B., 2014), these satellite images have been commonly used to map surface water (Shanlong, Ninglei, Bingfang, Yongping, & Zelalem, 2015).

1.2 Rationale of Study

This study presents an innovative method that uses tools provided by Arc Map[®] to delineate the potential boundary for the reservoir and then utilize that area for surface area and volume estimations at different times even if the satellite data is not available. The estimations made by this analysis could help guide discussion over potential uses of the reservoir, ecological impacts, and human consumption use.

The combination of rockslides and their associated landslide dammed lakes are significant geomorphic process to study, as these events have a direct link to the risk and hazard faced by local communities working and living in these areas. By understanding the emplacement and deposit dynamics of enormous rockslides and/or the outburst flood scenarios from naturally impounded reservoirs, we can attempt to lessen the direct impacts these events have to indigenous communities.

The multiple fluctuations in water levels in Lake Attabad provide a good field site for the study. In this study, quasi global freely available topographic datasets were chosen as the major data sources that provide the input data for lake level elevation whereas the most important input source data for Lake Bottom terrain reconstruction are the satellite imagery. The storage capacity was established for one or more different pool elevations and can be calculated by using the spatial information analysis on GIS.

1.3 Research Objectives

This study was aimed to make comparative analysis between two freely available global sets of data (SRTM3 v4.1, and GDEM2) for storage volume calculations of Attabad Lake in Hunza valley during filling, overtopping and partial draining. Our goal was also to describe the new method we developed to estimate lake volume, apply it to Lake Attabad, the largest artificial lake in NW Pakistan, and assess the method's accuracy for estimating lake volume in comparison to volumes calculated with other methods, the fitted polynomial equation of capacity curve and the lake storage with the results of NESPAK bathymetric data based on field survey.

In this paper we point out the efficiency of newly released worldwide high resolution SRTM-data (30m) and compare it with above DEMs in all aspects as well. How far it would be proved useful in determine lake volumes. We also described the discrepancy found among all datasets in volume estimations result. Different ways of comparison were also taken into account.

The main objective of this study is to analyze the performance of quasi global ASTER GDEM2 and void filled SRTM v.4.1 in calculating the volumes of Attabad rockslide dammed lake and the accuracy of the output using different comparison techniques are taken into account. To accomplish above tasks the following multiple objectives were addresses:

- ✓ Assess how SRTM4.1 plus GDEM2 limitations and uncertainty affect the storage estimations of impoundment
- ✓ Determine the utility of GIS and remote sensing data in quantifying the geometrics of the 2010 Attabad rockslide dammed lake

- ✓ Measure the filling and partial drainage of Lake Gojal (viz. water surface elevation, lake area and volume)
- ✓ Evaluate the utility of remote sensing data and techniques in characterizing the development and behavior of a rockslide-dammed lake
- ✓ Quantify the impact of Pakistan's rockslide-dammed lake mitigation attempts
- ✓ Examine and compare the SRTM4.1 volumetric calculations with the optical imagery DEM estimations
- ✓ Address the methodology that quantify accurate estimations of lake volumes at various stages of lake development
- ✓ Determine the Ratio of Volume to Area (RVA) index

1.4 Research Questions

The research presented in this thesis is guided by the following questions:

- ✓ What are the limitations of near global ASTER GDEM2 and void filled SRTM DEM?
- ✓ What is the vertical accuracy of void filled SRTM DEM when compared to ASTER GDEM2 and how it can be addressed?
- ✓ Which method would provide more precise results in determine volume estimations of Attabad lake and why?
- ✓ Which one of the topographic data set is more consistent with NESPAK field based survey results?
- ✓ How much discrepancy is found in either of DEMs while calculating lake geometrics (length, area, volume)?
- ✓ By which ways accuracy of the results would be assessed?
- ✓ What is the effect of resolution changes on the geometric calculation results?
- ✓ How does the newly introduce method calculate lake volume at specific date in the absence of satellite imagery?
- ✓ Why you choose GDEM2 and void filled SRTM DEM for proposed study?

1.5 Role of Digital Topographic Datasets in Present Study

This paper exhibits the utility of GIS as a decision support tool to compute the surface area of lake and amount of water volume for an appropriate dam crest height of the Attabad Dam (Clause, 2014). This application of GIS gives helpful information for planners and water managers. Water storage capacity and water surface area can be analyzed for different dam locations easier than reservoir surveys method to find the most suitable location for the dam construction (Ahmet IRVEM, 2011).

The quantity of water which can be stored in a reservoir or lake is called storage capacity or reservoir/lake capacity. However, this amount depends upon the how much water is inflowing and outflowing to and from the reservoir. The current techniques for calculating storage capacity are comprised of direct (field surveys) and indirect methods (use of topographical maps). Reservoir surveys that are conducted for water volume and surface areas estimations, apparently are time consuming and labor intensive, and hence assessment of surface water resources at appreciable costs. Geographic Information Systems (GIS) has extensively used in hydrological studies. The fundamental characteristics of GIS are processing, analysis and presentation of spatial data. These functionalities will enhance the reliability and feasibility of the decision making process in applications of the indirect methods (Ahmet IRVEM, 2011).

The use of digital elevation models (DEMs) has emerged as an important tool in the study of hydrological and geo-surface processes or for the quantification of the geometrics of catastrophic rockslides, rockslide-dammed lakes, different types of lakes molded by natural dams, and artificial reservoirs (Wang, Liao, Sun, & Gong, 2005) ; (Fujita, Suzuki, Nuimura, & Sakai, 2008) ; (Evans, et al., 2007) ; (Evans, Bishop, Fiedel, Valderrama, Delaney, & Oliver, 2009a) ; (Evans, et al., 2009b) ; (Evans, et al., 2009c) ; (Smith & Pavelsky, 2009) ; (Delaney & Evans, 2011) ; (Fan, C.J., Xu, Gorum, & Dai, 2012) ; (Suwandana E. , Kawamura, Sakuno, Y., & Raharjo, 2012) ; (Duan & Bastiaanssen, 2013) ; (Pan, Liao, Li, & Guo, 2013) ; (Wang, Chen, Song, Chen, Xie, & Liu, 2013). These data can be helpful in describing water surface elevations, topographic surfaces, and calculating 2D (area) and 3D (volume) values of hydrologic and geomorphic events. DEMs give a good demonstration of the terrain and are of

utmost significance as a starting point for further analysis (Piacentini, Ben, & Gerald, 2012). Terrain attributes are sensitive to DEM accuracy and cell size (Czubski, Kozak, & Kolecka, 2013). Landslides can directly be represented from a DEM (Hengl & Evans, 2009).

1.5.1 Why you choose these DEMs

We choose SRTM and ASTER-derived DEMs because these two post-processed elevation datasets provide the near global coverage and highest resolution in the study region.

The seamless dataset with voids filled in is acquired at the website of **CGIAR-CSI** (Consultative Group for International Agriculture Research Consortium for Spatial Information via (<http://srtm.csi.cgiar.org/>)). CIAT (Centro Internacional de Agricultura Tropical) have processed this data to offer seamless continuous topography surfaces and the NGA filled the voids using interpolation algorithms in conjunction with elevation data sources. By using new interpolation algorithms and better auxiliary DEMs, data available from this site has been upgraded to version 4.1 (Piacentini, Ben, & Gerald, 2012). In the original SRTM data those regions with no data have been filled using interpolation methods described by (Reuter, Nelson, A., & A., 2007). This version, thus, signify a major enhancement from previous ones because improved ocean mask has been used that comprises of some small islands which previously being lost in the cut data as well as single no-data line of pixels has also been fixed along meridians. SRTM uses C-band with wavelength of 5.6 cm (<https://lta.cr.usgs.gov/SRTM1Arc>).

SRTM 1 Arc-Second Global elevation data provide worldwide coverage at a resolution of 1 arc-second (30 meters) of void filled data and offer open distribution of this high-resolution global data set. There are still some tiles that may still contain voids. The SRTM 1 Arc-Second Global (30 meters) data set began to release in phases starting September 24, 2014. It is important to note that tiles above 50° north and below 50° south latitude are sampled at a resolution of 2 arc-second by 1 arc-second (<https://lta.cr.usgs.gov/SRTM1Arc>). As of January 2015, the most recent release embedded most of continental Asia (now including India), the East Indies, New Zealand, Australia, and western Pacific islands (<http://www2.jpl.nasa.gov/srtm/>).

A second version of ASTER GDEM came with the improvements in Geo location and elevation offset errors (**Khan, Richards, Parker, McRobie, & Mukhopadhyay, 2013**). The improvement in the contour level in GDEM2 is supposed to be linked to the successful elimination of anomalies and voids (artifacts) found in GDEM1 process which was originally released in June 2009. The ASTER GDEM1 was originally released in June 2009; however it was exposed to have a global bias of -5 m, and numerous inexplicable elevation artifacts (i.e. extreme unexplainable variations in elevation over short distances) (**Fujita, Suzuki, Nuimura, & Sakai, 2008**) ; (**Bolten & Waldhoff, 2010**) ; (**Wang, Yang, & Yao, 2011**) ; (**Suwandana E. , Kawamura, Sakuno, Y., & Raharjo, 2012**). GDEM2 removed the -5 m bias with the addition of enhanced water mask, higher horizontal accuracy, and the elimination of the unaccountable artifacts for some extend. This newer version (hereafter referred to as GDEM2) also enhanced the global vertical accuracy by 3 m from about 20 m to 17 m (**Meyer, et al., 2011**).

The GDEM2 dataset was generated from over 1.3 million ASTER VNIR stereo-pairs, and a horizontal resolution of about 30 m (**Meyer, et al., 2011**). If no cloud-free stereo-pairs available, the voids were manually filled with different datasets such as SRTM, provincial/state datasets, or (NED) national elevation datasets (**Meyer, et al., 2011**). We acquired ASTER GDEM2 dataset from the Japan Space Systems website (<http://gdem.ersdac.jspacesystems.or.jp/>).

Although the outcomes of this study may be site-specific but it is noteworthy that they still deliberated for the improvement of the following GDEM version DEMs. The quality of a DEM itself is chiefly rely on the exactness of the elevation values, the number of anomalies and the number of voids (artifacts) (**Suwandana E. , Kawamura, Sakuno, Kustiyanto, & Raharjo, 2012**).

For detail description of DEMs, please refer to **Appendix E: Detail Description of ASTGDEM V2_0N36E074**.

We used for this research above global scale GIS compatible open source DEMs which differ in coverage and precision and contained following specifications:

Table 1.1: Input Source Data Characteristics

DATA	ASTER GDEM2	CGIAR-CSI SRTM v.4.1	SRTM 1 Arc-Second Global
Data Supplier	METI/NASA	NGA/NASA	NGA/NASA
Acquisition technique	Satellite stereo images/pairs, VNIR	SAR Interferometry (IFSAR)	SAR Interferometry (IFSAR)
Acquisition Date	OCT. 2011	18 FEB. 2011	23 SEP. 2014
Period of data collection	2000 - 2010	11 days in 2000	11 days in 2000
Horizontal datum	WGS84	WGS84	WGS84
Vertical datum	EGM96 (Earth Gravitational Model 1996) ellipsoid	EGM96 geoid/ellipsoid	EGM96 geoid/ellipsoid
Horizontal Accuracy	±30m(abs.)95%CE	±20m(abs.)90%CE	±20m(abs.)90%CE
Vertical Accuracy	±20m(abs.)95%LE	±16m(abs.)90%LE	±16m(abs.)90%LE
Projection system	Geographic	Geographic	Geographic
Spatial resolution (arc-seconds)	1 arc-second (approx. 30m)	3 arc-second (approx. 90m)	1 arc-second (approx. 30m)
Vertical units	Integer meters	Integer meters	Integer meters
Data Format	GeoTIFF, signed 16 bits	GeoTIFF, signed 16 bits	Bill, signed 16 bits
Raster Size	1° x 1°tiles	5° x 5° tiles	1° x 1° tiles
RMSE specification (m)	8.86–18.31	16	16
Coverage	North 83 degrees to south 83 degrees	North 60 degrees to south 56 degrees	*North 60 degrees to south 56 degrees
Main distortion Factor	Clouds	Radar shadows, echo	Radar shadows, echo

The references of above table are taken from **(Khan, Richards, Parker, McRobie, & Mukhopadhyay, 2013)** ; **(Czubski, Kozak, & Kolecka, 2013)** ; **(Athmania & Achour, 2014)**.

*tiles above 50 degree north and below 50 degree south s latitudes are sampled at resolution of 2 arc-second by 1 arc-second (<https://lta.cr.usgs.gov/SRTM1Arc>).

1.6 Evaluation of Vertical Elevation Error of Topography in Digital Terrain Data

(Farr & Kobrick, 2000) assessed the maximum elevation error to be about 15 m globally of the SRTM dataset, while expect variations of the vertical error rely on the topography, exact location, and the combination of aspect and slope angle. **(Rodriguez, Morris, & Belz, 2006)** estimated a global error between 5 m and 14 m, and **(Becek, 2008)** calculated an error between - 5 m and 4 m in his investigation of international airport runway elevations, **(Farr, et al., 2007)** also analyzed vertical inaccuracies for particular areas of the Earth; they determined an average error for Eurasia that varies from 6m to 8m and they evaluated that in mountainous regions of northern Pakistan, the average vertical error in elevation changes from 10 m to 15 m.

By analyzing ASTERGDEM2 dataset, **(Bolten & Waldhoff, 2010)** determined a RMSE value of 8.02 m. **(Wang, Yang, & Yao, 2011)** calculated a RMSE value of 12.5 m, and the ASTER GDEM2 validation team found RMSE of 8.68 m. **(Meyer, et al., 2011)** used ICE Sat elevation data as their baseline and considered errors from specific regions. They calculated an average RMSE that lies between 10.38 m and 11.87 m over Eurasia. **(Meyer, et al., 2011)** also found a general error in Japan for mountainous regions as 15.1 m.

In order to assess the vertical accuracy of SRTM and GDEM2 elevation data, we compared the elevation of both ends of three runways in the Upper Indus with the official aeronautical data for civil aviation by adopting the **(Becek, 2008)** methodology (Table below). World Aeronautical Database provides information for runway elevation data and can be obtained via (<http://worldaerodata.com/>).

The runways are at Gilgit (62 km to the southwest of Attabad (35°55'07"N, 74°20'02'E)) and Skardu (125 km to the southeast (35°20'14"N, 75°32'01'E)).

The elevation difference for the SRTM dataset is found out to be ± 3 m over all the runways, with a RMSE of 0.0 m for Gilgit, and 1.0 m and 2.2 m for Skardu as given in table below. The GDEM2 showed a greater absolute elevation difference of ± 19 m for all the runways with a RMSE of 4.5 m for Gilgit, and 17.5 m and 15.9 m for Skardu as indicated in table (Delaney K. B., 2014).

Table 1.2: Comparison of actual vertical elevation of runways in the Attabad region (data from World Official Aeronautical Database acquired via. <http://worldaerodata.com/> with vertical elevation derived from SRTM and GDEM2 DEMs. RMSE for both DEMs is also stated.

Airport	Runway#	Elevation (m.a.s.l.)	SRTM (m.a.s.l.)	RMSE (m.a.s.l.)	GDEM2 (m.a.s.l.)	RMSE (m.a.s.l.)
Gilgit	07	1461	1461	0.0	1457	4.5
	25	1462	1462		1467	
Skardu#1	15	2227	2226	1.0	2210	17.5
	33	2230	2229		2212	
Skardu#2	14	2212	2209	2.2	2200	15.9
	32	2225	2226		2206	

1.7 Evaluation of Error of Area and Volume of River Impoundments in Digital Topography Data

To assess the precision of the two DEMs for calculating the volumes of landslide-dammed lakes in the Upper Indus, (Delaney K. B., 2014) compared the engineered volume estimated by WAPDA (Water and Power Development Authority of Pakistan) of the suggested Diamer-Basha dam reservoir with the volume of the reservoir determined from the SRTM and GDEM2 digital topographic data. The Diamer-Basha dam with 272 height will be built on the Indus River (Site

A of Code and Sirhindi, 1986) roughly 245 km downstream from Attabad and 95 km downstream from the 1841 Indus-damming landslide (**Delaney & Evans, 2011**) stated below. WAPDA facts and figures got from (<http://www.wapda.gov.pk>) tells that the dam will make an artificial reservoir to a maximum pool height of 1,160 m a.s.l, with an area of 110 km² and maximum storage capacity of 10 Gm³.

Considering the maximum pool height of 1,160 and by using the SRTM topography as the ground surface of the flooded upstream area of the Indus valley, we found out the overall volume and area of the reservoir to be 10.7 Gm³ and 109.5 km² respectively with a difference of +6.5% in volume and -0.5% in area. Taking the maximum pool height of 1,160 and using the ASTER GDEM2 digital topography, we estimated a total reservoir volume to be 11.3 Gm³ with an area of 120.5 km², thus a difference of +13% and +9.5%, correspondingly, from the engineered design specifications.

The results of this assessment gives us some clues i) SRTM 3-arcsecond (90m x 90m) digital data can give appropriate first-order topographic characterization of valley terrain in the Upper Indus, ii) Even though GDEM2 has a higher horizontal resolution but in spite of this it does not provide as much accurate results as SRTM digital terrain data gives in determining elevation of topographic surfaces in the Upper Indus, iii) SRTM data has greater accuracy for first-order estimations of areas and volumes of impounded water bodies in that region (**Delaney K. B., 2014**).

1.8 Outline of the Chapters

The research work undertaken in this thesis has been arranged into seven chapters.

Chapter 1 briefly summarizes **Introduction** i.e. about historical background related to Attabad Lake its Role of RS & GIS, importance of current study and objectives of research has also been included in this chapter.

Chapter 2 emphasizes on the studies carried out so far i.e. **Literature review** related to the background of work, data used, identification and mapping of Attabad Lake, hazards assessment and simulation of lake breach.

Chapter 3 intensely explores the importance of chosen **Study area** mentioning its geographical extent, geology, river basin, climate, vegetation and tourism. The entire Hunza valley has been discussed in detail.

Chapter 4 dedicated to the **Methodology** employed in the research work in detail. It starts with the preprocessing of datasets followed by the methods (Contour Interpolation Method, and Pixel by Pixel Method) used for volume calculations for Attabad Lake, comparative analysis of volumes among all DEMs (SRTM4.1, GDEM2, and SRTM3_1arcsec), also comparison with field observed Bathymetric data (NESPAK). It also describes the details of **Materials and datasets** used in the study such as EO-1 ALI, ASTER Terra, LANDSAT OLI, and Google Earth Imageries from 2010 to 2015 also SRTM models and ASTER GDEM2. Major highlights of collected field data has also been presented in this chapter.

Chapter 5 presents the **Results** obtained from geometric (length, area, volume, runoff etc.) calculation of Attabad Lake, trend line analysis, accuracy assessment results, also involves qualitative and quantitative analysis.

Chapter 6 of the **Discussion** gives the interpretations of the results by keeping in view the arguments of the researchers and we also consider the similar work and background in order to interpret our results.

Chapter 7 highlights **Conclusions and limitations** on the implications of research. It also highlights the limitation and future scope of the project.

2 LITERATURE REVIEW

2.1 History Behind the Formation of Landslide Dammed Lakes

The remnants of landslide dams are predominant in the incised river valleys of the northwest Himalayas (Pakistan and India) and the adjacent Pamir Mountains of Tajikistan and Afghanistan (Delaney K. B., 2014). Landslide dams are come into being when debris created by a mass movement of rock, in the form of a landslide or a rock avalanche, obstructs surface drainage (Evans, Delaney, Hermanns, Storm, & Scarascia-Mugnozza, 2011); (Fan, C.J., Xu, Gorum, & Dai, 2012). As a consequence of this obstruction a landslide-dammed lake may generate, flooding valley surfaces upstream from the dam; the landslide-dammed lake may exist as a perpetual component of landscape, suffer stable draining for a long time, fill up with sediment, or experience catastrophic failure at some stage in its lifespan causing a destructive outburst flood downstream (Evans & Clague, 1988); (Cosat & Schuster, 1988); (Korup, Montgomery, & Hewitt, 2010); (Evans, Delaney, Hermanns, Storm, & Scarascia-Mugnozza, 2011); (Delaney & Evans, 2011); (Fan, C.J., Xu, Gorum, & Dai, 2012). The creation and probable failure of landslide dams is therefore an essential element of rockslide hazard in mountainous terrain and plays a significant role in evolution of mountainous landscape (Delaney K. B., 2014).

2.2 Highlights of related studies in northwest Himalayas and Adjacent Areas

Literature review have suggested that large amount of landslide debris are found in the Pamir and Himalaya mountain regions of Central Asia, some of them have impounded surface waters creating major landslide-dammed lakes in current-historical time and in pre-historical period (Hewitt, 1968) ; (Hewitt, 1982); (Hewitt, 1998); (Korup, Montgomery, & Hewitt, 2010); (Delaney & Evans, 2011); (Delaney K. B., 2014). Previous studies have also revealed that some factors intricate in this high incidence of landslide dams contain deep narrow valleys forming from the incised high mountainous terrain that make a valley topography favorable for damming, massive rock slope failure with high frequency, and dynamic collisional tectonics causing

frequent major earthquakes and high degree uplift (**Ouimet, Whipple, Royden, Sun, & Chen, 2007**).

2.3 Historical Landslide Dams III – 2010 Upper Hunza at Attabad

The Attabad landslide is a second major landslide that occurred at about 13:00 h on January 4, 2010 at a location (34°18'24"N, 74°49'17"E) in northern Pakistan (**Kargel, Leonard, Crippen, Delaney, Evans, & Schneider, 2010**). As a result of immense rock slope failure, Hunza River was completely blocked. The debris mass is found out to be in the order of 55 Mm³ (**Delaney & Evans, 2011**); (**Ekström & Stark, 2013**); (**Petley, et al., 2010**) and (**Schneider, Huggel, Cochachin, Guillén, & Garcia, 2014**) give a slightly lower landslide mass (est. 45 Mm³). Some spectators noted that the overall volume of rock mass entailed one large, and some other smaller mass movements (**Petley D. , 2011**); (**Iqbal, Shah, Chaudhary, & Baig, 2014**). The 2010 landslide took place just 2.5 km upstream of the 1858 valley-blocking landslide defined below.

The landslide mobilized valley filled sediments from the Hunza valley floor that liquefied and moved over the valley floor up to a downstream distance of 2.7km. Chunk of the mudflow fragments removed the valley side engulfing portion of a village downstream of Attabad, killing almost 20 people. The landslide blocked the Hunza River and a landslide-dammed lake (Lake Gojal) instantly began to form upstream. The minimum dam elevation is calculated as ca. 119 m for a maximum overflow crest height of about 2444m.a.s.l before the spillway excavation over the debris (**Delaney K. B., 2014**).

The land mass crushed the valley floor and liquefied lake and fluvial sediments in the valley bottom causing destructive mudflows that moved both upstream and downstream. Liquefied sediments in valley bottom rose to the opposed side of valley and flowed towards the back crossways the deposit surface, shelling the fragmented rock mass with fine-grained muddy slurry. Nearly 3 kilometers downstream to Sarat, a second mud flow ran where it caused in the deaths of 19 people (**Petley, et al., 2010**); (**Petley D. , 2011**); (**Schneider, Huggel, Cochachin, Guillén, & Garcia, 2014**); (**Iqbal, Shah, Chaudhary, & Baig, 2014**).

The highest sliding mass height on the source gradient was 3,004 m a.s.l., and the total travel distance was 1,390 m horizontally in a SSW direction. The horizontal movement was controlled by the contrasting valley wall that brought about a copious landslide deposit, and thus a higher dam, than an otherwise unrestricted flow (Fig. 2.1). (Delaney K. B., 2014) estimated the elevation of the slope as 679 m (H) with the SRTM DEM, which yields an $H/L = 0.488$ and a fahrböschung ($\tan^{-1} H/L$) of 26° .



Figure 2.1: Aerial view of Attabad landslide (Viewing downstream) on January 17, 2010 (Day 13 of impoundment) and natural debris dam features also highlighted that blocked the Hunza River forming Attabad Lake, filling in lower foreground [Pamir Times photograph]

As lake waters boost up they swamped many villages, large tracts of cultivated land adjoining to the Hunza, and the Karakoram Highway of 22km joining Pakistan and China, upsetting road

travel and commercial passage between the two countries (Cook & Butz, 2013) ; (Shah, Ali, & Baig, 2013); (Suwandana E. , Kawamura, Sakuno, Y., & Raharjo, 2012).



Figure 2.2: Aerial upstream view of 2010 Hunza landslide-dammed lake in northern Pakistan. This Pamir Times Photograph was taken on May 13, 2010 (127 day of impoundment) when lake waters constantly rising and filling the Hunza valley with pool height to be 2432 m.a.s.l. Another 12m increase was seen in lake prior to overtopping on May 29, 2010.

Pakistani authorities began the construction of a spillway over the debris for getting an eventual controlled overflow on 29 January (day 25 of impoundment), completing it around May 15 (day 128). The spillway excavation let down the dam effective crest by about 15 m that was analogous to a maximum possible lake elevation of 2,435m.a.s.l. By July 20, 2010, stable overtopping continues as Pakistan authorities deliberate some more drainage/partial drainage approaches.

No large scale and good quality topographic data was available to us. Despite of calibrating the DEMs both SRTM-3 and GDEM2 based on runway elevations as described in previous chapter, we also tested the DEM accuracy by discussing to news reports that directed that the waters of landslide dammed lake touched the Karakoram Highway Bridge piers on February 10 (day 37) across the Hunza River placed just about 10.5 km upstream of the landslide dam at Gulmit. The altitude of the bridge piers is assessed 2,375m.a.s.l and 2,372m.a.s.l from SRTM-3 and GDEM2 respectively so correspondingly discrepancy in lake level on that date is found out to be only 1m and 4m from the NDMA data; the SRTM-3 and GDEM2 DEM shows that the lake volume was 61.95 Mm³ and 70.92 Mm³ in that order at the pool elevation of 2,375m.a.s.l on day 37 (**Delaney K. B., 2014**).

In the course of filling, leakage started to appear on nearly March 5 (day 60) at a pool height of ca. 2,387m.a.s.l in the downstream face. Preliminary approximations of leakage were made on March 9 (day 64) and estimated 18,348m³ per day. By March 17 (day 72), this leakage had risen to 40,367m³ per day. Leakage then seemed at several sites in the downstream face and outflow through the debris had markedly increased. Due to that fact interior erosion inside the landslide debris and the creation of sink holes on the debris surface occurred.

Regardless of this indication of considerable leakage powers the landslide integrity remained intact and the lake level persistently rose up to the date of overtopping (29 May), over the carved spillway. The lake level at the time of overtopping on 29 May (day 143) was computed from the SRTM4.1 and GDEM2 to be 2,433m.a.s.l and 2424m.a.s.l correspondingly. At this maximum pool elevation the lake extent was noted from these DEMs. To verify our maximum pool elevation we superimposed the desired contour from these DEMs on the ASTER June 1 image; the contour and the lake outline corresponded almost exactly.

Lake levels constantly increased up to 3m with an equivalent additional volume of ca. 30 Mm³ even after overtopping by June 3 (5 days), meanwhile lake inflow exceeded the Lake Outflow (during summer flood). However, the lake level had become stable from 5 June (Fig. 2.3) as outflow in the spillway raised, and stable overtopping initiated. Pamir Times photos after overtopping reveal the channel widening due to deepening through head-ward erosion from the

bottommost part of the spillway and by widening through lateral undercutting and leakage erosion of the spillway walls.



Figure 2.3: This photo of Focus Humanitarian Assistance depicts that the large boulder is falling into the water on the right hand image, presumably showing that channel widening is occurring. This pair indicates the downslope side of the channel where slow evolution of spillway is taking place (major change in between two images)

According to FWO (Frontier Works Organization), almost 24 m depth had achieved by digging 7 million cft of earth debris. On the orders of NESPAK specialists, further excavation of spillway had been shut because more carving in could become hazardous. They were continuously checking the inflow, discharge and increase of water levels. There was no threat of dam bursting with current discharge of about 60 cuses at that time because as per experts danger rises when discharge exceeds 200 cuses (FWO, 2010).



Figure 2.4: Photograph of Focus Humanitarian Assistance is taken on June 10, 2010 (12 days after overtopping), reveals flow along the spillway is prominently increased that controlled by the large boulder in the middle of the channel, also the deepening and the widening of the lower part of the channel with the formation of rapid is evident.

Military Engineers along with FWO were also functioning at the demand of NDMA to decrease the troubles of the residents smashed by natural disaster by taking material and people crossways the 11 km stretched lake. In order to facilitate them, Defence Engineers had begun a boat service from 14 Feb 2010 and were handling 17 boats for this task. So far they had transported over 7,500 individuals and 80 tons of fuel and food supplies (FWO, 2010) and also see **Appendix-B: Descriptions About Attabad Lake Level Reduction.**

2.4 Present Status of Attabad Lake

Pakistani experts have been dynamic in mitigating the hazard to downstream communities and the threat at the landslide. Not only these specialists have been getting effective control on

overtopping and reducing the maximum volume of the lake through the carving of spillway over the debris but they have also been attentive in monitoring the lake, evacuating vulnerable areas, delineating probable flood zones downstream, and mounting a siren-based warning system in case of a disastrous breach being commenced. The Hunza landslide-dammed lake sustained its stable overtopping of the spillway over the debris till July 25, 2010 (day 200 of impoundment). As Pakistani professionals take into account engineering strategies to reduce the lake level, lake level has been retained roughly at 2,435m.a.s.l., therefore refining the upstream deluging of large swathes of the Hunza Valley and the Karakoram Highway (**Delaney K. B., 2014**).

2.5 Tracking and Quantification of Attabad Lake with NASA Imagery

2.5.1 March 16, 2010 (72 Days of Impoundment)

A landslide took place on January 4, 2010 in Hunza Valley of northern Pakistan. The preliminary catastrophe submerged the Attabad village, killing 20 persons and destroying 26 houses. With passage of weeks, situation became complicated because landslide did more than abolish a village. It also obstructed the Hunza River, forming an 11-kilometer (7-mile) long lake that inundated 3 miles (5 kilometers) of the Karakoram Highway and flooded many villages. The landfalls often blocked the highway which mostly cleared in days but work was still under way in mid-March 2010 at Attabad, also see **Appendix C: Local GIS Data For Attabad Lake**.

Acquired on March 16, 2010, by the Advanced Land Imager (ALI) on NASA's Earth Observing-1 (EO-1) satellite, this natural-color image shows the lake formed by the landslide of January 4. North is to the right because this image has been rotated. In the upper left corner of the image, the dark rocks cover the river and the V-shaped turquoise lake stretches out behind the slide. The Karakoram Highway adjoining the temporary lake is a faint meandering line of pale brown. A bridge across the Hunza River has been underwater due to rising water. The bridge joins the settlements of Shaskit and Gulmit on the area's only route to and from China (**Cook & Butz, 2013**) ; (**Shah, Ali, & Baig, 2013**) ; (**Schneider, Huggel, Cochachin, Guillén, & Garcia, 2014**).



Figure 2.5: EO-1 satellite image acquired from <http://earthobservatory.nasa.gov/> on March 16th 2010 displaying the Attabad landslide in Northwest Pakistan and debris dam and the extent of landslide-dammed Lake Attabad, 72 days after impoundment. The image has been rotated so that north is to the right.

According to news reports, this lake not only displaced about 1,500 people by submerging their houses but it also cut off everybody—an estimated 3,000 people—from the outside world between Attabad and the flooded bridge. By late January, Chinese engineers had begun working with Pakistan’s army team to dig a spillway through the landslide but the landslide size made for slow progress (FWO, 2010).

As of January 25, Geologist David Petley (Petley, March 11, 2010) reported that the lake’s level was increasing around 3.6 feet (1.1 meters) per day, and from February 10, water was increasing around 24 inches (60 centimeters) per day. Water was percolating through the earthen dam, probably from the newly produced lake by March 11. The leakage raised threats that the water might fissure the dam and deluge villages downstream (Carreiro, March 16, 2010).

2.5.2 May 2, 2010 (116 Days of Impoundment)



Figure: 2.6: This landslide lake false color image taken by ASTER on the Terra satellite on May2, 2010 representing water in blue, vegetation in red and bare rock in shades of beige and gray. North is on the right.

On January 4, 2010, a landslide blocked the Hunza River in northern Pakistan, generating a lake that endangered to overspill its rocky dam and inundate downstream communities. As of mid-March 2010, the lake was 10 kilometers (7 miles) long. As of early May, the lake had stretched out well beyond its mid-March extent. As spring proceeded, high temperatures began melting snow, which increased the inflow speed to the lake (Petley D. , May 10, 2010) ; (Petley D. , May 8, 2010).

This false-color image of the landslide lake was obtained by the Advanced Space-borne Thermal Emission and Reflection Radiometer (ASTER) on the Terra satellite on May 2, 2010. This image represents vegetation in red, water in blue and bare rock in shades of beige and gray. The

estimated extent of the lake on March 16, 2010, seems as a white outline. In the above image, north is to the right due to rotation.

The river-blocking landslide seems adjacent to the upper left margin of this image. As compared to their mid-March extents, water levels have increased subsequent to the landslide and higher water is apparent along the whole lake. In mid-March, the Hunza River was a narrow tributary lying north of the landslide lake. However, the water body is extended well in this scene, past the former lake extent.

Paralleled to the closely lying large barren slopes, low, broad plains associated with settlements along the river support abundant vegetation (shown in red in this image). As the settlements exist along with the rapidly rising rockslide lake which partially immersed homes and trees, as well as locals flee their houses to rescue construction materials (**Petley D. , May 9, 2010**).

2.5.3 May 25, 2010 (139 Days of Impoundment)

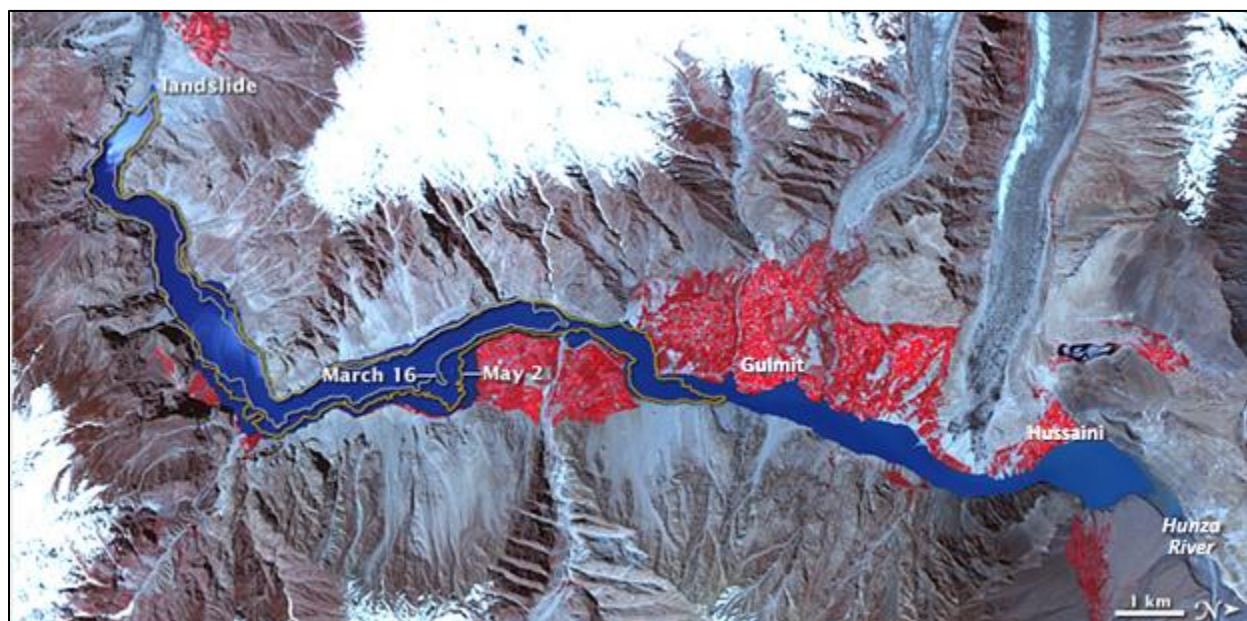


Figure: 2.7: ASTER on NASA's Terra satellite obtained this landslide lake image in false color on May 25, 2010 indicating water with blue or vegetation with red color and bare rocks in tones of beige and gray. North is to the right so that river flowing southward to the image.

The lake creating ahead of landslide that blocked that Hunza River on January 4, 2010 in Pakistan seemed very close to reaching an overtopping point in late May, according to geologist David Petley of the International Landslide Centre in the United Kingdom. Snow were melting due to warmer temperatures in the mountains upstream and triggering the lake to grow.

The Advanced Space borne Thermal Emission and Reflection Radiometer (ASTER) on NASA's Terra satellite taken this false-color image of the landslide lake on the Hunza River on May 25, 2010. Note that north is at right; the river flows southward to the image. Bare rock is in shades of gray-brown, vegetation is red and water is blue. On the basis of previous satellite imageries, the lake level of 16th March and 2nd May are drawn on the image. In middle of March, the lake had backed up just about the mid-point of the scene; as of May 2, it reached over the two-thirds of the image. Since May 25, it extended across the entire image (**Petley D. , May 27, 2010**).

2.5.4 June 1, 2010 (146 Days of Impoundment)

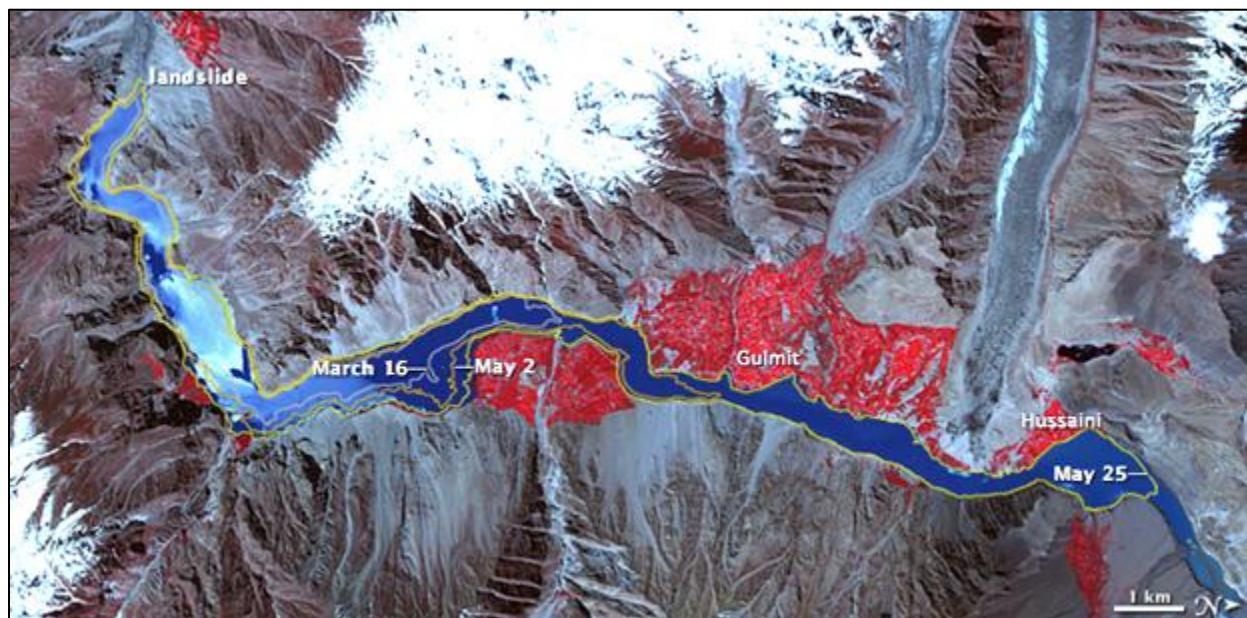


Figure 2.8: False color image of Landslide Lake was captured on June 1, 2010, demonstrating the water in varying tones of blue, vegetation in red and bare rocks in tones of brown and gray, also illustrating the previous lake levels past by Gulmit and Hussaini settlements. North is at right in this image.

A lake built by a landslide in northwest Pakistan constantly rising all over the month of May 2010. The lake stretched northward up to the Hunza River, passed by the Gulmit and Hussain settlements. The geologist David Petley of the International Landslide Centre in the United Kingdom reported that the danger of a breach for now continual increasing (**Petley D. , June 1, 2010**).

The Advanced Space borne Thermal Emission and Reflection Radiometer (ASTER) on June 1, 2010 captured this false-color image of the landslide lake by the Terra satellite. Water looks in varying shades of blue. Vegetation is shown in red whereas bare rock is in shades of brown and gray. North appears at right because of image rotation. The Hunza River flows southward to the image, and water backing ahead of landslide has gradually moved toward the north. Colored lines donate the lake's previous levels: March 16 by gray, May 2 by burnt orange, and May 25 by yellow. This image displays that the landslide lake had stretched 2 to 3 kilometers north of its May 25 extent up to June 1.

2.5.5 July 2, 2010 (177 Days of Impoundment)



Figure 2.9: In this EO-1 satellite true color image, the lake appears to have overtopped the rocky dam on July 2, 2010 which backing up the waters of the river past the settlements of Shishkat, Gulmit, and Hussaini. Hunza River flows towards south in this rotated image in which north is at right.

In early January of 2010, a rockslide filled the Hunza Valley portion in northwestern Pakistan by producing a natural dam across the Hunza River at Atta Abad. Since early June, a considerable lake had generated, preventing the river water past the settlements of Shishkat, Gulmit, and Hussaini. In this image the lake seems to have overflowed the dam on July 2, 2010, and water was spilling out through a man-made spillway. The Advanced Land Imager (ALI) on NASA's Earth Observing-1 (EO-1) satellite got this true-color image of the rockslide lake on July 2, 2010. Due to rotated image, north appears to the right. The Hunza River flows toward the south, and water backed up behind the landslide has slowly spread toward the north (**Sheikh, 2010**).

Situation reports of David Petley (geologist of the International Landslide Centre in the United Kingdom) indicated that the discharge or outflow channel may be constrained by some heavy boulders which result in precluding the channel from eroding as speedily as would otherwise be expected. Use of explosives is considered as one of the option by local authorities for further clearing the spillway and permitting the lake to drain more rapidly (**Petley D. , June 26, 2010**).

2.5.6 July 7, 2010 (182 Days of Impoundment)



Figure: 2.10: This natural color image of Landslide Lake (blue-green) and of newly operational spillway was obtained on July7, 2010 by ALI on NASA's EO-1 satellite. North is to the right and no considerable rise in lake level at that time.



Figure: 2.11: Detailed view of Landslide Lake on Hunza River Overflows into Spillway acquired July 7, 2010. Water pouring out the spillway looks white because of its rapid flow while rest of the lake looks blue-green in color.

Alongside the Hunza River in northwestern Pakistan, a lake had been forming for months behind a rockslide dam that created in January 2010. Army laborers and engineers worked energetically on a spillway to release the growing lake, which had backed up past many settlements. Ultimately, the lake started flowing over the spillway in late May 2010. From the news of David Petley, the lake levels had seemingly stabilized by July 6.

The Advanced Land Imager (ALI) on NASA's Earth Observing-1 (EO-1) satellite took this true-color image on July 7, 2010 of the rockslide lake and its recently operational spillway. The top image demonstrates a wider view and the bottom scene illustrates a detailed view of the region outlined in white above. North is at the right in this image. No significant variation in lake level observed at that time.

Water coming out the spillway seems white, probably resulting from its fast flow. The rest of the lake looks almost uniform blue-green. Mostly brown and bare parcel of land exist around the Hunza Valley, but pockets of cultivated land accompanying with settlements appear adjacent to the riverbanks. On the adjoining mountain peaks, snow cover remains, and tiny glaciers snake in the direction of the river valley.

The rockslide lake displaced around 1,500 people in the first half of 2010 and according to news (Petley D. , July 6, 2010) bulletin it also separated nearly 3,000 natives from the external world by destroying a central bridge. Due to progressing water levels behind the rockslide, a number of people ruined their houses to salvage building materials. In the meantime, downstream communities encountered a flood hazard due to the fact that the landslide lake may burst through the rocky dam abruptly. Accomplishment of the spillway was expected to decrease the danger of such a disastrous event.

2.5.7 August 23, 2010

In January 2010, a landslide commenced the creation of a protruding lake along the Hunza River in northwestern Pakistan. In late May, water finally started flowing over a spillway constructed to decrease the speedily growing water level and avoid a disastrous outburst flood.



Figure: 2.12: Stabilized water channel was observed on July 7, 2010 in this natural color image, showing the channel that filled with water nearly 1.5 to 2 km upstream from the settlement.



Figure: 2.13: Comparatively empty channel was noted on Aug 23, 2010, a few weeks later from July 7, 2010. An obvious reduction in water level is seen to NE of Hussaini.

Geologist David Petley at the International Landslide Centre informed that the level of lake had become stable by July 6 noticeably. On NASA's Earth Observing-1 (EO-1) satellite, the Advanced Land Imager (ALI) took these true-color images of the rockslide lake. An upstream area from the spillway after water started flowing over it is clearly depicted in above scenes.

The top image displays the lake at July 7, 2010 afterward its water level apparently stabilized. The bottom image is taken on August 23, 2010 that indicates the similar lake after some week. The water level has reduced remarkably to the northeast of Hussaini.

Upstream from the town, water filled the channel about 1.5 to 2 kilometers on July 7. The channel at August 23, 2010 seems almost empty about 1 kilometer upstream (**Petley D. , July 6, 2010**).

2.5.8 October 3, 2010



Figure: 2.14: NASA's EO-1 satellite acquired this natural color image on Oct.3, 2010 by ALI, suggesting the decline in water level at upstream margin of lake since July, 2010 and river also returning to its former bed whereas long shadow describing the change in season in this scene

A rockslide close to Attabad, Pakistan, dumped masses of rock into the Hunza River in early January 2010. The natural dam obstructed the river, triggering a lake to develop behind it and inundating roads, towns, and meadows for miles. Bridges across the Hunza River were underwater and the Karakorum Highway, an important trade route with China and the main road through the region was disrupted (Cook & Butz, 2013); (Shah, Ali, & Baig, 2013); (Schneider, Huggel, Cochachin, Guillén, & Garcia, 2014); (Delaney K. B., 2014). When water reached a spillway in late May so it had been excavated to relieve pressure and to avoid a tragic outpouring flood. Geologist David Petley stated in its report that the lake level was peaked in early July but had steadily been decreasing as the water flow from melting glaciers into the lake had declined

and the spillway had extended to allow more water out of the lake (**Petley D. , September 1, 2010**).

The true-color image of October 3, 2010, captured by the Advanced Land Imager (ALI) on NASA's Earth Observing-1 (EO-1) satellite, illustrates the drop in water levels at the upstream margin of the lake by July. An approximation of the river's course since September 2009 is shown on the October image, rely on NASA's Terra satellite imagery of ASTER.

By July, the lake had recoiled predominantly nearby Hussaini town. The river braided pattern had formed the muddy islands which seemed again after months underwater. The river had been coming back to its earlier bed as the water had retreated. Since August 23, the minor change was observed, signifying that the new lake might be momentarily stabilized at this extend. Relative to the direct rays of mid-summer, the elongated shadows was seen in the October image (**Taylor A. , June 4, 2010**) dictating the change of seasons.

2.5.9 August 3, 2011

On January 4, 2010, a landslide struck the Hunza Valley in northern Pakistan, blocking the Hunza River and abolishing a village. As water backed up behind the rocky dam, the growing lake forced natives to demolish their homes. Due to suppressing a bridge, overland access was cut off to the outside world. Engineers and military workers excavated a spillway through the dam because of this water eventually started flowing through it in late May 2010.

The Hunza Valley did not coming back to normal even though the spillway had released pressure on the landslide lake. Assessed this natural-color image on August 3, 2011 by the Advanced Land Imager (ALI) on NASA's Earth Observing-1 (EO-1) satellite, depicts the rocky dam and enduring lake a head of it. The top image is presenting wide-area view while the bottom scene giving a close-up of the boxed area from the top. North is to the right because both images are rotated. White water is flowing over the spillway at the southwestern end of the lake. On the other hand, water looks like blue-green.



Figure 2.15: Lake (blue-green) lingering behind the earthen dam in this true color image, acquired on Aug.3, 2011 by ALI on NASA's Terra satellite. Dam crest changed slightly between July 2010 and August 2011, also spillway revealed into the box area. North arrow is at right due to rotation of image.



Figure 2.16: Close-up view depicting the white water rushing through the spillway from the SW side of the lake

Geologist David Petley (International Landslide Centre at Durham University) has hunted down the effects of Hunza rockslide from January 2010. With the help of spillway, lake levels of

Hunza most likely stabilized by early July 2010. Over the subsequent 13 months, water pouring through the spillway eroded the rockslide dam, broadening the flow channel. Up till now, flow out of the lake and the river valley downstream continued controlled by the narrow inlet through the dam crest. Petley (**Petley D. , August 24, 2010**) noted the minor change in crest between July 2010 and August 2011; also refer to **Appendix-D: Hunza Landslide Relief** for details.

2.6 Blasting of Attabad Lake Spillway on 15 MAY 2012

On 15 May 2012, under the supervision of CEO FWO, fourth coffer dam at Attabad was blasted at 1035 hours causing in discharge of 35000 cusecs of water from the lake.



Figure 2.17: Snapshot provided by FWO on 15 MAY 2012 at the time of blasting of Attabad Lake Spillway.

Lake level may be further lower down, as a consequence of blasting the coffer dam and deepening the spillway (**FWO, 2012**).

3 STUDY AREA

*All stuff described below is prior to the disaster period of Attabad landslide.

3.1 Location, Accessibility and Extend

The Attabad village is situated in the extremes north of Pakistan (in Gilgit-Baltistan Province). It is placed at a distance of 760 km from Islamabad, about 130 km upstream of Gilgit town (inset figure), which signs the confluence of the Indus and Hunza rivers, 30kms north east of Aliabad and 5.5 km from Karakorum Highway (KKH) near Sarat on steep slopes in Hunza valley (**Hussain & Awan, 2009**). The village was located approximately 600 m above the riverbed on the western wall of the Hunza Valley (**Petley D. , 2010**).

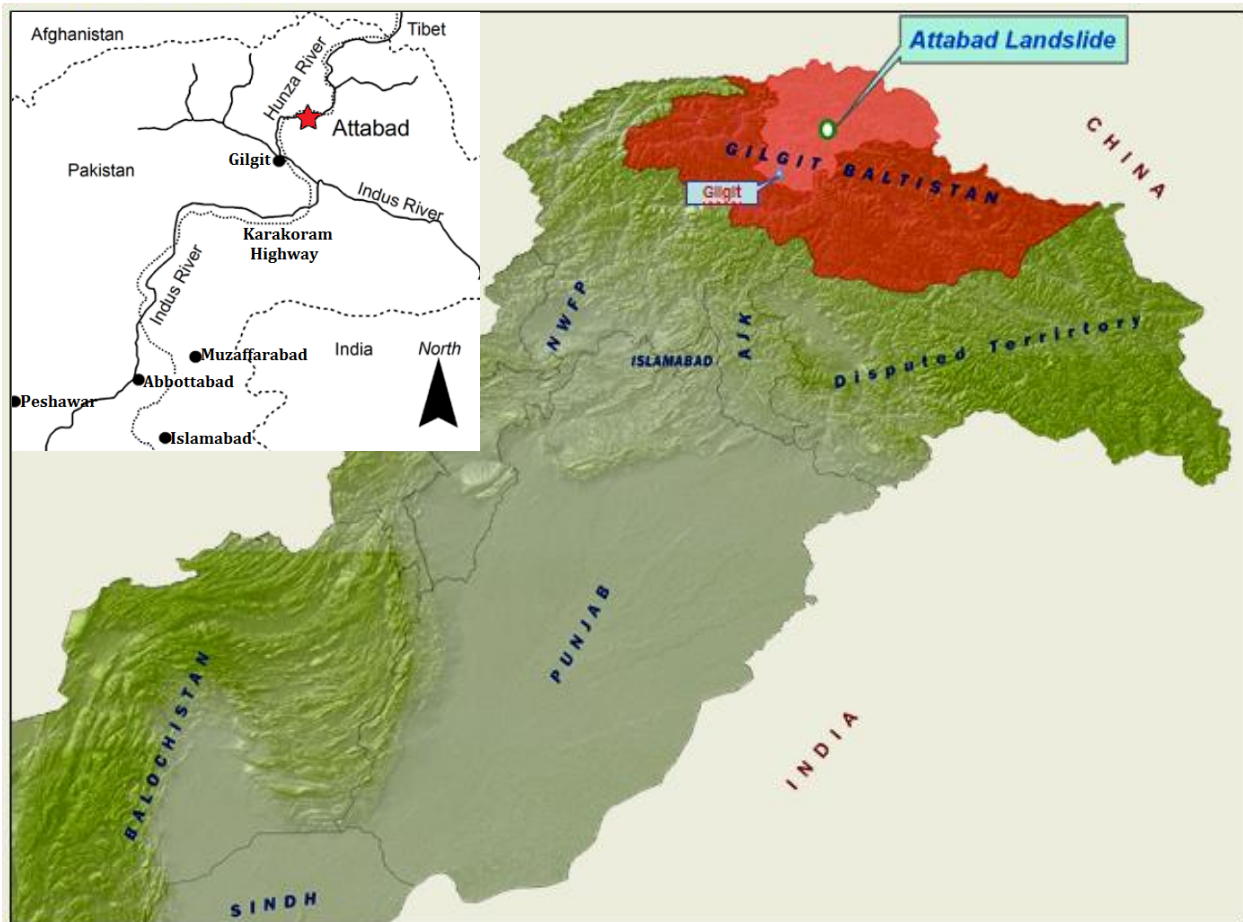


Figure 3.1: Location map of Attabad landslide

Attabad village is positioned just about 109 Km North East of Gilgit and nearly 19 Km East of Hunza where a small natural lake Attabad existed. All weather metaled road passes by way of the Hunza Valley linking Islamabad with Gilgit as well as further to Khunjrab pass. Very narrow, uneven, steep and unmetaled road takes to Attabad village while overpassing Hunza River by suspension bridge near Sarat from KKH (**Hussain & Awan, 2009**).

It lies between coordinates given below in the SOP (Survey of Pakistan) sheet No. **42L/15**.

Upper Left	36°19'08.50''	Lower Right	36°18'35.36''
	74°47'58.41''		74°49'02.45''

3.2 Geology and Tectonics

The geology of the Attabad region is complicated because of extreme tectonics that disturbs this region (**Hussain & Awan, 2009**). The place is underlain by malformed and sheared Precambrian paragneisses and orthogneisses of the Baltit Group. These rocks are extensively affected by enormous dispositions. Some indigenous faulting is apparent. Bedrocks are covered with thick and widespread deposits of fluvio-glacial and Holocene colluvium, typically comprising of cobbles, gravels and boulders along with a sandy matrix. Some marks of shearing are evident in these deposits (**Petley D. , 2011**).

The geology of the source region of the Attabad landslide contains two lithologic units isolated by a main (NW-SE) thrust fault related within the Main Karakoram Thrust zone (**Searle, 1991**). The younger unit at the upper part (northern limit) of the rockslide source area is the Hunza pluton (Red fill in Fig. 3.2). This rock type contains chiefly granodiorites, comprising plagioclase, biotite, quartz, hornblende, and potassium feldspar, in concentrations ranging from granite to diorite (**Searle, 1991**). (**Le Fort, Michard, Sonet, & Zimmermann, 1983**) predicted life time of this rock formation to be 95 ± 5 Ma.

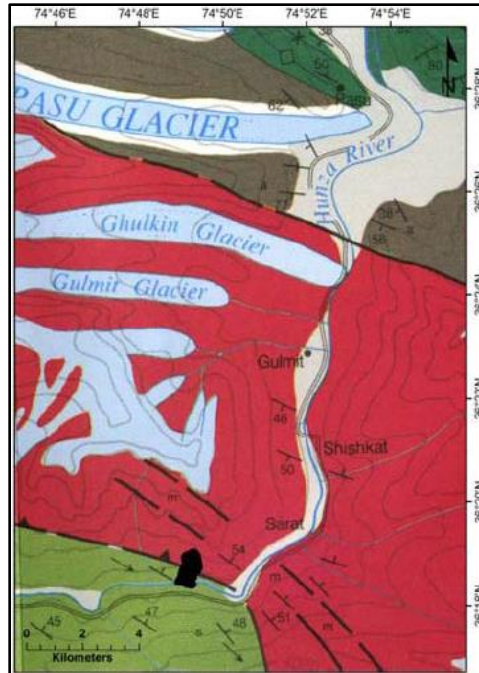


Figure 3.2: Geology of the Attabad region in northern Pakistan. The rockslide overlying the two major geologic formations is shown in black polygon, (Red: Hunza Plutonic Unit; Light Green: Dumordu Unit) and a thrust fault reviewed (Searle, 1991).

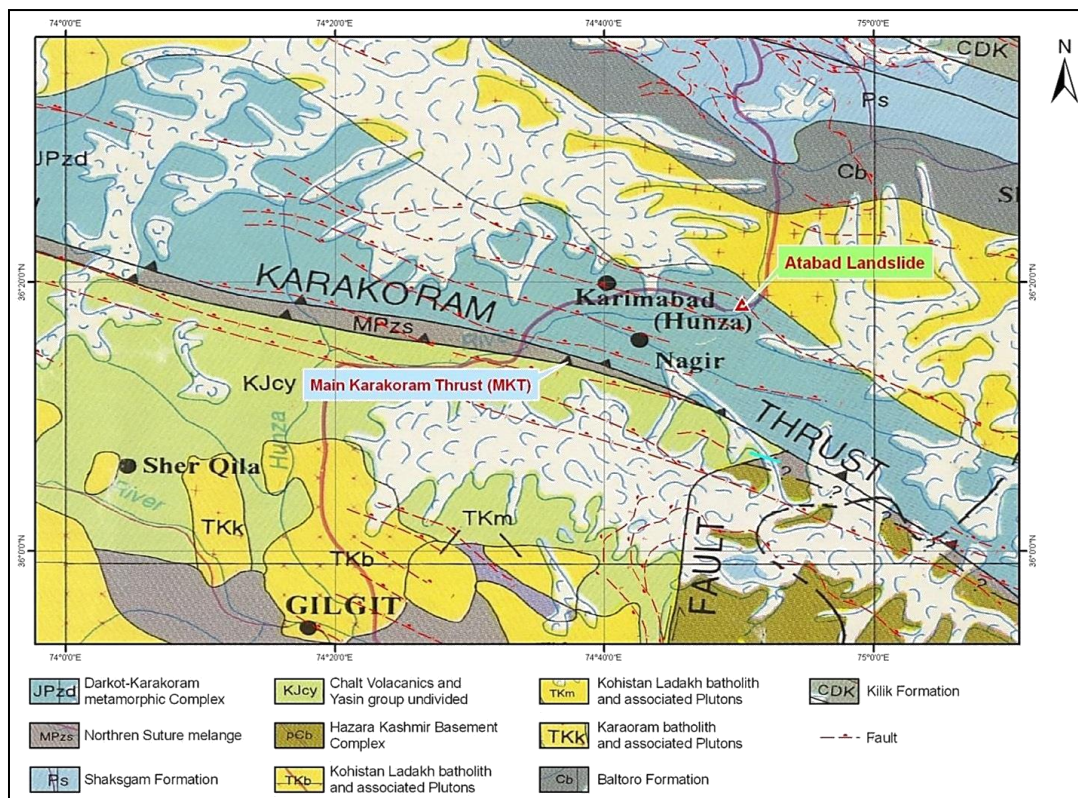


Figure 3.3: Geological map of landslide area

The lower part of the landslide source zone contains the older rock formation which is the Dumordu Metasedimentary Unit (Light Green fill in Fig. 3.2). This unit contains meta-sedimentary marble, with trivial aggregates of interbedded amphibolites, orthoquartzites, pelites, and conglomerates (Searle, 1991). The foliations are dipping 45° to 50° to the NNE particularly in the Dumordu meta-sedimentary marbles almost directly opposite to the movement direction of the Attabad landslide (Fig. 3.2).

On the other hand, the site and sliding direction of the rockslide (SW) corresponds to the dip and presence of a collision-related thrust fault (Fig. 3.2) that put the older Dumordu meta-sedimentary unit above the Hunza Pluton (Delaney K. B., 2014).

The rock units renowned in Hunza valley with probable period are summarized in table below:

Table 3.1: Key Rock Units Renowned in Hunza Valley (Hussain & Awan, 2009)

Serial No.	Group	Period	Lithology
I.	Baltit Group	Pre-cambrian-lower Paleozoic	Gneiss, quartzite, marble, Schist, and dolomitic limestone
II.	Chalt ophiolitic melang zone	Late cretairccous to early tertiary	Quartz-biotite schist, garnet mica schist, staurolite schist, phyllite, quartzite, slate, marble, cherry conglomerate, and dolomitic limestone
III.	Karakoram Granodiorite	Pliocene	Granodiorite
IV.	Glacial Moraines, Terraces, River deposits	Quaternary	Morains, Terrace deposits and stream gravel

3.2.1 Type of Landslide Strata

The landslide mass comprised of clayey and slushy soil which sticks to the machinery and causes it to sink during mitigation work.

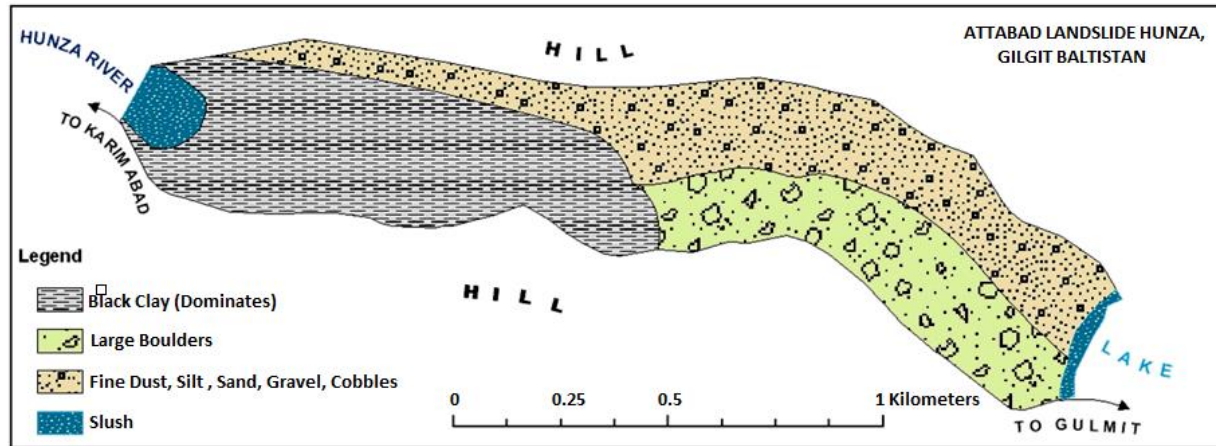


Figure 3.4: Distribution of landslide material based on visual observation

3.2.2 Huge Boulders

Heavy boulders of sizes more than 100 m³ were come across during cut. When again blasting has to done with time, these boulders slowed the pace of work [59].

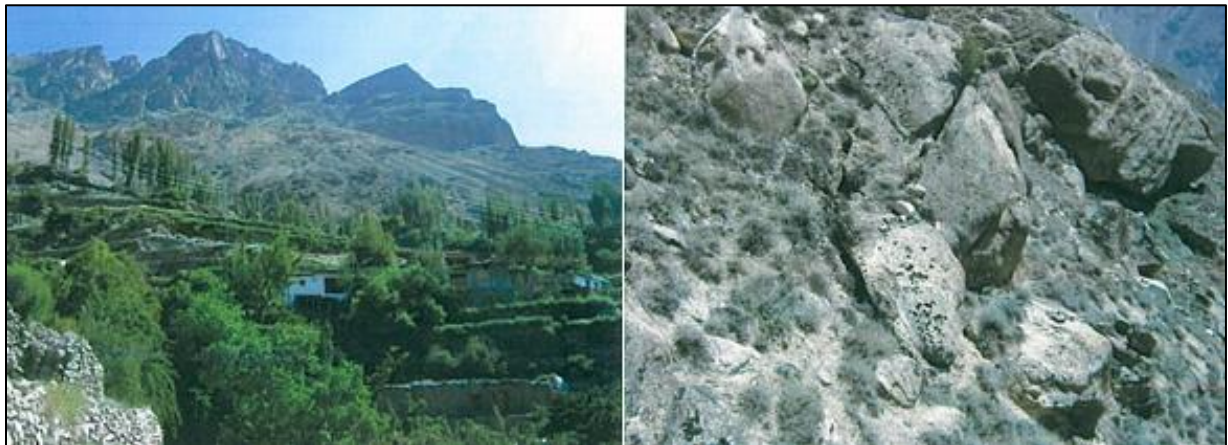


Figure 3.5: Boulders lying at high degree backslope directly hit Attabad (Hussain & Awan, 2009)

3.2.3 Network of Cracks

The network of cracks and fissures existing in the region are the possible cause of any future catastrophe and may result into loss of property and life. Three main patterns of cracks have been

detected on the backslopes and one network of crack has been identified at the terrace (**Hussain & Awan, 2009**).

According to spectators, numerous large cracks had appeared in the rockslope that suffered failure in 2010 at altitudes just above Attabad village resulting seismic activity in 2002 (**Petley D. , 2011**); (**Iqbal, Shah, Chaudhary, & Baig, 2014**). These cracks became wider (both by depth and laterally along the slope) and further widespread between their early discovery in 2002 and the rock slope failure in 2010 (**Petley D. , 2011**); (**Iqbal, Shah, Chaudhary, & Baig, 2014**).



Figure 3.6: Types of cracks lying at different locations

In the report of Geological Survey of Pakistan for NDMA, it was evident that **Crack No.1** was produced from eastern most part of terraces which stretched into the rockslopes into more three subdivisions and generated a whole slip surface. **Crack No.2** was placed at the center of eastern most part of the rockslopes **Crack N0.3** was a semicircular crack emerged from the left side of

the rock slopes that travelled along major multidirectional displacements into the upper sections of rockslopes and extended downslope into the Barali Shoe Nala and into the terraces at the end. **Crack No.4** was occurred in the terraces that affected the houses as well as cultivated regions too, it was also directly affected the Attabad population. There were so many other cracks existing in the region that were either minor individual cracks or have some association with the major cracks. Reporters had been monitored the displacement along these cracks constantly and observed edge letdowns, soil downfall and terraces settlement as a consequence of this, specifically in the snow melt and rainy periods of March to April (**Hussain & Awan, 2009**).

Table 3.2: Discovery of cracks in the affected area (Hussain & Awan, 2009)

	Location	Coordinates	Strike of Crack	Vertical Settlement/ Depth (ft.)	Horizontal Settlement (ft.)	Activity Status
Crack No.1	Lower part	36.31337 N 74.81796 E	N70E	Nil	3.6	Active
	Middle part	36.31349 N 74.81857 E	N75E	10	16	
	Upper part	36.31368 N 74.81989 E	EW	5	10	
	Top/end part	36.31432 N 74.82018 E	N30E	6	5	
Crack No.2	Middle part	36.31406 N 74.82198 E	EW	8	2	Active
Crack No.3	Left margins	36.31502 N 74.82468 E	N50W	5	6	Very Active
	Crown of crack	36.31760 N 74.82327 E	N60W	16	15	
	Lower part	36.31528 N 74.81668 E	N60E	3	4	
Crack No.4	At Terraces	36.31475 N 74.81785 E	EW	4	3	Very Active



Figure 3.7: House damaged due to failure of slope at terraces (Hussain & Awan, 2009)

3.3 Topography and Geomorphology

The Karakorum Himalayas range passes through the Hunza valley in NW to SE direction. High snow covered mountains with steep hills and narrow valleys are topographic characteristics. The difference between valleys and peaks varies from 2200m and 2700m. The drainage of the area is controlled by Hisper and Hunza rivers. To the south of investigated area, the world's 11th highest peak Rakaposhi (7788m) exists. Pasu Glacier is in the North of the said region.

As compared to any other place in the world, the Hunza valleys that cut Karakoram Mountains have highest contrasting relief and great vertical elevation difference over a short horizontal distance. Hunza valley increases from 1850m to the Rakaposhi cliff at 7788m, a vertical distance above 11km. The highest valley regions possess sharp ridges, pyramidal and without plateau topographies. Mass driven activity is at large scale in that area because of slope failure weathered by frost action (Hussain & Awan, 2009).

The slope morphology of Hunza valley has many kinds. Snow packed high cliffs are particular associated with scree slopes, rock slope, mudflow and are existing all through the Hunza valley. The moraines have asymmetrical topography (Hussain & Awan, 2009).

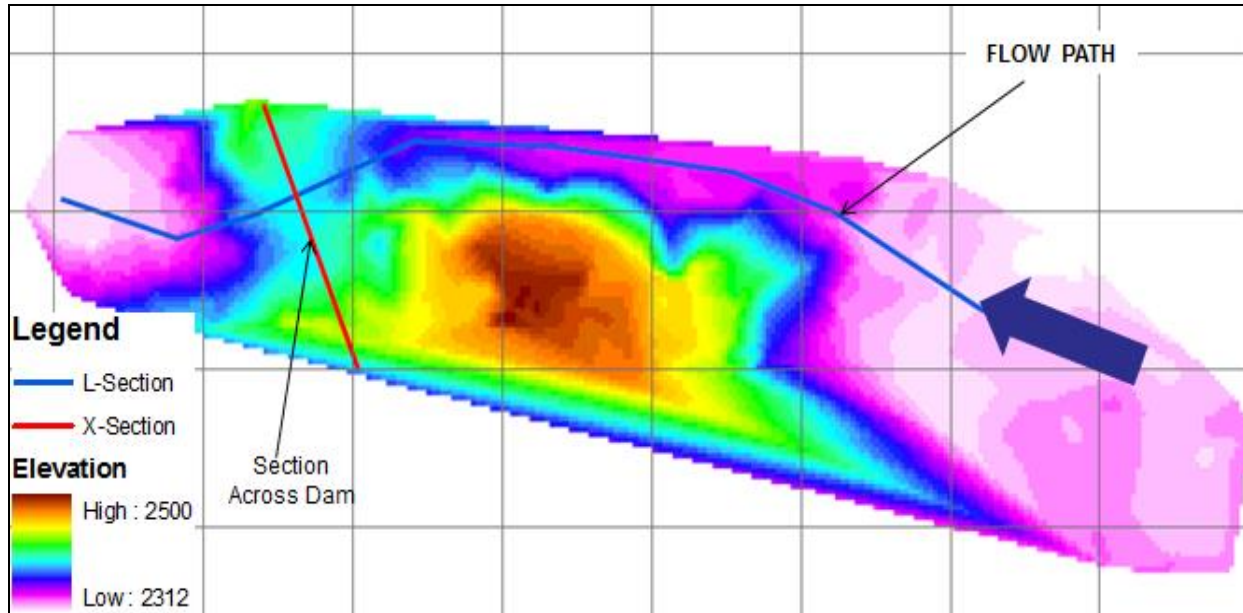


Figure 3.8 Topographic Survey of landslide by NESPAK Engineers

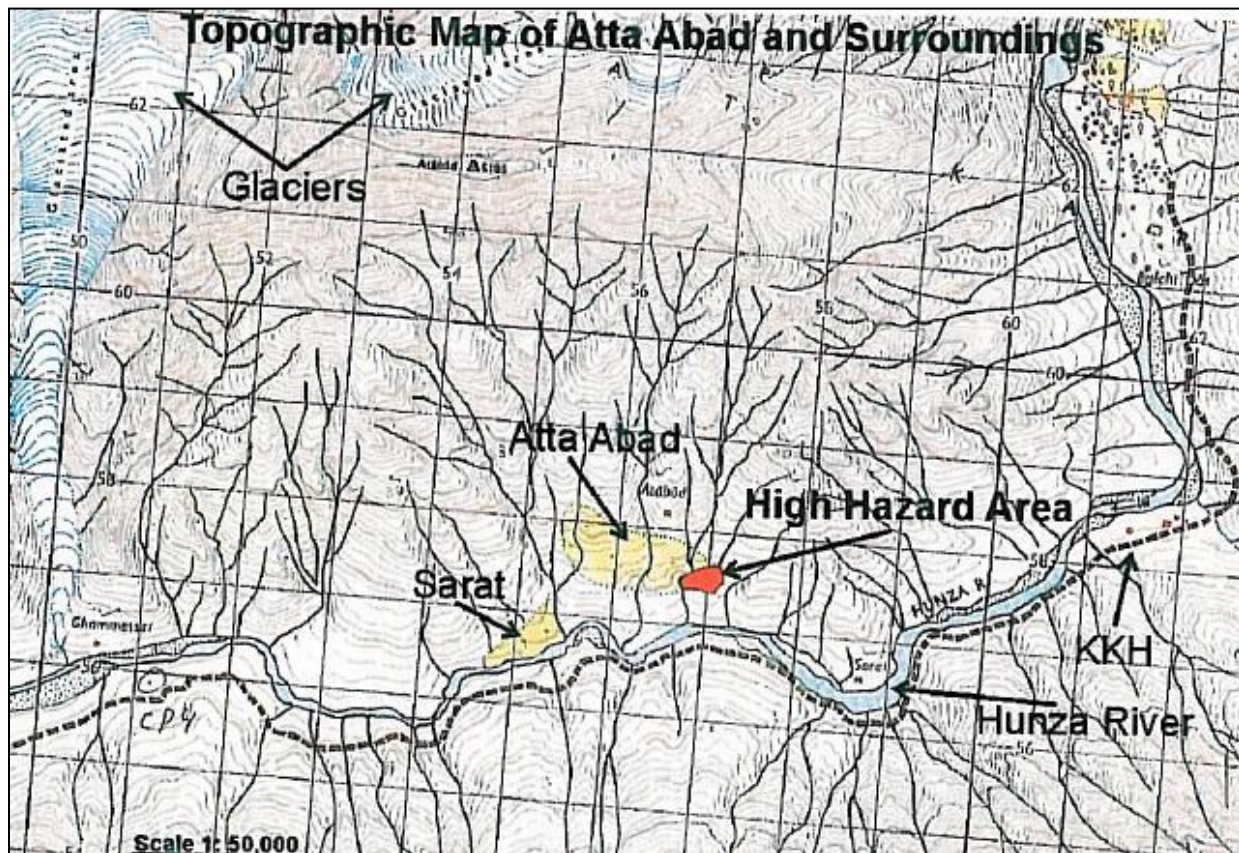


Figure 3.9: Topographic map of Attabad and surroundings provided by Survey of Pakistan

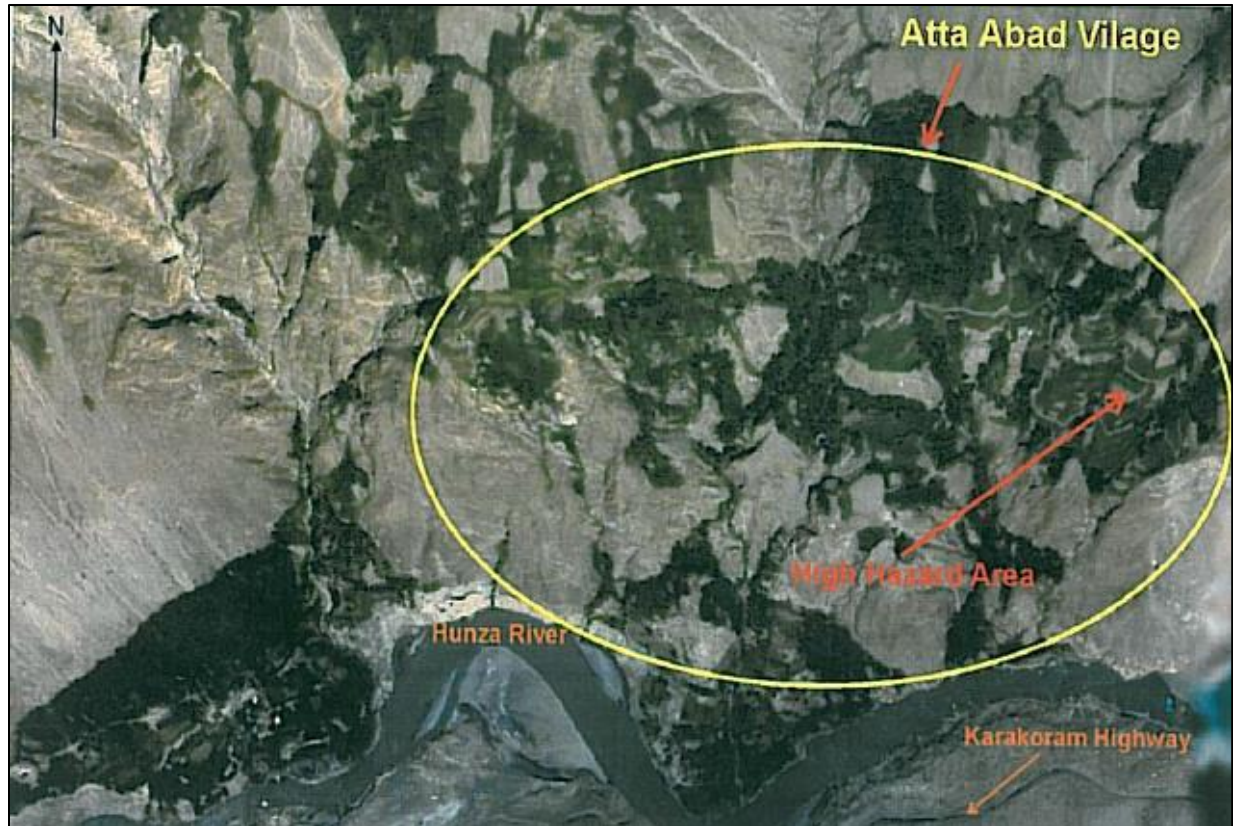


Figure 3.10: Ariel view of Attabad village and surroundings (Hussain & Awan, 2009)

3.4 Climate

The climate in this part of Pakistan is mostly arid and high summer temperatures ranges from 25 to 30°C but temperatures in the winter goes below zero. Sometimes winter temperature would fall below -15°C so making it very difficult for machinery and men to work in case of land sliding. Extreme weather has been present in the slide area that turns into rainy and snowy weather time to time (FWO, 2010).

During winter, Hunza and investigated regions are extremely cold with severe climate. But spring and summer are rather pleasant. Usually two to three feet (24-36 inches) snow falls in this region in winter. The coldest month of the winter is January. March and April become hazardous months triggering rock falls and mud flow as a consequence of snow melting. Rain is very short and scanty (Hussain & Awan, 2009).

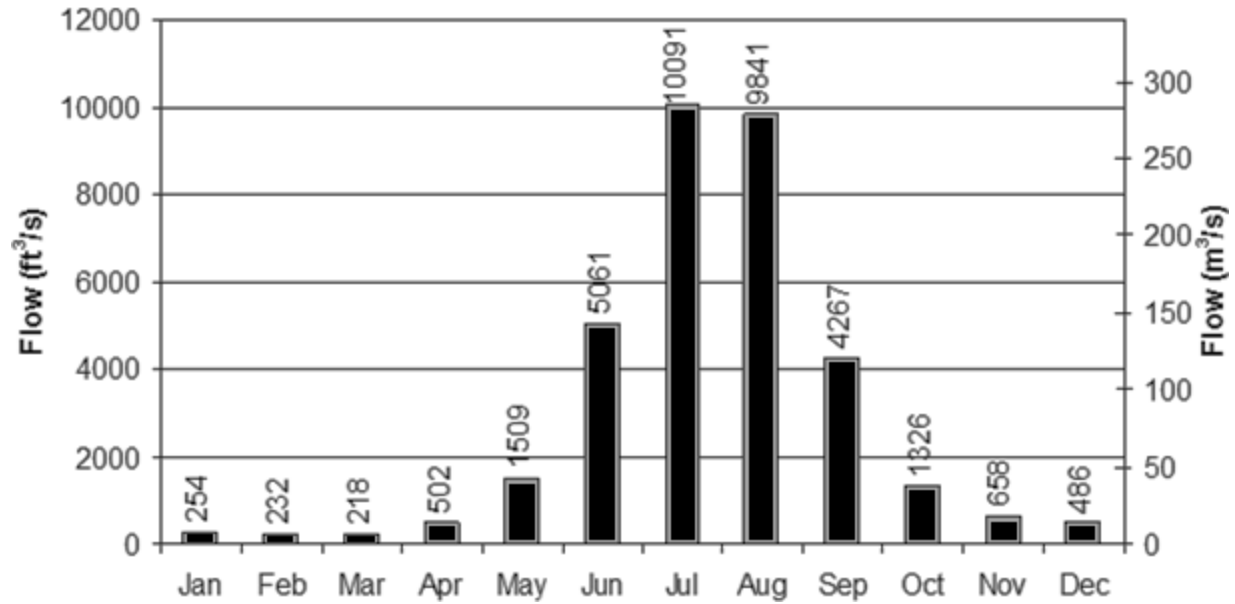


Figure 3.11: Estimated monthly average flows at landslide location

3.5 Fruits

Natives of Attabad village depend on potato and apricot as main currency crop, although major fruits of Hunza valley are walnuts, apricots, apples, almonds, pears, grapes and peaches (Hussain & Awan, 2009).

4 METHODOLOGY

4.1 Data Sources

For quantifying the filling, overtopping, and consequent partial draining of Attabad Lake, we utilized different types of data from various data sources given below:

- 1) SRTM-3 and GDEM2 digital topographic data, detailed defined in Introduction section.
- 2) Multi-temporal satellite images from 2010 to 2015 of Attabad Lake, described below.
- 3) Facts and figures and all information about Attabad Lake formation was published on the following authentic internet websites:
 - i. <http://www.ndma.gov.pk/> - NDMA (National Disaster Management Authority) provided measurements of lake depth from filling to overtopping (no data was distributed after July 30, 2010 when overtopping became stable).
 - ii. <http://www.nespak.com.pk/> - Retrieved bathymetric survey data on lake surface levels and valley bottom terrain till July 2011 from NESPAK (National Engineering Services of Pakistan).
 - iii. <http://pamirtimes.net/> - This Pakistani news website (*PAMIR TIMES*) primarily gave qualitative descriptions and photographs related to the filling and fractional draining of Attabad Lake.
 - iv. <http://earthobservatory.nasa.gov/NaturalHazards/> - Georeferenced satellite Images in GeoTIFF format with complete updates on them (16th March 2010, 02nd May 2010, 25th May 2010, 01st June 2010, 02nd July 2010, 07th July 2010, 23rd August 2010, 03rd October 2010, and 03rd August 2011) were found out here.
 - v. <http://www.local.com.pk/hunza/> - .kml layers (16th March 2010, 02nd May 2010, 25th May 2010) were got from here so that all layers could overlay on Google Earth[®] imagery and able to see lake extend at that time.
- 4) WAPDA (Water and Power Development Authority) of Pakistan supplied data through Khalil Ahmad Ghauri.

Large scale (>1:250,000) topographic maps were not available to us for the study area as well as no fieldwork was conducted at Attabad.

4.1.1 Optical Satellite Imagery

We made use of ten optical images from three satellite platforms: EO-1 ALI, ASTER Terra and LANDSAT8 OLI. These all satellite platforms have adequate temporal resolution and sufficient data archives to precisely display the growth and shrinkage of Attabad Lake from the early landslide in 2010 to its status in 2015. EO-1 and ASTER georeferenced images in GeoTIFF format were directly accessed from the NASA website: <http://earthobservatory.nasa.gov/NaturalHazards/> while EROS USGS (United States Geological Survey) Landsat 8 imagery was downloaded from Earth Explorer. We also utilized Google Earth imagery of 08th November 2012.

The EO-1 imagery (16th March 2010, 02nd July 2010, 07th July 2010, 23rd August 2010, 03rd October 2010, and 03rd August 2011) has the highest panchromatic spatial resolution of 10m, with an elongated image extent of 36 km x 82 km, and gathers data across 8 spectral bands for analysis (**USGS, Earth observing 1 (EO-1), 2011**). The ASTER imagery (02nd May 2010, 25th May 2010, and 01st June 2010) has a (non-panchromatic) horizontal resolution of 15 m, covering an area of 60 km x 60 km, and utilizing 14 spectral bands for analysis (**NASA, 2004**). The LANDSAT8 OLI imagery (02nd May 2013, 25th August 2014 and 08th May 2015) has a panchromatic spatial resolution of 15 m, covering an area of 183 km x 190 km, and collects data across 11 spectral bands, and has WRS path 149 and row 035 of it (**USGS, 2013**).

We processed and analyzed DEMs and optical images in ESRI ArcGIS[®] 10.1. This involves mosaics of DEM tiles and exporting of digital terrain data for process analysis. These images were collected, preprocessed and processed in a way to delineate lakes surface areas. No rectification of images was required because all of them were already georeferenced and rectified into UTM zone 43. Next, these images were enhanced in a way to differentiate between lakes and surroundings. The consistency and quality of DEM was tested both visually and logically.

Table 4.1: Remote Sensing data used for study

Data Type	Acquisition Time	Spatial Resolution (m)
EO-1 ALI	16 th March 2010, 02 nd July 2010, 07 th July 2010, 23 rd August 2010, 03 rd October 2010, and 03 rd August 2011	10
ASTER Terra	02 nd May 2010, 25 th May 2010, and 01 st June 2010	15
Google Earth	08 th November 2012	15
LANDSAT OLI	02 nd May 2013, 25 th August 2014 and 08 th May 2015	15

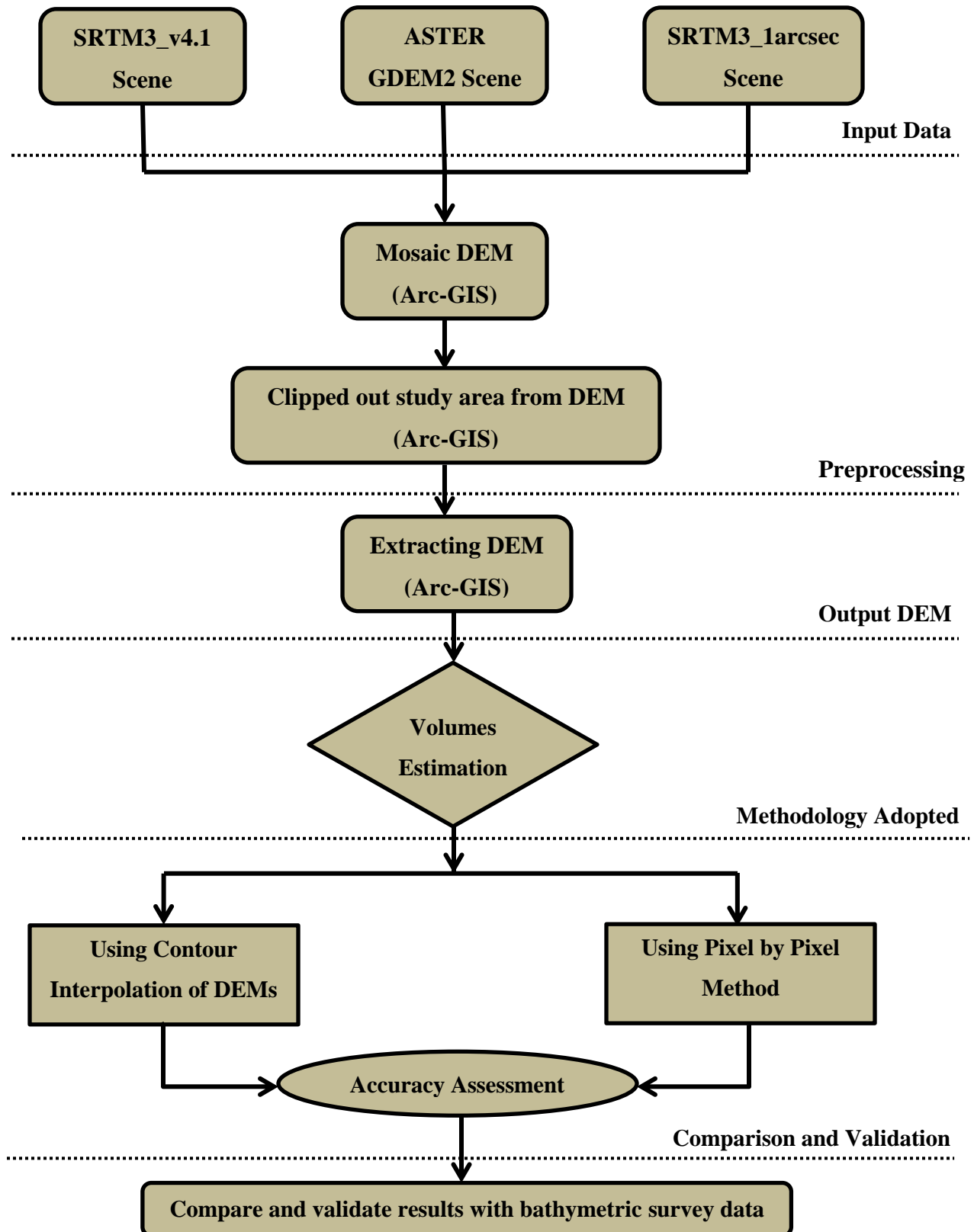
4.2 Materials

Six major software packages were employed for the data processing, visualization and analysis of the results. These involved the ESRI Arc-GIS 10.1, Global Mapper, MATLAB, Google Earth Pro and Microsoft office.

Table 4.2: Software utilized for the current study

Software Used	Purpose
ESRI Arc-GIS 10.1	Mosaicing, creating shape file, merging, clipping, digitizing, DEM profiling and analysis, performing geometric calculations, 3D visualization, map layout
Global Mapper	Raster to vector conversion, conversion of ESRI shape file (.shp) into Google Earth shape file (.kml/.kmz), Hillshade Mapping
MATLAB R2011a	Plotting, symbolizing and visualizing data
Google Earth Pro	For calculating perimeter of the lake
Microsoft Excel 2010	Perform calculations, analyze information, and visualize data in spreadsheets by making graphs, charts, and tables
Microsoft Word 2010	For creating, editing and compiling of documents

4.3 General Validation Approach



4.4 Analysis of Contour Interpolation of DEMs for Estimating Lake Volumes

We used the contour interpolation technique along with SRTM and GDEM2 datasets for the first order geometrics (length, area, volume, depth) approximations of the rockslide-dammed lake. This technique utilizes the contour function of the ArcGIS® 10.1 3D Analyst tool in combination with the elevation data. This interpolation generates contours based on a comparison between the neighboring DEM heights thus evaluating the elevations between center points of the discrete grid cells.

In this technique each generated contour denotes the lake level in the topographic data. We supposed a local datum of 2322m.a.s.l. at the landslide location for the river valley floor, assuming a lake depth of 0 m (figure 4.1), and a maximum lake elevation 2434m.a.s.l. We interpolated twelve 10 m-interval contours within these height limits from the DEMs and used these contours as an estimation for the lake shorelines in the period of reservoir filling (Table 4.3). We calculated values of area and volume for every interpolated contour level of the lake from both digital data sets (Table 4.3).

We added the NDMA defined lake depths for attaining the lake elevation above sea level in meters to the elevation of our assumed NESPAK based local datum (2322 m.a.s.l.), starting on 27 day of impoundment (31st Jan. 2010). In this way we plotted a filling curve of lake depths and pool height elevations during the filling of Attabad Lake as indicated in figure 4.1.

We were also able to check the vertical accuracy of the SRTM and ASTER GDEM2 by referring to local news reports and the NDMA lake depth data; for example, on February 10, 2010 (day 37) Attabad Lake had reportedly reached the piers of the Karakoram Highway Bridge located at Gulmit, upstream of the impoundment. The elevation of the SRTM grid cell under the bridge piers at this location is recorded as 2375 m.a.s.l., which is within 2 m of the elevation (2377 m.a.s.l.) indicated by the NDMA lake depth (ca. 52 m) reported on that day while GDEM2 gave the elevation 2369 m.a.s.l.

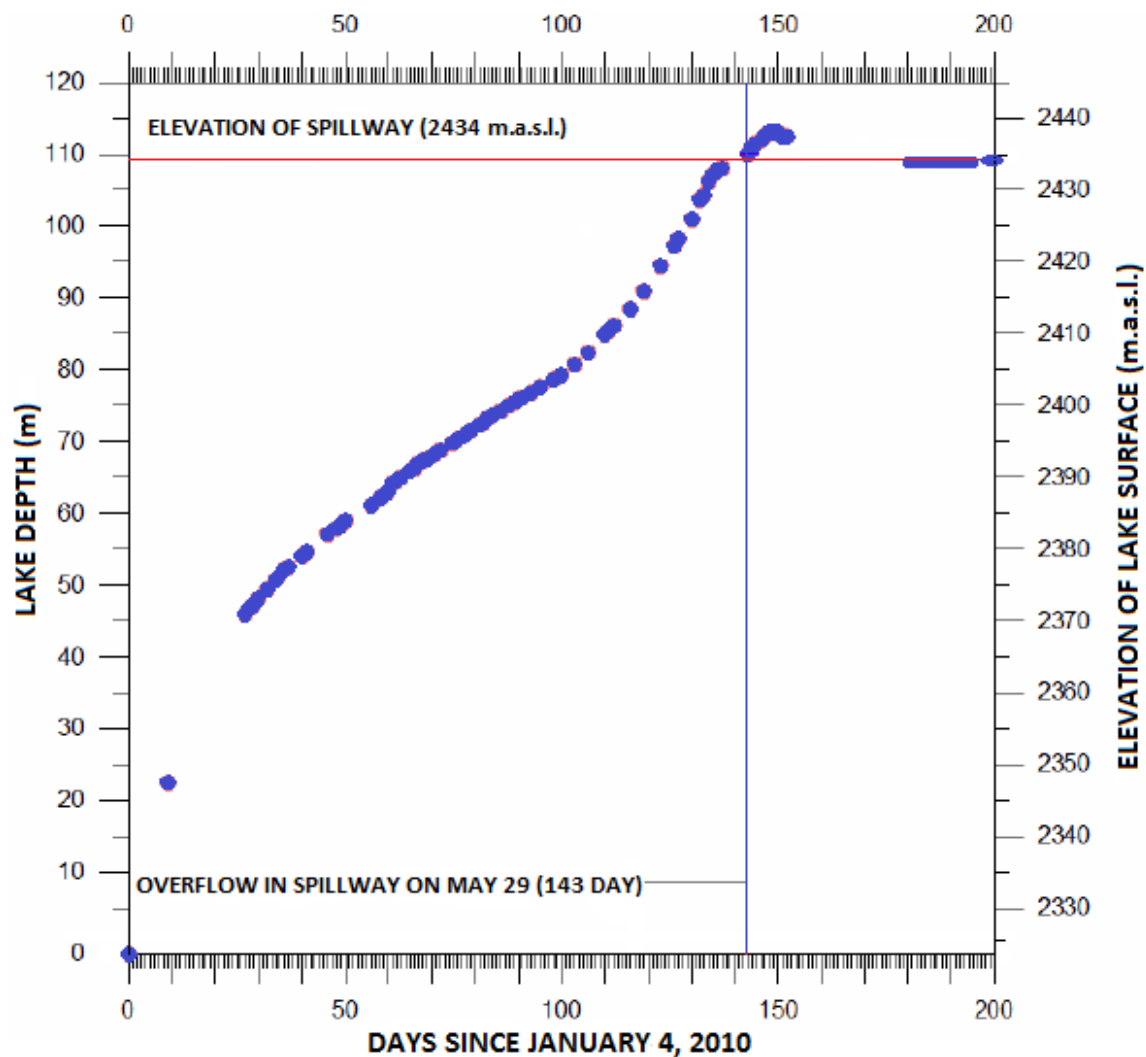


Figure 4.1: Data about filling curve of lake depths and water surface elevations of Attabad Lake during landslide-dammed lake development and was derived from the National Disaster Management Authority (NDMA) Pakistan.

By using contour interpolation utility of Arc GIS[®] 10.1 in conjunction with digital topographic datasets (SRTM-3 and GDEM2), we made first order estimations of area and volume of Attabad Lake for a range of pool surface elevation during filling and partial draining of Lake as described in table. For the sake of being compared our contour interpolated calculations with NESPAK (bathymetric) field survey results, we hereby assumed datum to be 2322 m.a.s.l (also see **Appendix-A: Elevation Capacity Curves of Attabad Lake** for detail).

Table 4.3: Table illustrates the first order geometric (area, volume) estimations of Attabad Lake extracted from contour interpolation of SRTM-3 and ASTER GDEM2 digital terrain data and compare it to the NESPAK data based on bathymetric field survey. Lake filling information is also given.

		NESPAK		SRTM-3 v.4.1		GDEM2		SRTM-3_1arcsec	
Lake Height	Height Above River	Surface Area	Volume	Surface Area	Volume	Surface Area	Volume	Surface Area	Volume
m.a.s.l.	m	km ²	Mm ³	km ²	Mm ³	km ²	Mm ³	km ²	Mm ³
2434	112	9.29	328.85	11.17	416.4	11.45	443.96	11.79	427.38
2424	102	6.86	248.06	9.42	316.34	9.8	346.44	9.89	323.97
2414	92	5.02	189.29	7.17	236.83	8.14	264.15	7.52	242.13
2404	82	3.99	144.91	4.87	173.39	6.54	196.89	5.42	182.61
2394	72	3.33	108.32	4.2	129.52	4.68	143.24	4.44	138.31
2384	62	2.71	78.15	3.61	92.09	3.98	103.81	3.77	99.66
2374	52	2.23	53.42	2.98	60.47	3.26	70.6	3.13	67.03
2364	42	1.77	33.34	2.37	25.14	2.54	43.85	2.42	40.49
2354	32	1.28	18.02	1.45	17.23	1.78	23.85	1.57	21.69
2344	22	0.78	7.67	0.88	6.54	1.1	10.48	0.99	9.69
2334	12	0.408	1.88	0.29	1.27	0.48	3.25	0.48	2.84
2324	02	0.0708	0.063	0.0101	0.0095	0.12	0.68	0.084	0.13
2322	0	0	0	0.00248	0.0024	0.098	0.48	0.031	0.03

Bathymetric surveys of NESPAK were undertaken in the period of July 2011, they notified elevations rely on a recently established benchmark surveyed in by (SOP) Survey of Pakistan. NESPAK (2014) reported the height of the river valley at the upstream side of the landslide dam to be 2322 m.a.s.l. which parallels to a local datum as noted above with a lake depth of zero (Khali Ahmad Ghauri (WAPDA)).

Furthermore, NESPAK determined a maximum lake elevation of 2434 m.a.s.l. only 1meter and 16meter below the elevation in that order determined from the SRTM-3 and GDEM2.

While we assessing these three data sets we checked that GDEM2 values in both area and volume for a given lake surface elevation are consistently larger than the SRTM-3 values (Table 4.3); this discrepancy becomes larger as water surface elevation and lake volume increases.

We performed a comparison between the NESPAK data rely on bathymetric survey (July 2011) and the estimated volume derived during the first order contour assessment of SRTM and GDEM2 data (fig. 4.2). It is obvious from NESPAK results that it undervalues the lake volume for a given elevation of water surface.

The discrepancies in volume calculations play a major role in outburst flood modeling or in hazard assessment. Three sets of data NESPAK (328.85 Mm³), SRTM-3 (416.40 Mm³) and GDEM2 (443.96 Mm³) - a series of 115.11 Mm³- represents the maximum volume at the full elevation of Attabad Lake ~2434m.a.s.l.

The gradient of the rating curve demonstrates a major change between 2404m.a.s.l. and 2414m.a.s.l. in all DEMs and the NESPAK data .This reflects the influence of the knick-point in the Hunza River valley nearby Shishkat at ca. 2405m.a.s.l. produced from the deposits of alluvial fan complex on the western shoreline.

The difference between the digital datasets and NESPAK data utilized in this study probably due to the fact of very limited number of cross-sections taken by NESPAK in the upper stretches (north of Shishkat) of Attabad Lake. Total 29 cross-sections were measured all along the 22 km of Attabad Lake according to NESPAK and just 4 of these cross-sections were obtained in the upper 9.5 km of the lake while 25 cross-sections were taken in the lower 12.5 km.

The following diagram (fig. 4.2) is graphically demonstrating the volumes estimated from the Contour Interpolation of SRTM4.1, ASTER GDEM2, and SRTM3_1arcsec global and showing the difference in between them.

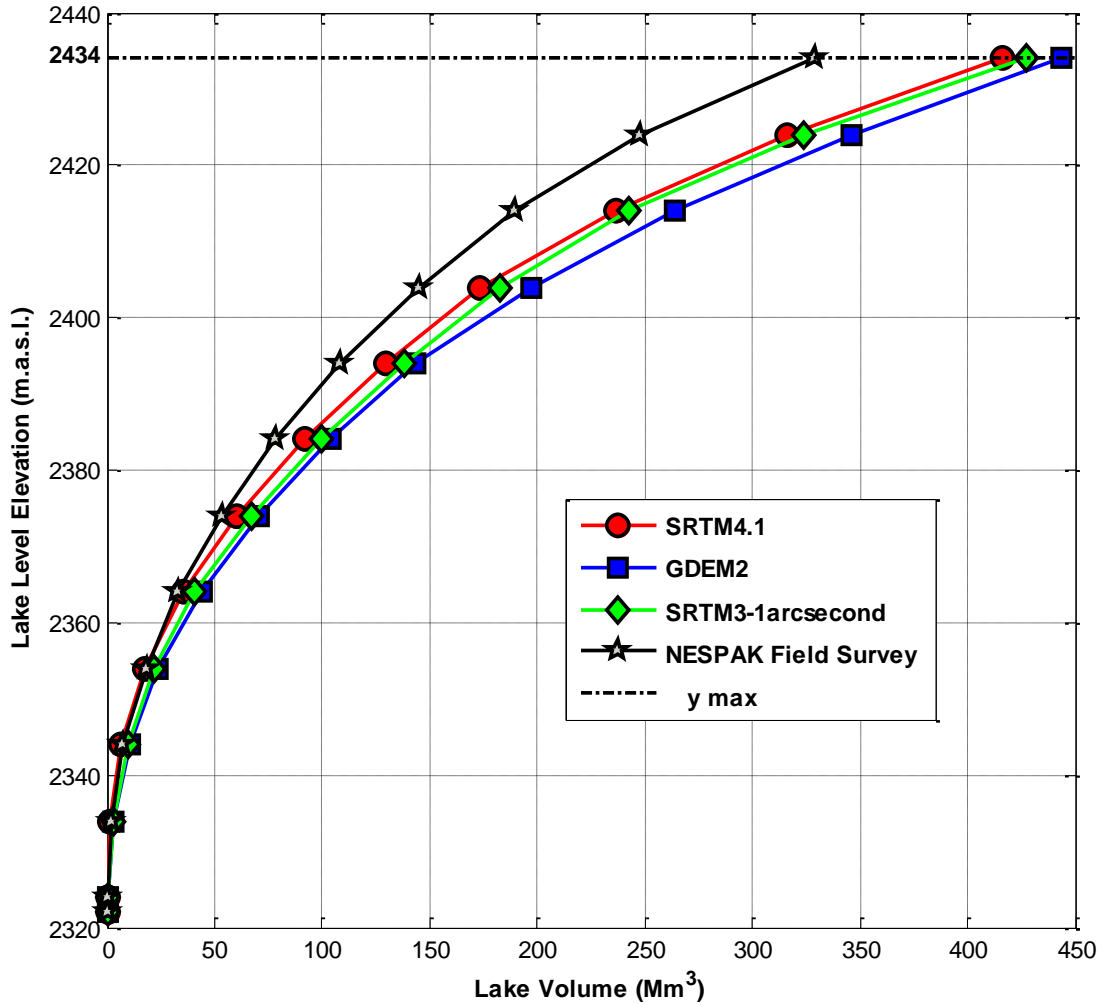


Figure 4.2: Plot of lake level elevations (m.a.s.l) and their volumes determined from the contour interpolation of SRTM4.1 (circles), GDEM2 (squares) and SRTM-3_1arcsec (diamond) DEMs and the NESPAK bathymetric data depend on field survey (stars). Datum is taken as 2322m.a.s.l. Dark black horizontal dashed line marks the approximated maximum lake elevation reached by Attabad Lake after stable overtopping started (2434m.a.s.l.).

Next, we are going to introduce another method that based on digitized shoreline that is used to accurately quantify the volumes of Lake at different stages of development and shrinkage.

4.5 Interpreting Pixel-by-Pixel Shoreline Methodology for Quantifying Lake Volumes

This pixel by pixel methodology that relies on a more rigorous delimitation of Lake Shoreline elevation proved to be very helpful in achieving the precise estimations of area and volume throughout the filling, overtopping, and partial draining of Attabad Lake. With this technique we attained a mean pool elevation of reservoir by a fusion of satellite imagery and DEM data. **(Dong, et al., 2014)** and **(Delaney K. B., 2014)** adopted the same procedure that contains the steps as follow. The Lake shoreline for distinct satellite imagery was visually traced out creating a polyline in GIS. After the formation of shoreline, the elevation was recorded of each SRTM 90m x 90m, GDEM2 30m x 30m, and SRTM-3 30m x 30m grid cell exact lying beneath this polyline for the whole perimeter of the lake. The number of counted grid cells of the analyzed lake shorelines ranged from 95 to 218 (for SRTM4.1), 158 to 372 (for GDEM2), and 137 to 355 (for SRTM-3_1arcsec). Then we obtained average value of these measurements as an approximation of the true lake elevation, and made their comparison where possible to field observed values. The associated histogram for each lake indicates the elevation ranges of shoreline.

Due to long term unavailability of NDMA data, aerial photography was used to maintain a historical record of lake level and volume for Attabad Lake. Thus, aerial photographs of the Attabad Lake were collected and rectified. Remote sensing and GIS software were utilized to store, analyze, and visualize the data and results for Attabad Lake. The key analytical steps started with the detection of the lake boundary from each photograph. This boundary was then used to detect the surface elevation of the lake that depends on the location of lake edge on a model DEM (digital elevation model). Volume of Lake was estimated using the Lake boundary, surface elevation and model DEM. Finally, the generated record of lake level and volume was compared with the field survey data to notice the correlations and trends **(Christensen & Bergman, 2005)**.

For all sorts of geometric calculations and terrain analysis, it is necessary that horizontal units of grid cells must match with the units used for elevation (meters).

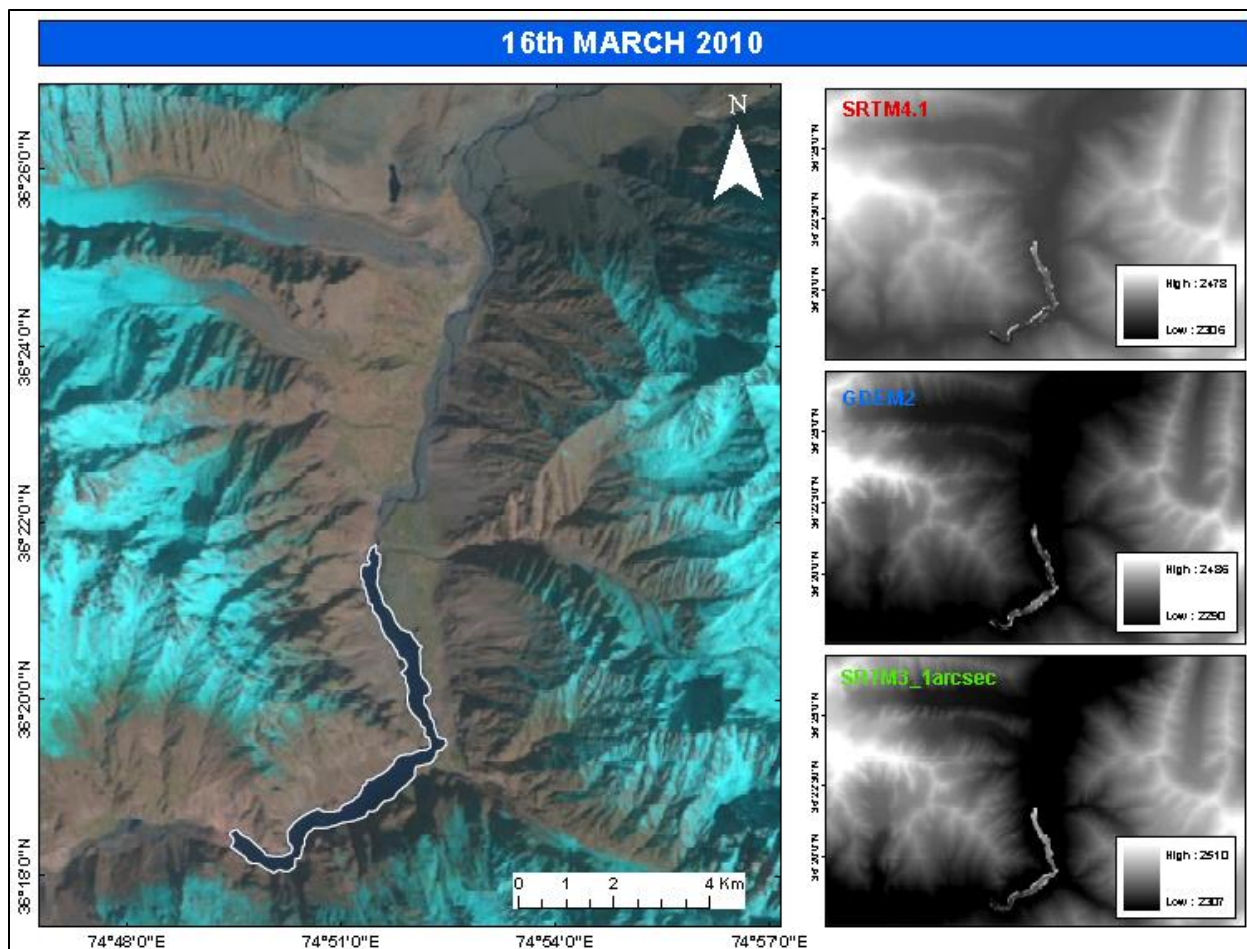


Figure 4.3: EO-1 ALI satellite imagery taken on 16th March 2010 indicating the Lake boundary in white color. NDMA provided the Lake Level Elevation 2389.3 at this time while datum assumed to be 2322 m.a.s.l.

An average lake level Elevation (m.a.s.l.) determined from pixel by pixel method on that date to be 2392.15 (for SRTM4.1), 2389.15 (for GDEM2) and 2391.6 (for SRTM3_1arcsec) so counted grid cells corresponding to them around the perimeter of the Lake are 95 (SRTM4.1), 158 (GDEM2) and 137 (SRTM3_1arcsec). The NDMA measured a lake depth of 67.3 m at that time showing an elevation of 2389.3m a.s.l; a difference of only -2.85, +0.15 m and -2.35 in that order. Thus at that elevation volume of Attabad Lake were calculated and the difference in volume using these two methods were also noted and wrote in tabular form. For the same lake shoreline elevation, contour interpolation method overestimates the volumes like for SRTM4.1, GDEM2, and SRTM3_1arcsec it calculated values as 128.30 Mm³ (82.78Mm³), 143.60 Mm³ (124.33 Mm³), and 134.10 Mm³ (117.43 Mm³) while the values in brackets represent the volumes based on pixel by pixel methodology.

02nd MAY 2010: ASTER satellite captured the Lake Gojal in false-colour composite was imaged by the ASTER on May 02, 2010 in figure 4.4:

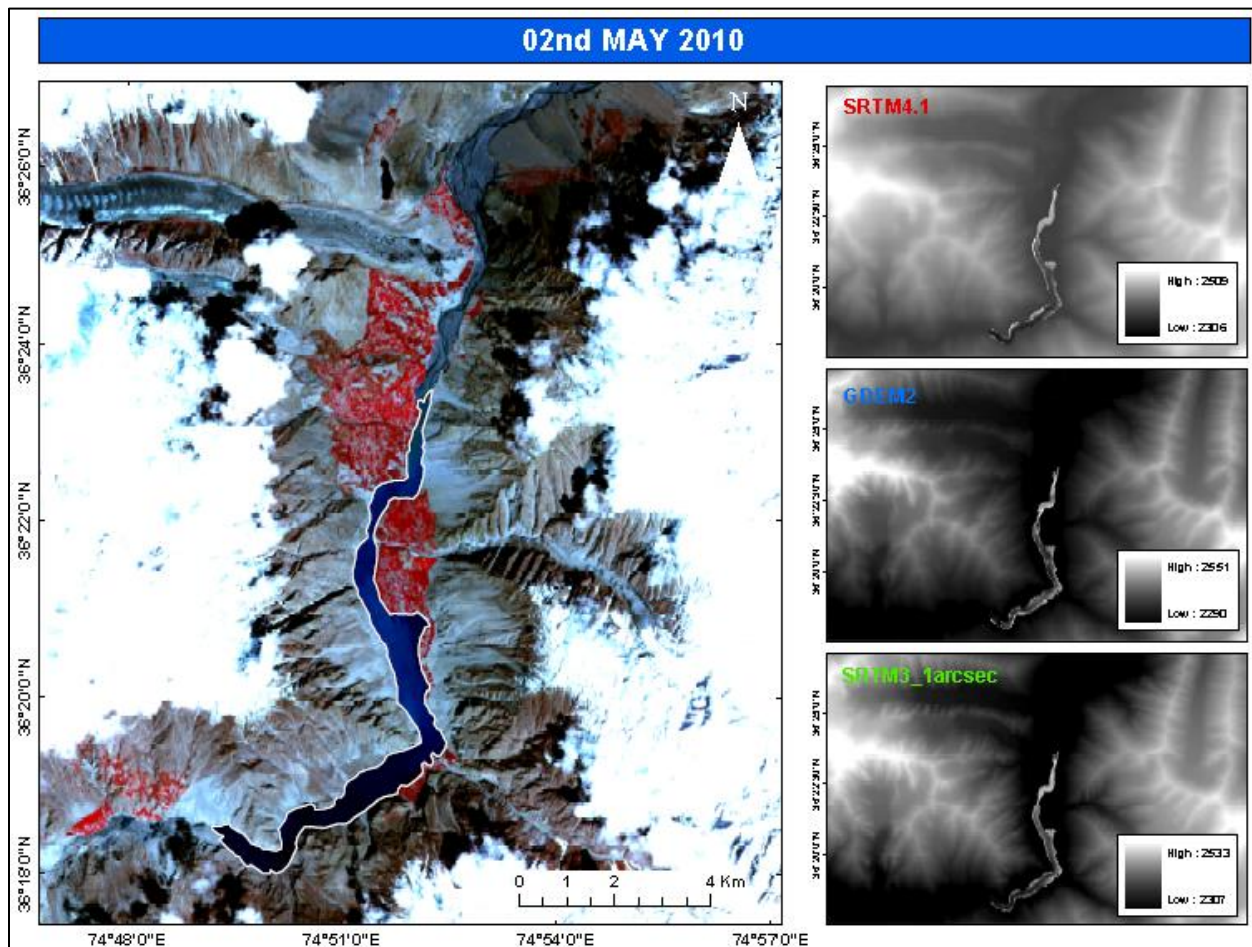


Figure 4.4: Attabad Lake imaged on 02nd May 2010 by the ASTER satellite at the time of filling, digitized shoreline shown in white. The shoreline elevation measurements are determined from the pixel-by-pixel method.

The mean pool height and the number of pixels around the periphery of lake on 02nd May were found out to be 2408.7 m a.s.l with 132 counts of SRTM4.1; 2415.2m a.s.l with 226 counts of GDEM2 and 2408.2m a.s.l with 147 counts of SRTM3_1arcsec. As no report published on 02nd May, the NDMA recorded a lake depth of 88.4 m on 03rd May that representing a lake level of 2,410.4 m a.s.l. A vertical difference of +1.7 m, -4.8 m, +2.2 m were observed for SRTM4.1, GDEM2, and SRTM3_1arcsec respectively. At this elevation differences in volumes calculated from pixel by pixel method and contour interpolation method were found out to be 243.37 Mm³ (187.27 Mm³), 267.57 Mm³ (240.28 Mm³), and 251.22 Mm³ (229.81 Mm³), it clearly shows that

contour interpolation method yields only approximations of volumes but proposed pixel based methodology gives precise results. Volumes in brackets indicate the delimited shoreline volumes calculated from pixel based methodology.

25th May 2010: During the filling process, the lake was imaged again by the ASTER satellite on May 25, 2010.

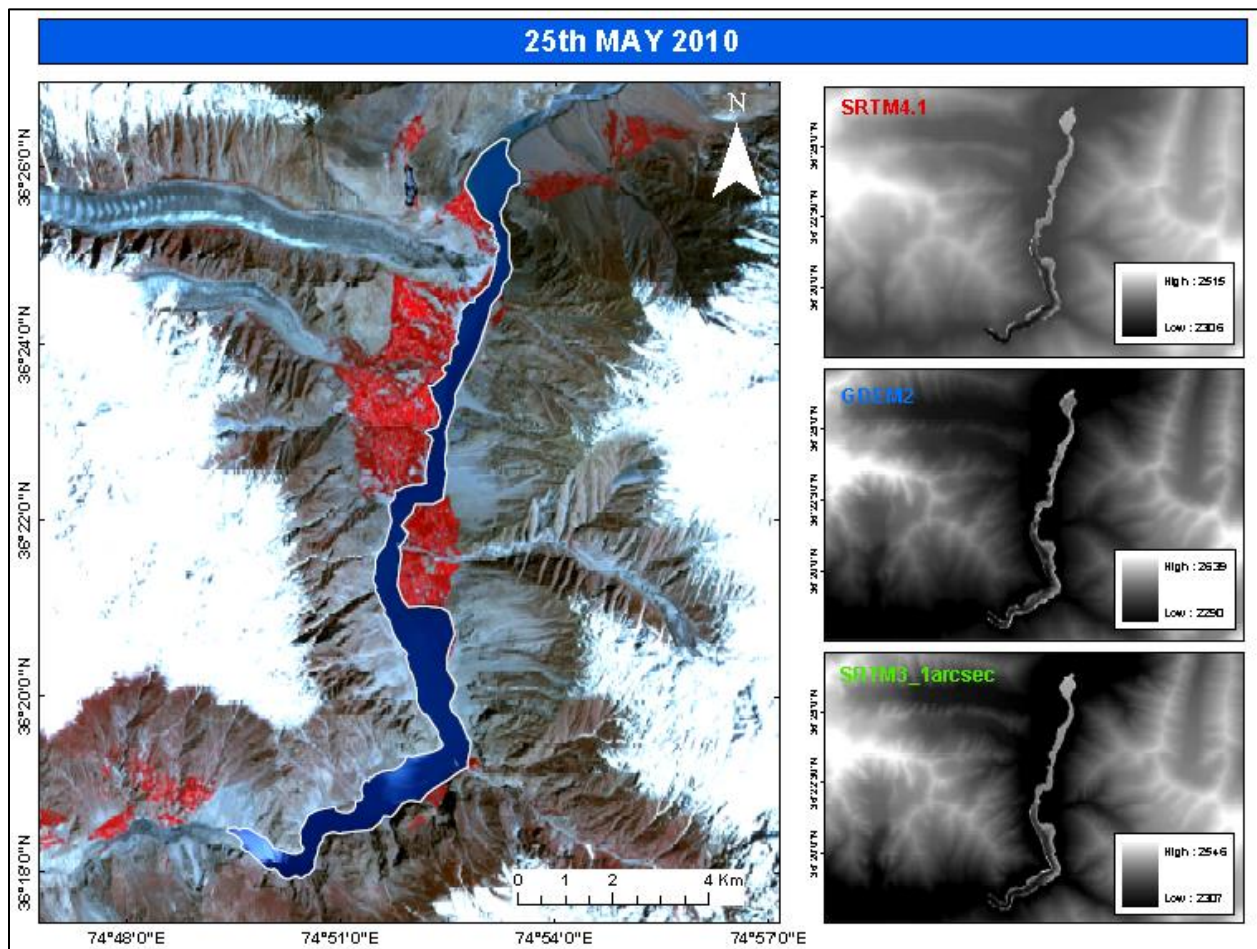


Figure 4.5: Digitized shoreline placed on ASTER satellite imagery showing the Attabad Lake extent of 25th May 2010. Lake level progressively reached to the overtopping level.

The mean pool height determined from the SRTM4.1, GDEM2, SRTM3_1arcsec on 25th May as: 2430.7m a.s.l., 2433.7m a.s.l., 2430.7m a.s.l. in that order and were calculated from 142, 265, and 191 grid cells sequentially.

The lake depth data of NDMA recorded 108.4 m depth on that date indicating a lake elevation of 2430.4 m a.s.l., a vertical difference of -0.3 for SRTM based DEMs and +3.3 for GDEM2.

With the help of pixel by pixel method more precise volume estimations 413.12 Mm³ (352.04 Mm³), 450.70Mm³ (420.70 Mm³) and 251.22 Mm³ (229.81 Mm³) in that sequence at this elevation can get from SRTM4.1, GDEM2, and SRTM3-1arcsec, where volumes given outside the brackets were estimated from Contour interpolation methods.

01st June 2010: Attabad Lake was imaged again by the ASTER satellite two days later on 01st June 2010 when overtopping had started over the spillway and also observed the farthest lake stretch detected by satellites. At that time, the NDMA informs that lake depth has increased from 1.62 m to 111.6 m above the overtopping level of 2434m.a.s.l. to a level of 2435.6m.a.s.l. on 01st June 2010. NDMA records that the lake depth rises 4 m further from 29th May 2010 to 02nd July 2010, afterwards lake level drops.

The average pool height elevation on June 01st were determined from the SRTM 4.1 is 2,433.1 m a.s.l. while 2438.1m a.s.l. for GDEM2 and 2432.6m a.s.l. for SRTM3_1arcsec is 2438.56 m a.s.l. whereas counted grid cells corresponding to them were 172, 283, and 242 respectively.

The Lake level elevation were 2434.2 m a.s.l on that time indicating a lake depth of 112.2 m reported by NDMA with a vertical difference of +1.1 m (for SRTM4.1). -3.9 (for GDEM2), and +1.6 (for SRTM3_1arcsec).

At that lake level, the shoreline traced by the pixel-by-pixel method gave us the volume of Attabad lake to be 383.57 Mm³ (for SRTM4.1), 454.89 Mm³ (for GDEM2) and 439.56 Mm³ (for SRTM3_1arcsec) which we consider as the maximum lake volume reached.

This is relatively comparable to the first-order DEM contour interpolation calculation of 461.35 Mm³, 497.07 Mm³, and 460.84 Mm³ for the maximum volume of the lake at 2,434 m a.s.l.

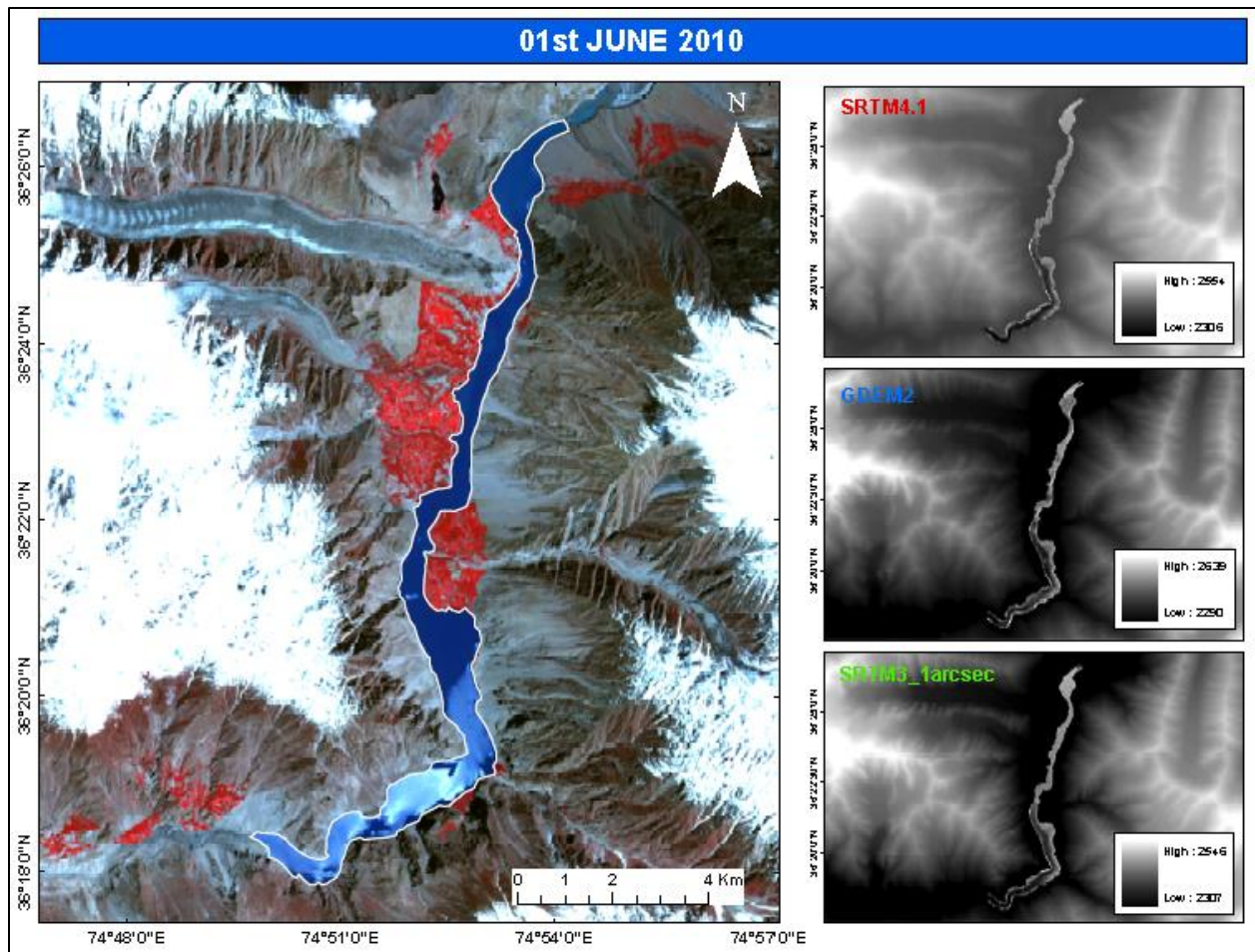


Figure 4.6: ASTER image taken on 01st June 2010 two days after overtopping of Attabad Lake; shoreline displayed in white presenting larger extend of it. NDMA recorded the Lake depth of 112.2 m on that date.

07th July 2010: With the aid of EO-1 ALI satellite, the Attabad Lake was imaged on 07th July 2010 (182 days of impoundment), when overtopping had been stabilized.

The NDMA indicated in their reports that the Lake Level had increased above the overtopping level of 2434m.a.s.l. to a level of 2,438.6 m a.s.l. on 06th July 2010.

NDMA informed that the lake depth increased ~ 4.5 m more from 29th May 2010 to 06th July 2010, at that time the lake level became stabilized.

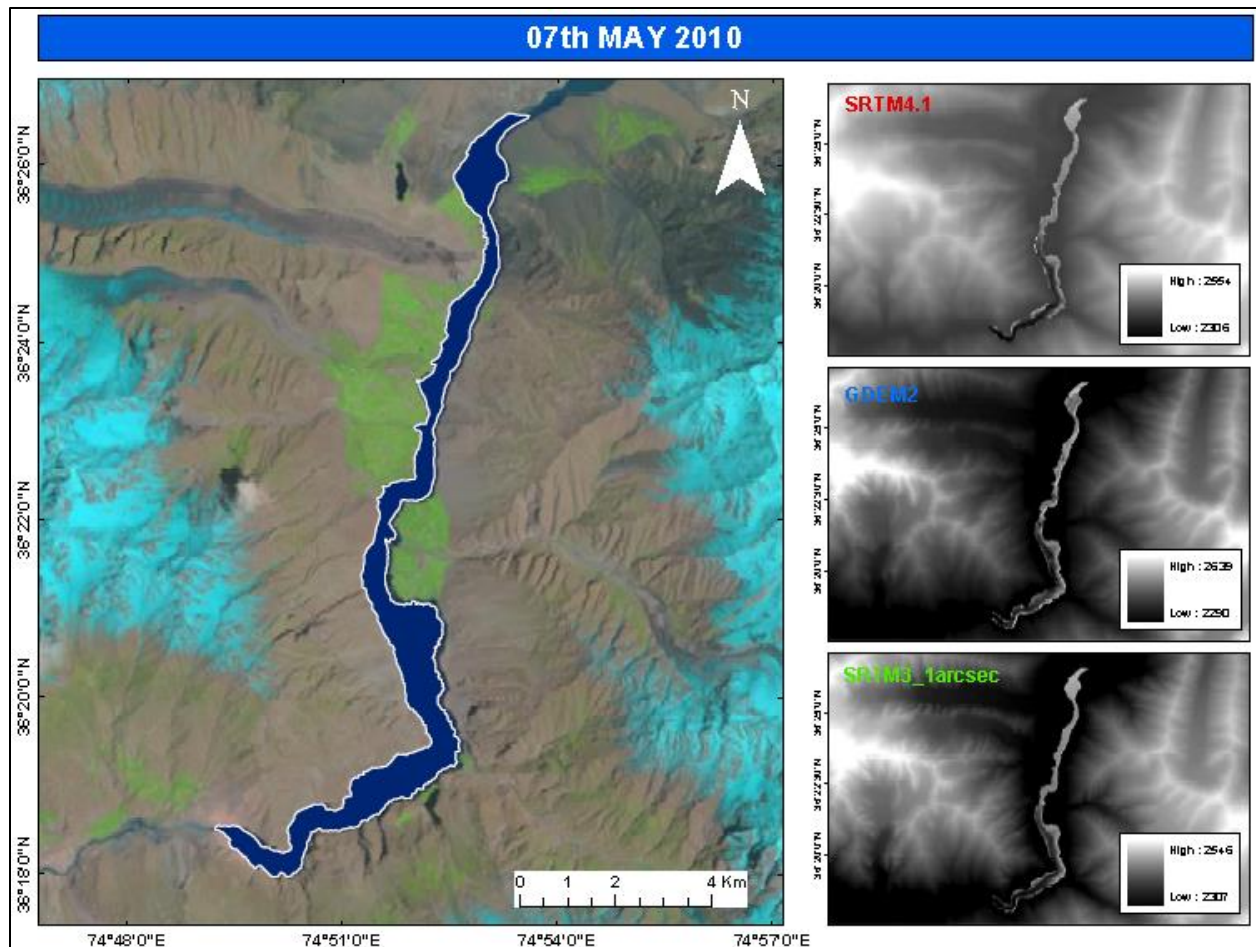


Figure 4.7: EO-1 ALI satellite image of Attabad Lake was captured on 07th July 2010 (182 days of impoundment), one day before on 06th July 2010. the lake level had been stabilized and at that time NDMA showed the lake depth of ~ 116.7 m in their report.

On 7th July 2010, the estimated average Lake elevation from pixel by pixel method were 2,433.1 m a.s.l. (for SRTM4.1) while 2439.6 m a.s.l. for GDEM2 and 2437.17 m a.s.l. for SRTM3_1arcsec is 2438.8 m a.s.l. whereas counted grid cells associated with them were 218, 372, and 296 respectively. The Lake level elevation on 6th July 2010 was ~2438.6 m a.s.l (a day prior to 7th July), signifying a lake depth of ~ 116.7 m - located on NDMA Lake depth graphs - with a perpendicular inconsistency of +1.0 m (for SRTM4.1). -1.43 (for GDEM2), and +0.2 (for SRTM3_1arcsec). The shoreline traced by the pixel-by-pixel method at that pool level give us the volume of Attabad lake to be 421.32 Mm³ (for SRTM4.1), 488.91 Mm³ (for GDEM2) and 460.84 Mm³ (for SRTM3_1arcsec) that regarded as the greatest Lake Volume – but there are no more evidences of ~ 2438.8 m lake depth except from NDMA observed graphs.

This is comparative to the first-order DEM contour interpolation approximations of 461.35 Mm³, 497.07 Mm³, and 460.84 Mm³ at that sequence (in below table) for the maximum volume of the lake at 2,438.6 m a.s.l.

After 30th July 2010, the NDMA did not give any more information about Attabad lake depth. Above stated pixel-by-pixel methodology, however, provided adequate results in approximating the lake levels from a combination of satellite imagery and digital terrain data.

Estimated average pool elevations vary from pool elevations measured from the NDMA field surveyed lake depth data (considering a datum of 2322ma.s.l.) in a range from -2.85m to +3.00m (for SRTM-3), -3.9m to +6.5m (for GDEM2) and -2.35m to +3.5m (SRTM3-1arcseconds).

Within RMSE specifications of DEMs, the average elevation data varies from ± 0.6 to ± 3.00 (for SRTM4.1), ± 0.0 to ± 6.5 (for GDEM2) and ± 1.00 to ± 3.5 (for STRM3-1arcseconds).

International Sedimentation Research Institute of Pakistan, Pakistan Water and Power Development Authority (ISRIP-WAPDA) reported that the Attabad lake reached to an elevation of 2434.57m.a.s.l on 31st July 2011.

During the draining of Attabad Lake, unluckily no more field data was determined. In the course of post-overtopping, we made an attempt to derive the lake elevations when fractional draining occurred by taking into account the pixel-by-pixel methodology and applied it onto satellite images: EO-1 ALI imagery of 03rd Aug 2011, Google earth imagery of 08th Nov 2012, Landsat8 imageries of 02nd May 2013, 25th Aug.2014 and 08th May 2015.

The EO-1 ALI satellite imaged the Attabad Lake (Fig. 4.8) on 04th Aug 2011 within 4 days of the survey accomplished by ISRIP-WAPDA. The Attabad lake geometrics (depth, surface area, and volume) after a year of controlled overtopping in association with digging and supplementary eroding of the engineered spillway- had somewhat decreased from its supreme extend attained in July 2010.

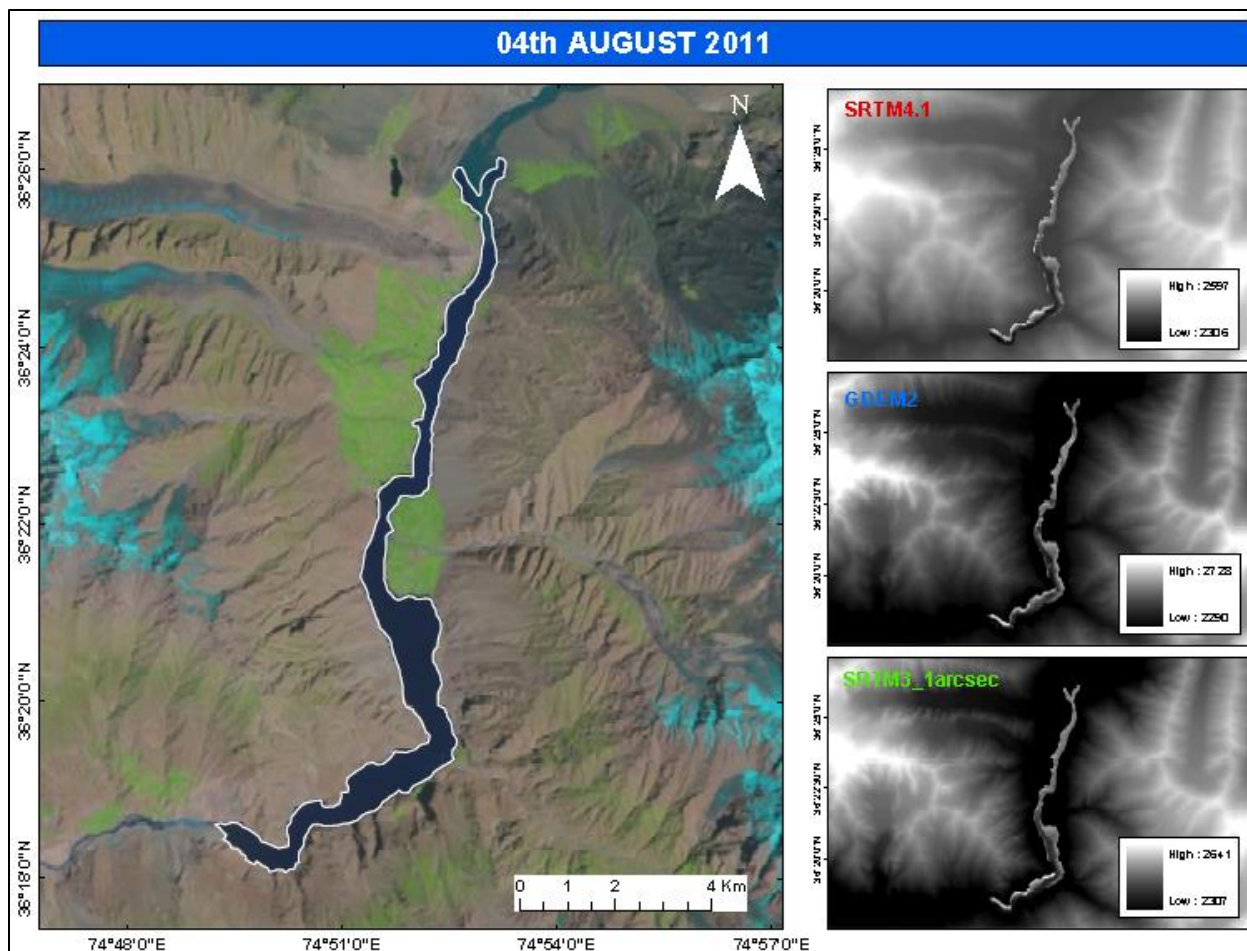


Figure 4.8: Post-overtopping image of Attabad Lake was taken on 04th August 2011 by EO-1 ALI satellite. Lake portion highlighted in white. A significantly decreased in volume was observed at that time as obvious from figure. ISRIP-WAPDA measured the lake level elevation on 31st July 2011 by considering the datum to be 2,322 m a.s.l.

The average Lake height observed from the DEMs on 04th August 2011 was 2,433.8 m a.s.l. (for SRTM4.1), 2,429.3 m a.s.l. (for GDEM2), and 2,435.8 m a.s.l. (for SRTM3_1arcsec), calculated from 158, 185, and 165 grid cells of them respectively. In that order, the volume of Attabad Lake at this altitude estimated by the pixel by pixel method was 399.46 Mm³ (428.57 Mm³), 455.00 Mm³ (469.93 Mm³), 431.61 Mm³ (441.10 Mm³), the volumes enclosed in bracket derived from contour interpolation technique. The Attabad lake successively dropped in volume to ~ 35 Mm³ from the peak volume consequent to overtopping in early July 2010 as seen above.

Just about 4 days before the EO-1 ALI imagery at 31st July 2011, NESPAK tasked the International Sedimentation Research Institute of Pakistan, Pakistan Water and Power

Development Authority (ISRIP-WAPDA) for getting done the field bathymetric estimations of Attabad Lake. They noticed the lake level elevation at that time was 2,434.6 m a.s.l (Gauri, 2015). Hence a difference of only +0.8 m (for SRTM4.1), -5.3 m, +1.2 m (SRTM3_1arcsec) was seen from observed level.

08th November 2012: It is the Google Earth Imagery, and Attabad Lake was digitized by the help of Google earth tools and then this .kml layer was converted into ESRI (.shp) shape file so that volume calculations of Lake at that time was made possible with the help of 3D Analyst tool of Volume and Area in Arc map.

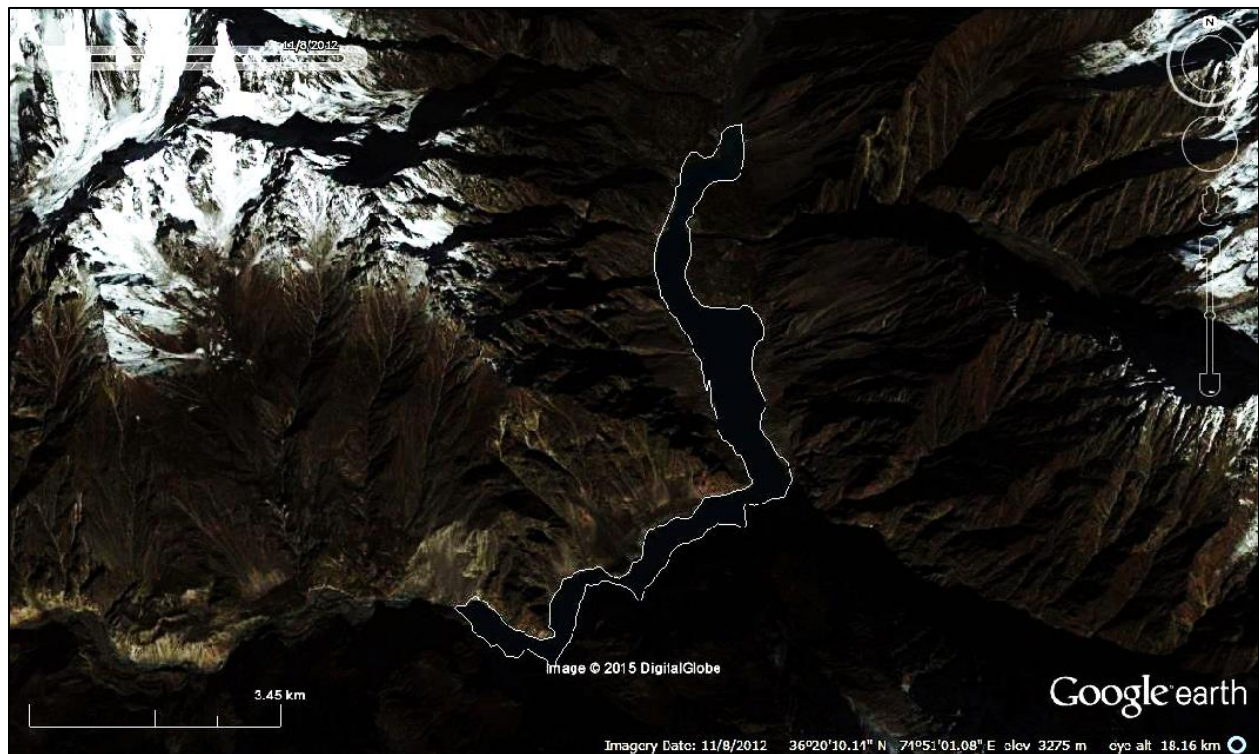


Figure 4.9: Digitized shoreline represented in white is overlaid on Google earth imagery. During the course of 2012, no other satellite imagery of Attabad was available. Attabad Lake edge elevation determined at the given date was 08th November 2012. Darkness in figure indicates the long shadows of winter.

The average pool height at that date measured from SRTM4.1, GDEM2, and SRTM3_1arcsec were 2413.5 m a.s.l., 2408.5 m a.s.l., and 2412.5 m a.s.l. in that order and the counted number of pixels were 143 (for SRTM4.1), 192 (GDEM2), and 182 (for SRTM3_1arcsec). The respective

volumes for them on particular described elevation were 159.54 Mm³ (268.60 Mm³), 230.03 Mm³ (287.58 Mm³), and 148.52 Mm³ (162.57 Mm³). All volumes in the brackets were the outcome of contour interpolation method.

02nd May 2013: LANDSAT8 satellite captured this image of Attabad Lake on 18th May 2013 when the excavation and additional erosion resulted in the high rate of discharge over the spillway. A significant decrease in lake surface area and lake volume was observed from its peak in July 2010.

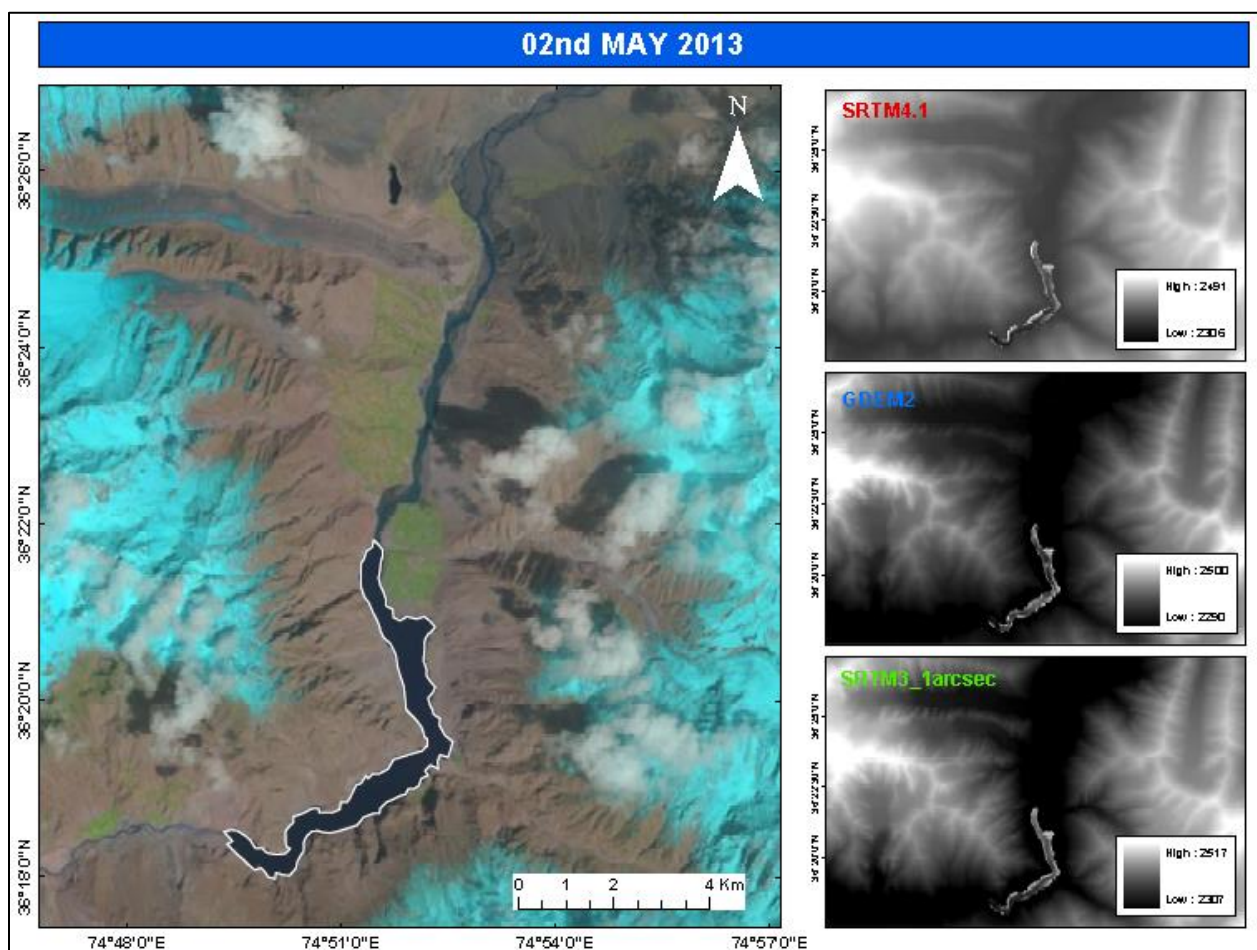


Figure 4.10: LANDSAT8 image of Attabad Lake taken on 02nd May 2013, displaying the delineated lake boundary in white. The lake edge elevation picked from Google earth was 2403 m a.s.l.

Elevation data employed in this study estimated the average pool height on 02nd May 2013 as 2,405.5 m a.s.l. for SRTM4.1, 2,405 m a.s.l. for GDEM2, and 2404.5 m a.s.l. and the counted

grid cells against them are 137, 185, and 180 sequentially. At this lake level in figure 4.10, the Attabad Lake volume approximated by the pixel-by-pixel method for SRTM4.1, GDEM2 and SRTM3_1arcsec are 159.54 Mm³ (195.38 Mm³), 198.05 Mm³ (208.41 Mm³), and 186.33 Mm³ (200.36 Mm³). Thus, from all pixel based calculations it can clearly see that the volume of impoundment successfully decreases to ~ 273.78 Mm³ (~65%) from its peak volume subsequent to overflowing in 2010.

23rd April 2014: This is the second last image that embedded in this research for the sake of being seen the Lake extent during this course of year, and compare it to the next year (2015) extend.

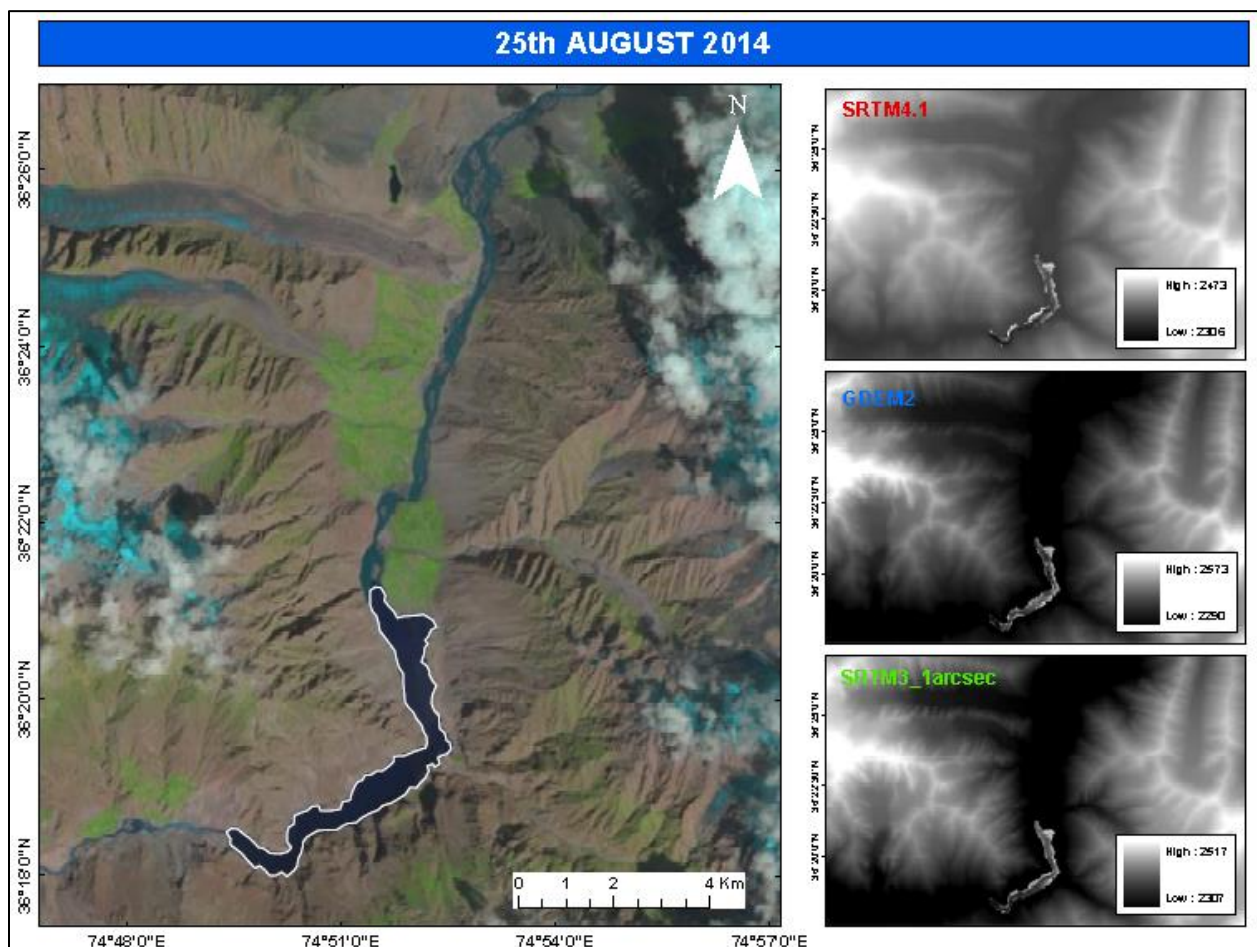


Figure 4.11: LANDSAT8 image of Attabad Lake acquired on 23rd April 2014, showing the delimited shoreline in white. Google earth displayed Lake edge elevation 2399 m a.s.l.

By following the pixel by pixel methodology, the mean pool height measured from the SRTM4.1, GDEM2 and SRTM3_1arcsec were 2400 m a.s.l., 2400.5 m a.s.l., and 2398.0 m a.s.l. in that order and in turn calculated number of pixels against them were 114, 193, and 170. The determined lake volume from pixel by pixel method at that Lake level were 134.70 Mm³ (\pm 169.97 Mm³) from SRTM4.1, 170.55 Mm³ (179.09 Mm³) from GDEM2, and 148.52 Mm³ (162.27 Mm³) while volumes surrounded by brackets are extracted from contour interpolated technique. With the help of these three elevation models we can able to judge that overall Attabad Lake volume reduces to \sim 286.62 Mm³ from the all-out overtopping volume (\sim 68%). This 68% gives us the indication remnant debris dam because this reduction is basically the greatest drop of volume as consequence of mitigation work as well as continuous erosion.

08th May 2015: The ultimately final and the latest LANDSAT8 OLI satellite imagery taken on 08th May 2015 and are applied to this study.

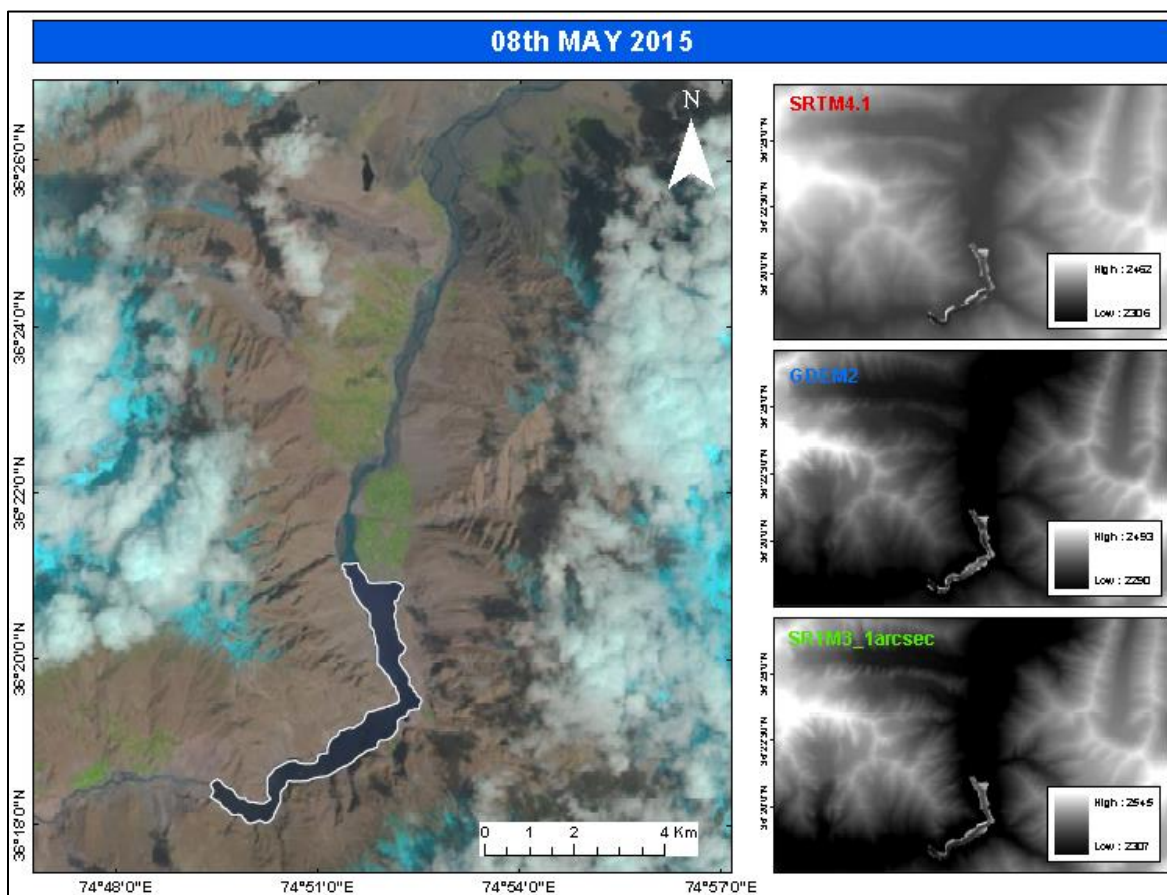


Figure 4.12: The most recent image of Attabad Lake is taken on 08th May 2015 by Landsat8 OLI satellite, depicting the delimited Lake boundary in white; also reduction in Lake Area is clearly visible.

In recent times, the mean pool elevation of Attabad Lake are attained by adopting the pixel based methodology that yields 2394 m a.s.l. for SRTM4.1, 2397 m a.s.l. for GDEM2, and 2393.5 m a.s.l. for SRTM3_1arcsec and their associated counted grid cells are 129, 181, and 175 respectively and in turn their resulted volumes at particular elevation are 114.65 Mm³ (156.41 Mm³), 158.75 Mm³ (167.33 Mm³), and 148.52 Mm³ (162.27 Mm³). Volumes inside brackets representing the Contour interpolated volumes.

Hence, by analyzing all DEMs and use of pixel by pixel method enables us to infer that the Attabad Lake Volume lower down to ~ 306.67 Mm³ from its maximum volume following to overtopping in early July 2010 so, ~72% reduction exhibit Attabad Lake currently. A considerable shrinkage of Attabad Lake is evidently described this figure 4.12, which gives us indication that Attabad Lake is no longer lake but a debris dam.

4.6 Comparison of DEM Based Analysis and Pixel-by-Pixel Approach

The digitized shoreline pixel based statistical methodology yields the lake volumes that are lesser than those volumes that are calculated by the first-order contour interpolation of DEMs (SRTM4.1, GDEM2, and SRTM3_1arcsec) for a specified Lake surface elevation (figures above). This may be caused by the fact that the actual shoreline is more precisely demarcated in this pixel-by-pixel approach which results in a smaller area relative to the lake area generated from the interpolated heights of SRTM4.1, GDEM2, and SRTM3_1arcsec DEM into contour data for a certain shoreline.

Therefore, in the presence of an extremely high-resolution temporal satellite image collection, along with perfectly observed field measurements of lake depth or absolute lake level elevation, the pixel-by-pixel technique are proved to be satisfactory in order to attain very accurate estimations of areas and volumes of impoundment.

For the range of Lake surface elevations included here, the first-order contour interpolated values of all DEMs (SRTM4.1, GDEM2, and SRTM3_1arcsec) give the impression of overestimation of the areas and the volumes of Attabad Lake as indicated in figures and tables below.

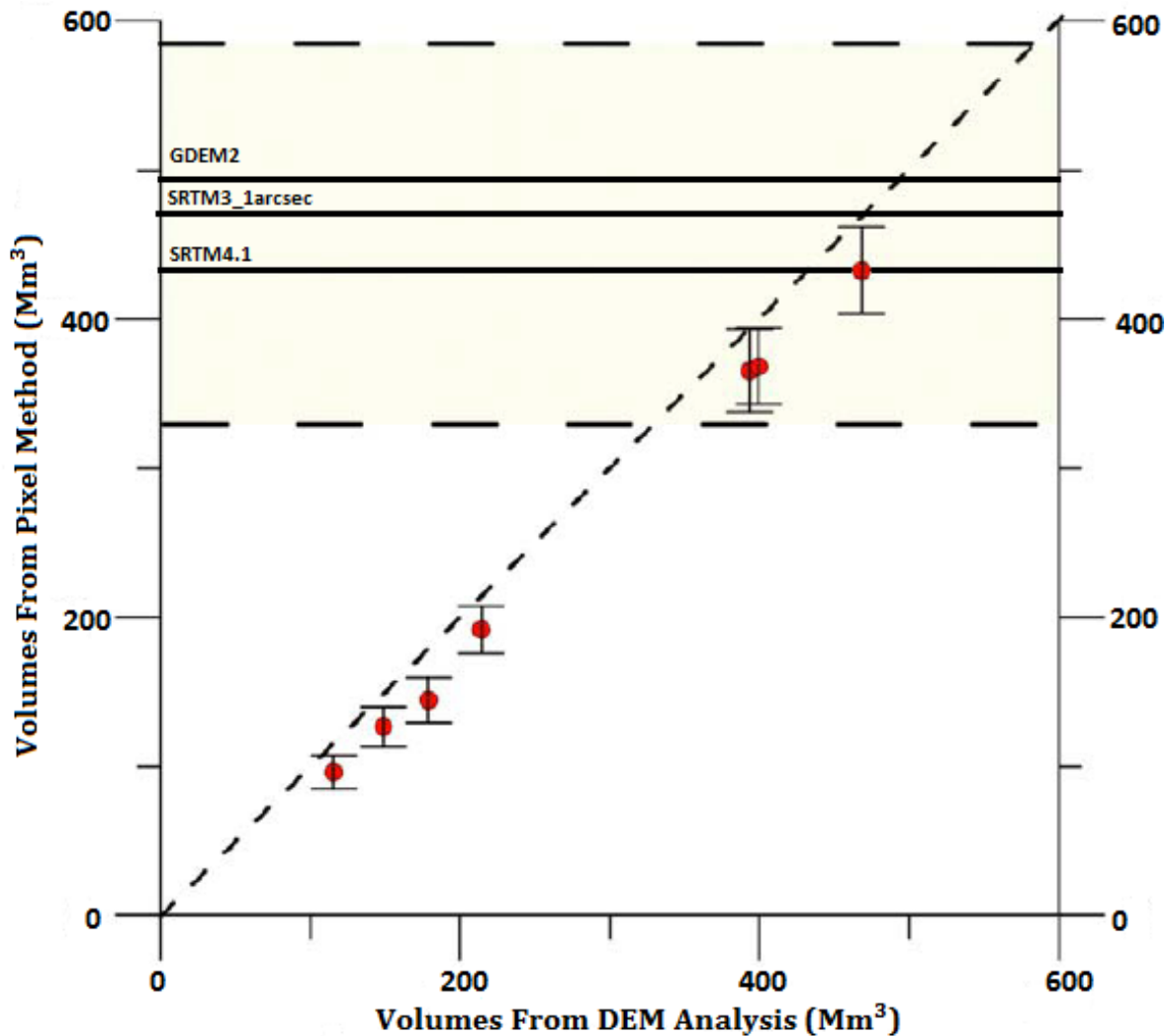


Figure 4.13: Plots showing the comparison between volumes of landslide-dammed Lake Attabad approximated by contour interpolation method for nine shorelines and the Lake Volumes calculated by the pixel-by-pixel approach for the same shorelines. It is observed that pixel by pixel method gives lower values of volumes relative to contour interpolated approach that overestimates volumes. Horizontal dashed line with fill represents a series of values of the greatest volume of Attabad Lake stated in the literature (refer text below) while the horizontal solid line showing the Volumes of Attabad Lake that are calculated by utilizing pixel based approach.

We examined the original volume (461.35 Mm³ for SRTM4.1, 497.07 Mm³ for GDEM2, and 470.91 Mm³ for SRTM3_1arcsec) estimations from the first-order contour interpolation of DEMs (Table 4.4) that lies within the specific errors of the volume evaluated from the pixel-by-pixel analysis (table 4.4; (421.32 Mm³ for SRTM4.1, 488.91 Mm³ for GDEM2, and 460.84 Mm³

for SRTM3_1arcsec) and corresponding difference ($\pm 40.03 \text{ Mm}^3$, $\pm 8.16 \text{ Mm}^3$, $\pm 10.07 \text{ Mm}^3$) for the highest pool elevation achieved by Attabad Lake.

This value is comparable to the estimations determined by (Iqbal, Shah, Chaudhary, & Baig, 2014) : 408 Mm^3 ; (NESPAK, May 2014.) : 329 Mm^3 ; (Butt, Umar, & Qamar, 2013) : 334 Mm^3 ; (Schneider, Huggel, Cochachin, Guillén, & Garcia, 2014) : 450 Mm^3 ; (Petley D. , 2011) : 450-500 Mm^3 ; (Kargel, Leonard, Crippen, Delaney, Evans, & Schneider, 2010) : 585-450 Mm^3 .

All the volumetric calculations that based on Pixel by Pixel methodology are given in tabular form below:

Table 4.4: Contrast between shoreline elevation data determined from NDMA Depths (Observed Data) or by Pixel Method and comparison of their associated volumes derived from Pixel by Pixel method or Contour Interpolation of DEMs (SRTM4.1, GDEM2 and SRTM3_1arcsec)

a) Calculations For SRTM4.1

Date of Imagery	Satellite Platforms	Elevations Derived from NDMA Data (m.a.s.l.)	Pixel Method Elevations (m.a.s.l.)	SRTM4.1 Volumes (Mm^3)	Pixel Method Volumes (Mm^3)
16 th Mar.2010	EO-1	2389.3 (67.3)	2392.1 ± 2.85	128.30	82.78 ± 45.45
02 nd May 2010	ASTER	2410.4 (~88.4)	2408.7 ± 1.7	243.37	187.27 ± 56.1
25 th May 2010	ASTER	2430.4 (108.4)	2430.7 ± 0.3	413.12	352.04 ± 61.08
01 st June 2010	ASTER	2434.2 (112.2)	2433.1 ± 1.1	461.35	383.57 ± 77.78
02 nd July 2010	EO-1	2438.3 (~116.3)	2439.6 ± 1.3	497.84	417.81 ± 80.03
07 th July 2010	EO-1	2438.6 (~116.7)	2439.6 ± 1.0	500.22	420.18 ± 80.04
04 th Aug. 2011	EO-1	2434.6 (WAPDA)	2433.8 ± 0.8	428.57	399.46 ± 29.11
08 th Nov.2012	Google Earth	2415 (Observed)	2413.5 ± 1.5	268.60	159.54 ± 109.06
02 nd May 2013	LANDSAT 8	2403 (Observed)	2405.5 ± 2.5	195.38	147.54 ± 47.84
25 th Aug.2014	LANDSAT 8	2399(Observed)	2400 ± 1.00	169.97	134.70 ± 35.27
08 th May 2015	LANDSAT 8	2397(Observed)	2394 ± 3.00	156.41	114.65 ± 41.76

b) Calculations For GDEM2

Date of Imagery	Satellite Platforms	Elevations Derived from NDMA Data (m.a.s.l.)	Pixel Method Elevations (m.a.s.l.)	GDEM2 Volumes (Mm ³)	Pixel Method Volumes (Mm ³)
16 th Mar.2010	EO-1	2389.3 (67.3)	2389.15 ± 0.15	143.60	124.33 ± 19.12
02 nd May 2010	ASTER	2410.4 (*88.4)	2415.2 ± 4.8	267.57	240.28 ± 27.29
25 th May 2010	ASTER	2430.4 (108.4)	2433.7 ± 3.3	450.70	420.70 ± 30.00
01 st June 2010	ASTER	2434.2 (112.2)	2438.1 ± 3.9	497.07	454.89 ± 42.18
02 nd July 2010	EO-1	2438.3 (~116.3)	2436.6 ± 1.7	542.86	492.55 ± 50.31
07 th July 2010	EO-1	2438.6 (~116.7)	2437.17 ± 1.43	549.55	495.33 ± 54.22
04 th Aug. 2011	EO-1	2434.6 (WAPDA)	2429.3 ± 5.3	469.93	455.00 ± 14.93
08 th Nov.2012	Google Earth	2415 (Observed)	2408.5 ± 6.5	287.58	230.03 ± 57.55
02 nd May 2013	LANDSAT 8	2403 (Observed)	2405 ± 2.00	208.41	198.05 ± 10.36
25 th Aug.2014	LANDSAT 8	2399 (Observed)	2400.5 ± 1.5	179.09	170.55 ± 8.5
08 th May 2015	LANDSAT 8	2397 (Observed)	2397 ± 0.0	167.33	158.75 ± 8.58

c) Calculations for SRTM3 1arcsec

Date of Imagery	Satellite Platforms	Elevations Derived from NDMA Data (m.a.s.l.)	Pixel Method Elevations (m.a.s.l.)	SRTM3 Volumes (Mm ³)	Pixel Method Volumes (Mm ³)
16 th Mar.2010	EO-1	2389.3 (67.3)	2391.6 ± 2.35	134.10	117.43 ± 16.67
02 nd May 2010	ASTER	2410.4 (*88.4)	2408.2 ± 2.2	251.22	229.81 ± 21.41
25 th May 2010	ASTER	2430.4 (108.4)	2430.7 ± 0.3	421.98	402.12 ± 19.86
01 st June 2010	ASTER	2434.2 (112.2)	2432.6 ± 1.6	470.91	439.56 ± 31.35
02 nd July 2010	EO-1	2438.3 (~116.3)	2438.15 ± 0.15	515.33	479.99 ± 35.34
07 th July 2010	EO-1	2438.6 (~116.7)	2438.8 ± 0.2	520.93	482.94 ± 37.99
04 th Aug. 2011	EO-1	2434.6 (WAPDA)	2435.8 ± 1.2	441.10	431.61 ± 9.49
08 th Nov.2012	Google Earth	2415 (Observed)	2412.5 ± 2.5	273.72	200.29 ± 73.43
02 nd May 2013	LANDSAT 8	2403 (Observed)	2404.5 ± 1.5	200.36	186.33 ± 14.3
25 th Aug.2014	LANDSAT 8	2399 (Observed)	2398 ± 1.00	173.35	162.73 ± 10.62
08 th May 2015	LANDSAT 8	2397 (Observed)	2393.5 ± 3.5	162.27	148.52 ± 13.75

5 RESULTS

5.1 Volume-Area and Volume-Elevation Relationship of Attabad Lake

We computed Volume-Area and Volume-Elevation relationships via ArcGIS® 3D Analyst > Surface Analyst > Area Volume Statistics Tool. By adding the lake depths provided by NDMA we determined the Lake elevation and then calculated their respective volume, and surface areas. Finally polynomials are fitted to Volume-Area and Volume-Elevation relationships which can be used further in the lake level simulation model.

We began the calculation from the lowest point 2322m height of plane and calculate statistics corresponding to it.

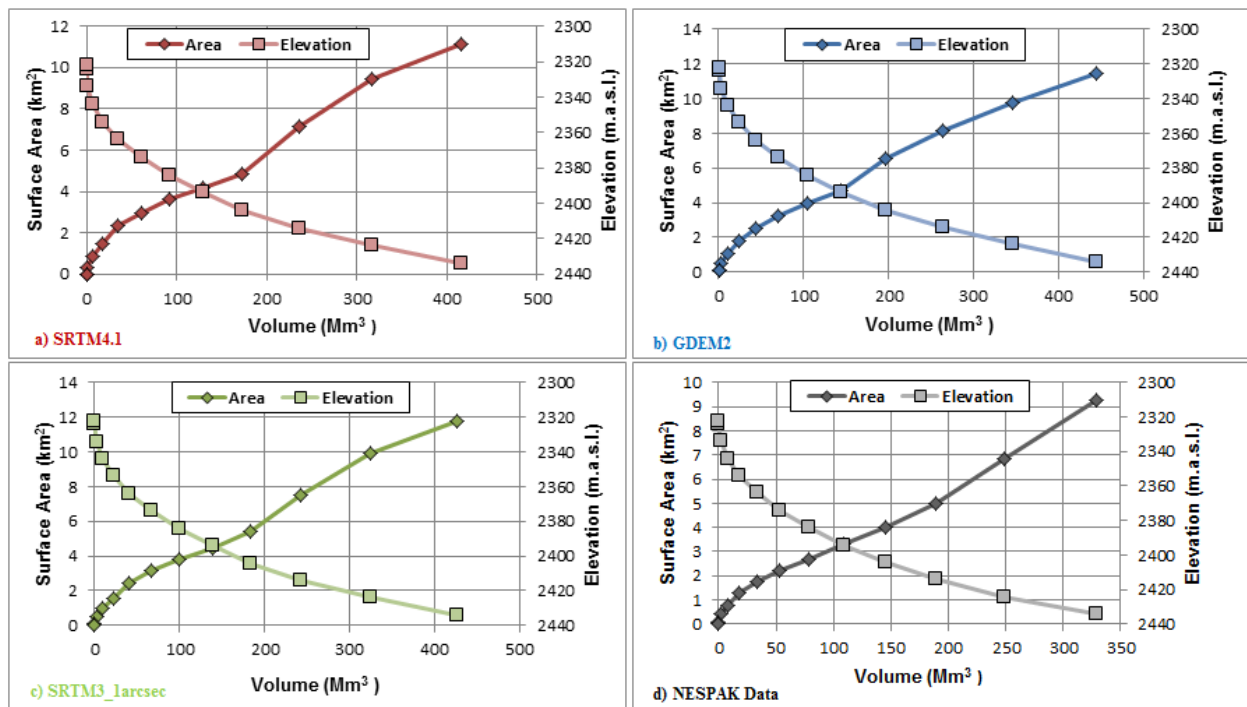


Figure 5.1: Scatter plot demonstrating the relationship between Volume-Area (indicated by diamond box) and Volume-Elevation (depicted by square box) of Attabad Lake determined from the geometric calculations of a) SRTM4.1, b) GDEM2, c) SRTM3_1arcsec and d) NESPAK Field Survey Data that correspondingly represented by red, blue, green and black color.

We computed the area and volume between the reference plane (perform calculations above or below this plane) and the surface, and also determined the projected area (2D) and surface area (3D) for the portion of the surface below the given base height (lake level). The volume denotes the million cubic areas between the plane and the top of the surface (**Wale, 2010**).

Scatter plots described above are more or less similar in shape for all dataset which reflect that all elevation data are more or less give the good estimation of volumes. The significance of their relationships is determined by using the following validation approaches.

5.2 Results of Accuracy Assessments

The accuracy assessment of our results is made possible by using the following approaches:

- ▶ Trend line Analysis
- ▶ Percentage Difference (PD)
- ▶ Standard Error (S)

For an accuracy measurement, the values achieved by two approaches would be in perfect agreement when R^2 equal to 1 and stand error close to zero.

5.2.1 Trend Line Analysis

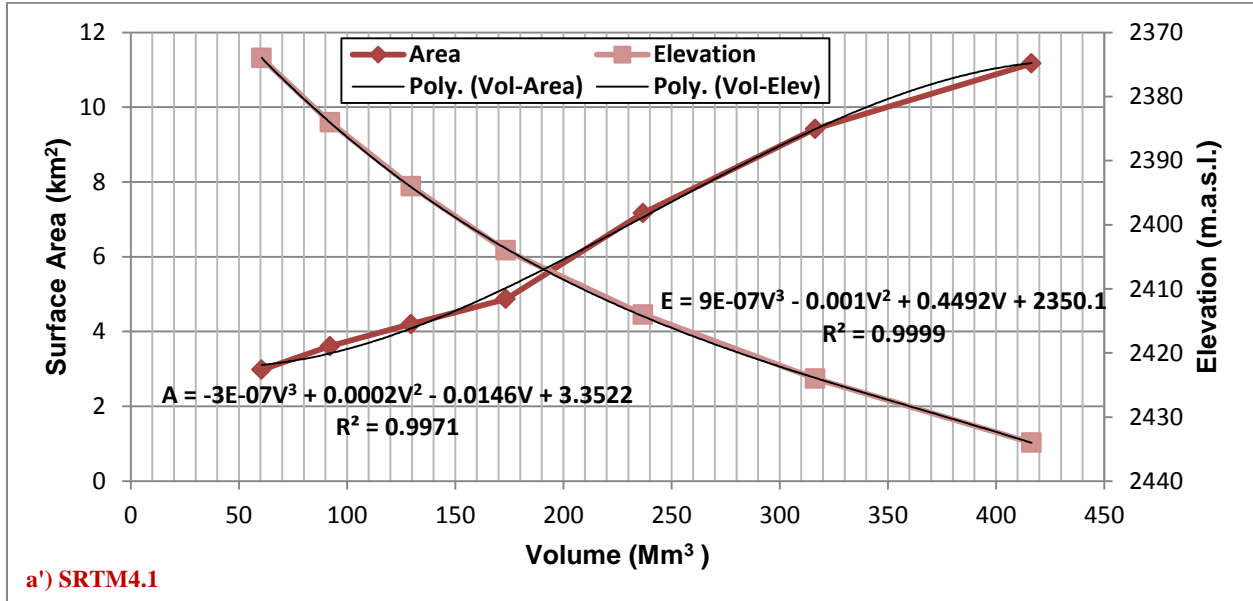
Polynomial is fitted to the data by using the excel trend line function.

We determine the equation of the polynomial trend line which is visually used to represent the trend in the data. These equations can be seen on the scatter charts presented above for all datasets. The R-squared (R^2) correlation coefficient in this equation depicts how well this equation fits the data or estimate the fit. As the R^2 approaches to 1.00 it means the trend line is better fitted to the data (**P.Lutus, 2013**). This is also computed and showed on the graph.

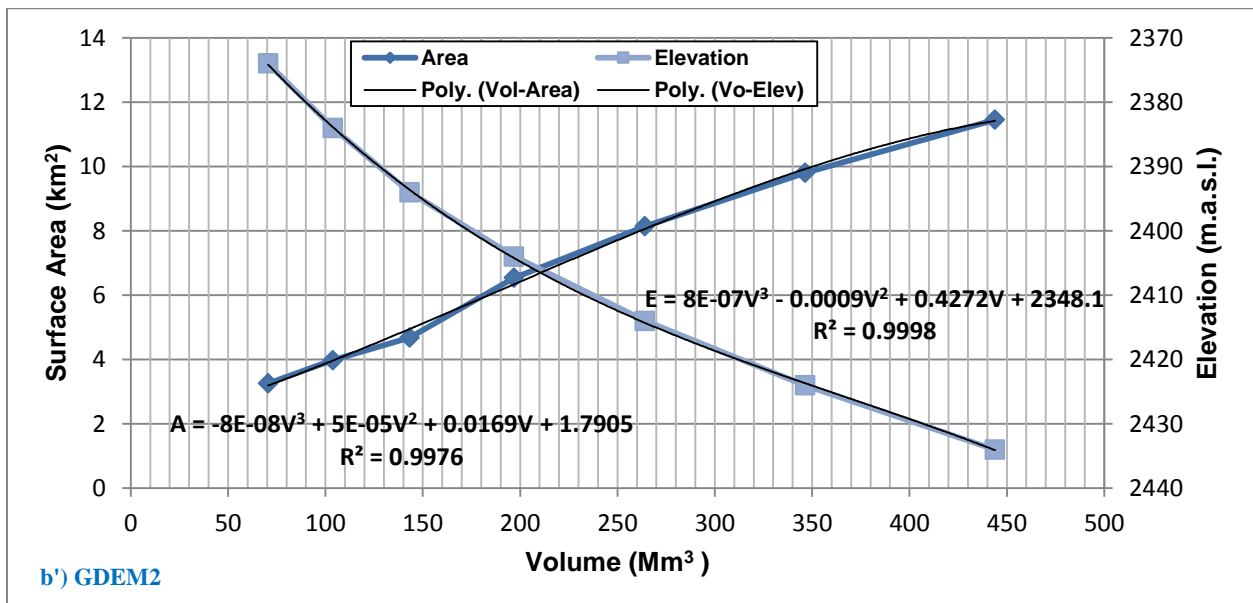
The two polynomial equations are displayed on the chart. One of them expresses the relationship between Volume (V) and Elevation (E) and the other one describes the correlation between Volume (V) and Area (A) of Attabad Lake. These trend lines can be regarded as a satisfactory approximation of the true results. For our datasets, we have measurements of volume, area and

elevations that are attained through the calculations made in ArcGIS 10.1 with 3D Analyst extension while the NESPAK readings are collected from the field survey data.

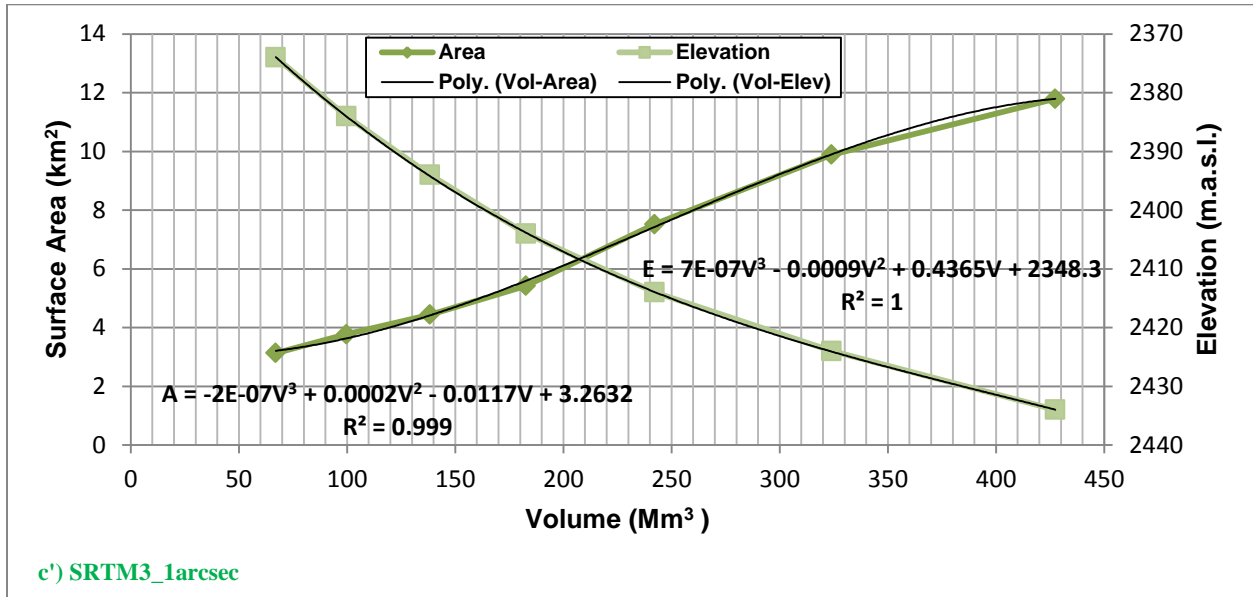
a) SRTM4.1 based results fitted with Polynomial Trend Line



b) GDEM2 based results fitted with Polynomial Trend Line



c) SRTM3-1arcsec based results fitted with Polynomial Trend Line



d) SRTM3-1arcsec based results fitted with Polynomial Trend Line

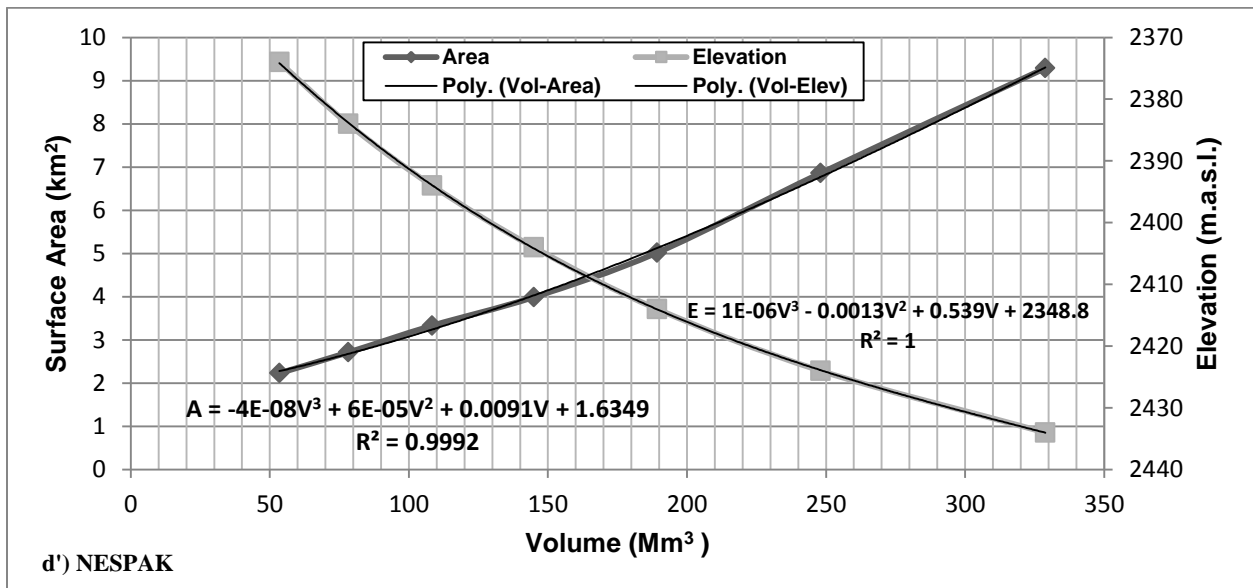


Figure 5.2: Polynomials of order 3 are fitted to the data by utilizing Excel's TRENDLINE function while the R-squared (R^2) value on chart visually displaying the trend in the data.

The following polynomial equations are acquired from above trend line analysis which indicate that SRTM3_1arcsec is highly correlated to the NESPAK data yielding $R^2 = 1$ (against Volume (V) to Elevation (E)) and $R^2 = 0.999$ for volume to area.

$A = -4E-08V^3 + 6E-05V^2 + 0.0091V + 1.6349$	$R^2 = 0.9992$ NESPAK Data
$A = -2E-07V^3 + 0.0002V^2 - 0.0117V + 3.2632$	$R^2 = 0.999$ SRTM3_1arcsec
$E = 1E-06V^3 - 0.0013V^2 + 0.539V + 2348.8$	$R^2 = 1$ NESPAK Data
$E = 7E-07V^3 - 0.0009V^2 + 0.4365V + 2348.3$	$R^2 = 1$ SRTM3_1arcsec

Results also reveal that the polynomial fitted equations for SRTM4.1 and GDEM2 does not give $R^2 = 1$ exactly but provided r-squared value very much closer to 1. SRTM4.1 is much nearer to 0.9999 in value of R-squared as compared to GDEM2 which has $R^2=0.9998$.

5.2.1.1 Using the R-squared coefficient calculation to estimate fit

After noting the R-squared value on the scatter plot, it is inferred that for NESPAK data it is much closer to 1.0 and the polynomial trend line seems to be well fitted as compared to other datasets. That is, the closer line moves across all the points. This is one of the reasons of using this data as reference for being compared our DEM based results. NESPAK reference data which best describes the polynomial fitted curve and the R-squared value due to the fact that it is the field observed data actually so that it gives

For this purpose let's glance at scatter plots. We noted that the equation for the polynomial trend line is different for different sets of data and R-squared value confirms this. SRTM3_1arcsec trend line is better fitted among all topographic datasets and indicating the 'true' relationship between Volume (V) and Lake Elevation as well as between Volume and area and its regression line closely passes through all data points as is the case of NESPAK data. It is 1 (for Vol. to Elev.) and 0.999 (for Vol. to Area) in figure compared to 1 and 0.9992 in figures with NESPAK data; exactly correlated with the NESPAK data. Though we would need to take in to account information such as the number of data points collected to make an accurate statistical prediction as to how well the polynomial curve represents the true relationship, we can generally say that

SRTM3_1arcsec represents a better representation of the relationship of volume-area or volume - elevation than SRTM4.1 and GDEM2 (Wallace, 2010), because SRTM3_1arcsec uses Radar technique and it is acquired without using any averaging or resampled method.

5.2.2 Percentage Difference (PD): A Method of Accuracy Assessment

Percentage Difference is another assessment method that is applied to our results in order to judge that how much percentage difference exist in volume calculations obtained from different DEMs i.e. SRTM4.1, GDEM2, and SRTM3_1arcsec. The less percentage difference indicates the better correlation between two values and if the %age difference becomes bigger it would yield less correlation between volumetric values of topographic datasets.

The Percentage Difference (PD) is calculated (James, 2015) as follows:

$$\text{Percentage Difference in Volumes} = \left| \frac{\text{First Value} - \text{Second Value}}{(\text{First Value} + \text{Second Value})/2} \right| \times 100\%$$

Table 5.1: Percentage Difference among three datasets (SRTM4.1, GDEM2, and SSRTM3_1arcsec) reveals how much difference exists in their volumes.

IMAGERY DATE	PERCENTAGE DIFFERENCE IN VOLUMES (PD)		
	$PD_{srtm4.1-gdem2}$	$PD_{gdem2-srtm3_1arcsec}$	$PD_{srtm4.1-srtm3_1arcsec}$
16 th Mar.2010	40.12%	5.70%	34.60%
02 nd May 2010	24.79%	4.45%	20.39%
25 th May 2010	17.77%	4.51%	13.28%
01 st June 2010	17.01%	3.42%	13.60%
02 nd July 2010	16.41%	2.58%	13.85%
07 th July 2010	16.41%	2.53%	13.89%
04 th Aug. 2011	13.00%	5.00%	7.73%
08 th Nov.2012	36.18%	13.82%	22.64%
02 nd May 2013	29.23%	6.09%	23.23%
25 th Aug.2014	23.48%	4.69%	18.84%
08 th May 2015	32.26%	6.65%	25.74%

The above table reveals that percentage difference (PD) in volumes calculated from pixel by pixel method as described in earlier section between SRTM4.1 and GDEM2 is greatest while between SRTM4.1 and SRTM3_1arcsec is not as larger as previous one reveals but for SRTM3_1arcsec and GDEM2 it is quite smaller.

Table 5.2: Percentage Difference in Volumes calculated from Contour Interpolation of DEMs- from Reference data based on field survey results of NESPAK

LAKE LEVEL (m.a.s.l.)	PERCENTAGE DIFFERENCE IN VOLUMES (PD)		
	<i>PD_{srtm4.1-reference}</i>	<i>PD_{gdem2-reference}</i>	<i>PD_{srtm3_1arcsec-reference}</i>
2434	22.49%	30%	26.05%
2424	24.19%	33.09%	26.54%
2414	22.31%	33.01%	24.49%
2404	17.89%	30.41%	23.02%
2394	17.82%	27.76%	24.31%
2384	16.37%	28.20%	24.19%
2374	12.38%	27.70%	22.59%
2434	22.49%	30%	26.05%
2424	24.19%	33.09%	26.54%
2414	22.31%	33.01%	24.49%
2404	17.89%	30.41%	23.02%

The table given above clearly reveals that the volumes estimated from the contour interpolation of SRTM4.1 exhibits lower %age difference in volumes from the Reference data that based on Bathymetric field survey data of Attabad Lake.

On the other hand volumes derived from SRTM3_1arcsec are ranked as second in precision while GDEM2 depicts Highest PD from reference data.

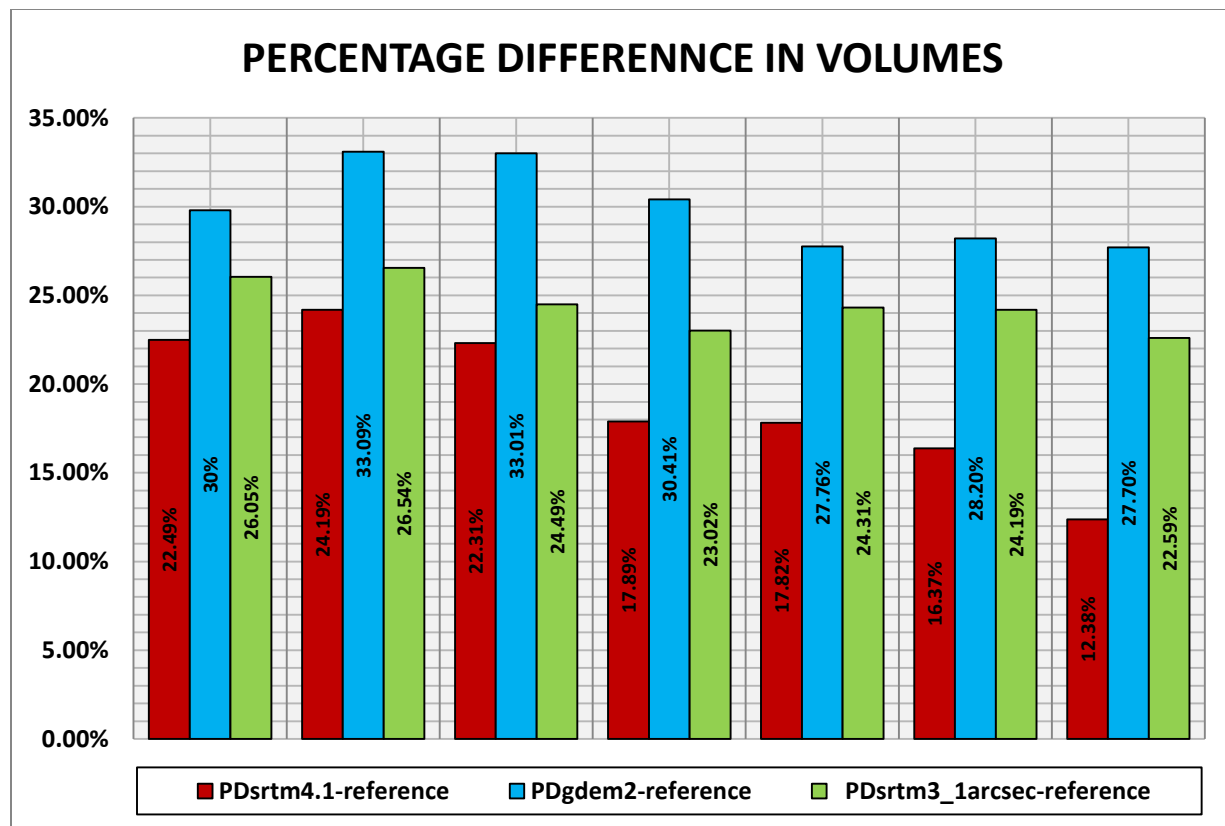


Figure 5.3: Red, green, and blue bars correspondingly representing the Percentage Difference (PD) in contour interpolated volumes of STRM4.1, GDEM2, and SRTM3_1arcsec from the reference NESPAK data based on field survey.

In comparison with NESPAK data, the percentage difference for SRTM4.1 contour interpolated volumes is small as compare to other DEMs and this difference exceeds with lake pool elevation as depicted in above graph.

5.2.3 Standard Error: A Way to Quantify Error

As R-squared determines how well a polynomial fits the data, there is also a different goodness-of-fit statistic commonly known as Standard Error (S). S delivers some more vital information that R-squared does not. Although both statistics gives an overall estimation of data fit (Frost, 2014).

S exemplifies the average distance that the observed values (volumetric values) fall from the fitted line. By using the units of the response variable (in our case volume Mm^3), it tells you how wrong the regression model is on average. Smaller values are better because it indicates that the observations are closer to the fitted line.

For all polynomial fitted plots, the standard error is shown in tabulated form below, which tells us that the average distance of the data points from the fitted line. In addition to R-squared, we use the standard error of the regression to assess the precision of the predictions made for volumes.

Table 5.3: Polynomial fitted Volume (V) to Area (A) and Volume (V) to Elevation Relationship for actual Attabad Lake levels also showing the correlation coefficient (R^2) and stand error (S) derived from SRTM4.1, GDEM2, SRTM3_1arcsec and NESPAK data

Polynomial fitted	Correlation coefficient (R^2)				Standard error (S)			
	SRTM4.1	GDEM2	SRTM3_1 arcsec	NESPAK Data	SRTM4.1	GDEM2	SRTM3_1 arcsec	NESPAK Data
Vol.-Area	0.9971	0.9976	0.999	0.9992	0.1833	0.1672	0.1139	0.0803
Vol.-Elev.	0.9999	0.9998	1	1	0.1966	0.2961	0.1309	0.154

From the observations described in table 5.3, it is evident that standard error is small 0.113 for SRTM3_1arcsec that closely match to the reference data and also tells that the average distance of the data points from the fitted line is about 1.3% (for volume –elevation).

Thus, from both assessment methods (R-squared (R^2), Standard Error), it is clear that SRTM3_1arcsec based results for volume calculations are highly correlated with field observed data providing R^2 and S to be 0.9992 and 0.1309 (for vol.-elevation) respectively, whereas the average distance of the data points from the fitted line is about 1.9% and 2.9% for SRTM4.1 and GDEM2 respectively for volume-elevation relationship.

5.3 Statistical Analysis

By observing the statistical parameters of Lake we derived the following results:

Table 5.4: Statistical Parameters for Attabad Lake derived from SRTM4.1, GDEM2, and SRTM3_1arcsec

Statistical Parameters	Count	Min.	Max.	Mean	Std. Dev.	Skewness	Kurtosis	1 st Quartile	Median	3 rd Quartile
SRTM4.1	4158	2320	2489	2429.1	30.941	-1.2907	4.4741	2417	2437	2450
GDEM2	9215	2307	2508	2430.2	41.65	-1.031	3.1255	2405	2447	2461
SRTM3_1arcsec	6883	2318	2498	2437.1	34.477	-1.5732	5.0685	2425	2449	2460

Skewness and kurtosis (**king & Julstorm, 1982**) was calculated for all datasets of Attabad Lake. Skewness represents a unitless measure of asymmetry in a distribution (**Shaw & Wheeler, 1985**). Positive Skewness shows a longer tail (highest values) to the right, while Negative Skewness shows a longer tail (lowest value) to the left. kurtosis is a unitless quantity represents the sharpness of the data peak. A quantity less than zero (0) indicate a flat Gaussian distribution, while a value greater than zero (0) indicates a peaked Gaussian distribution (**Disgus, 2015**). Our observations from all DEMs give the negative value of Kurtosis for all Attabad Lake whereas SRTM3_1arcsec is highly negatively skewed among all data sets.

The standard deviation can never be a negative number because it measures a distance (distances are never negative numbers). GDEM2 has the highest mean value thus it gives greatest value of standard deviation. As mean is affected by outliers so that of standard deviation as shown in table above. The standard deviation reveals the same units as that of source data represents.

SRTM3_1arcsec represents the highest value of median that lies in between 1st and 3rd Quartile as given in table. In fact, mean measures the central tendency of the data but do not provide any information about data distribution on either side of the median. Quartiles aid us to measure this (**Kalla, 2011**). First quartile of GDEM2 are much far away from the median as compare to

SRTM based DEMs it means that the data points that are smaller than the median are spread far apart, while the third quartile of all DEMs closer to the mean it indicates that the data points that are greater than the median are closely packed together.

The minimum (lowest value) and maximum (highest value) of DEMs gives us the more detailed picture of the Attabad Lake data. A set of five values that contains minimum, first quartile, median, third quartile and maximum are entitled as the ‘‘five number summary’’. We can display these five numbers in an effective way through a ‘‘boxplot or box and whisker graph’’ (Taylor, 2015).

5.3.1 Attribute (Contour) Analysis

Contour analysis done in Arc GIS[®] 10.1 is accompanied by following attributes:

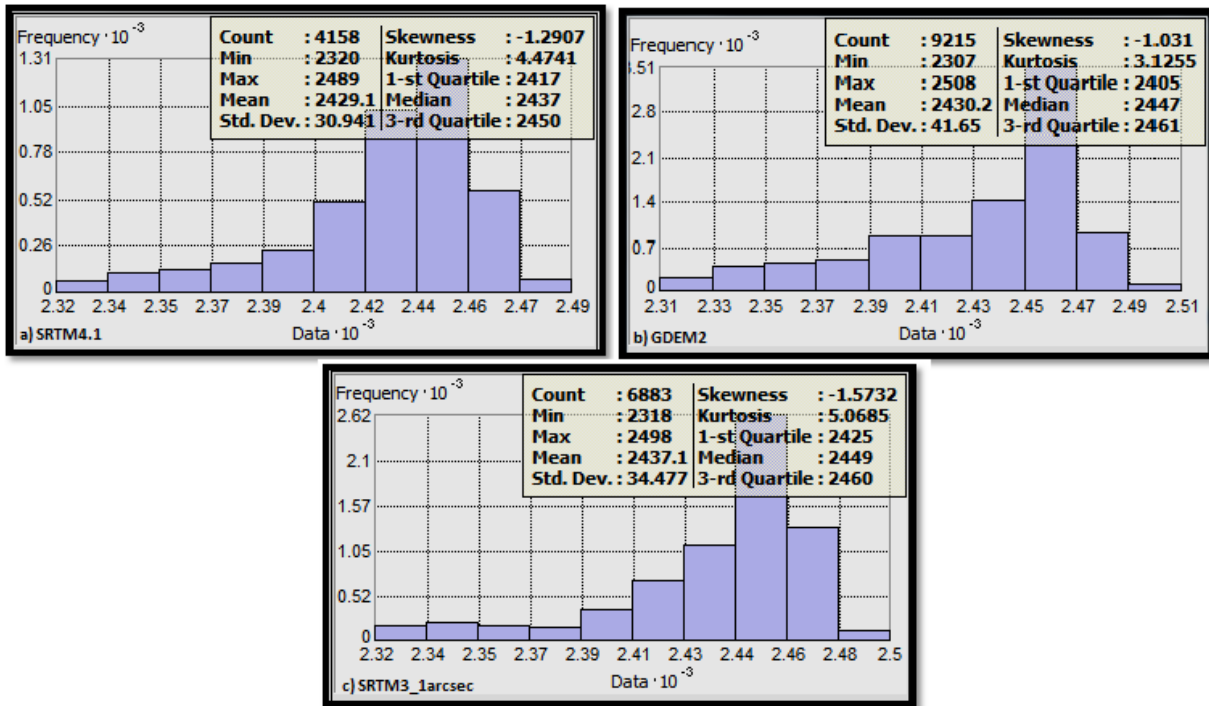


Figure 5.4: Graphical Representation of Contours for Attabad Lake derived from SRTM4.1, GDEM2, and SRTM3_1arcsec and statistical parameters associated with them are found out using ArcGIS[®] geospatial analysis.

During contour interpolation of SRTM4.1, GDEM2, and SRTM3_1arcsec, we got the above described statistical parameters that help us a lot for making our understanding better about DEMs.

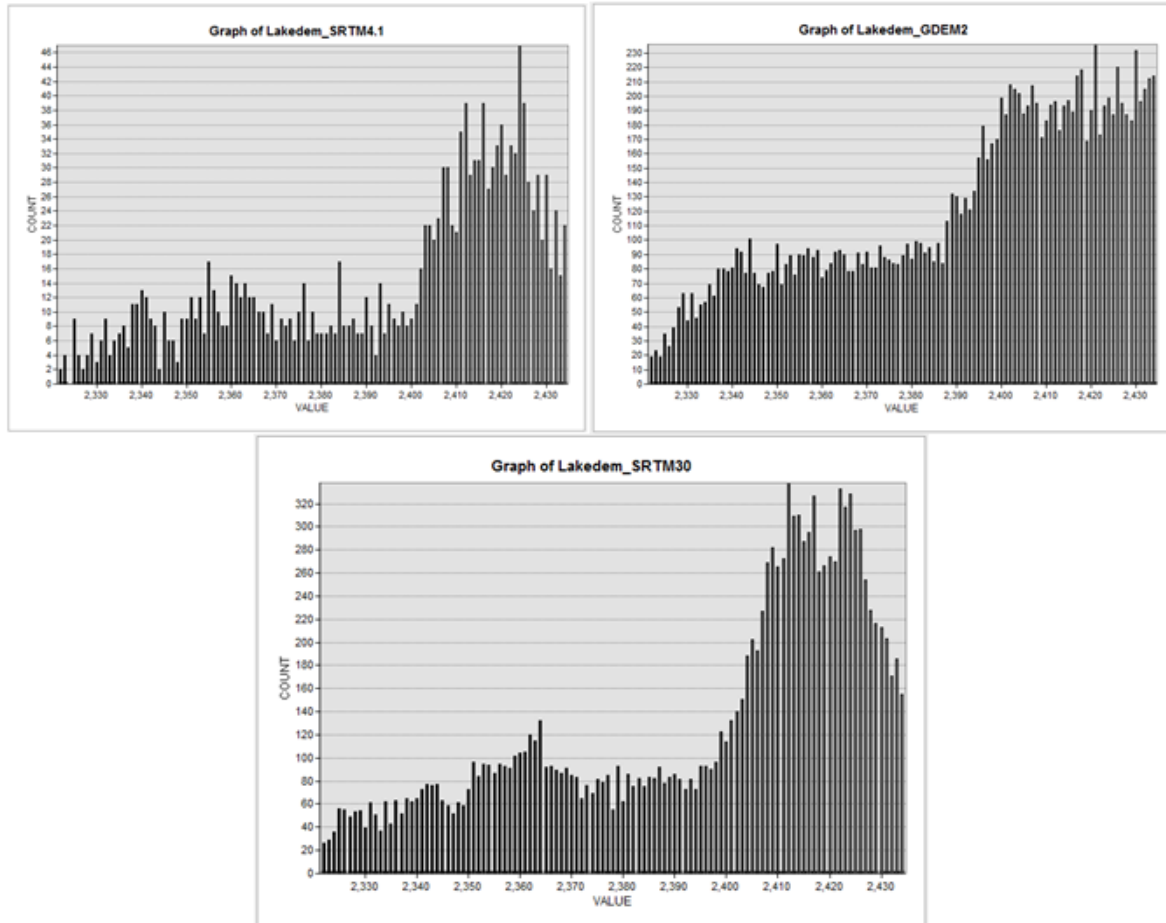


Figure 5.5: Graphical comparison of Attabad Lake DEM generated from SRTM4.1, GDEM2, and SRTM3_1arcsec elevation data.

The above diagram shows the COUNTS (number of pixels) of Attabad Lake DEM against VALUE presenting the Lake level Elevation.

5.3.2 Frequency Distribution of Attabad Lake

Statistical importance of frequency distributions is pronounced that enables us to make a detailed analysis of the work undertaken or the data inferred.

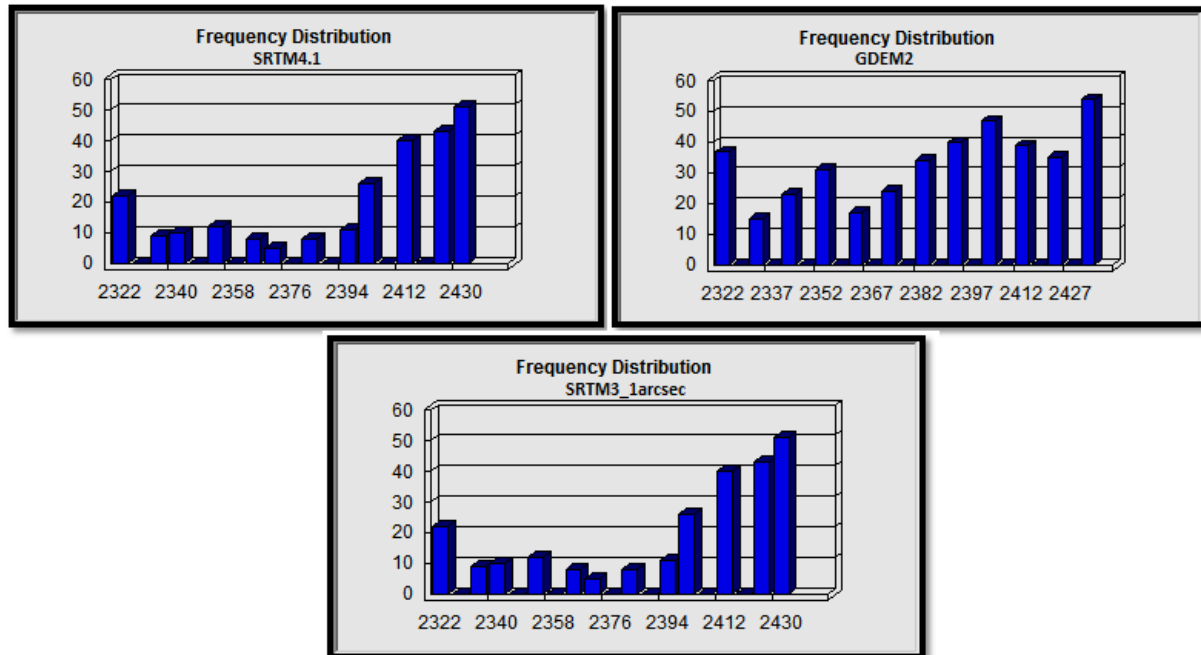


Figure 5.6: Comparison of Frequency Distribution of SRTM4.1, GDEM2, and SRTM3_1arcsec for Attabad Lake.

5.4 Visual Comparison

An easiest approach for comparing DEMs of the same area is made possible by making visual comparison of hill shade or shaded reflectance maps. Figures below show such comparisons, scaled so that the pixel resolution is suitable for a 1" DEM like the ASTER GDEM2 and SRTM3_1arcsec. Lowest resolution data like SRTM4.1" must be blown up to reach at this scale.

5.4.1 Hillshade Analysis

Hill shading produces a three-dimensional effect that provides a sense of visual relief for cartography. It is also responsible for a relative measure of incident light for analysis (Abuckley, 2008). Hillshade map of DEMs clearly reveals that SRTM3_1arcsec projects the terrain features better as compare to GDEM2. On the other hand, SRTM4.1 does not give good visual

representation of terrain but provide much more detail than other DEMs. (Guth, 2010) also agrees with this point.

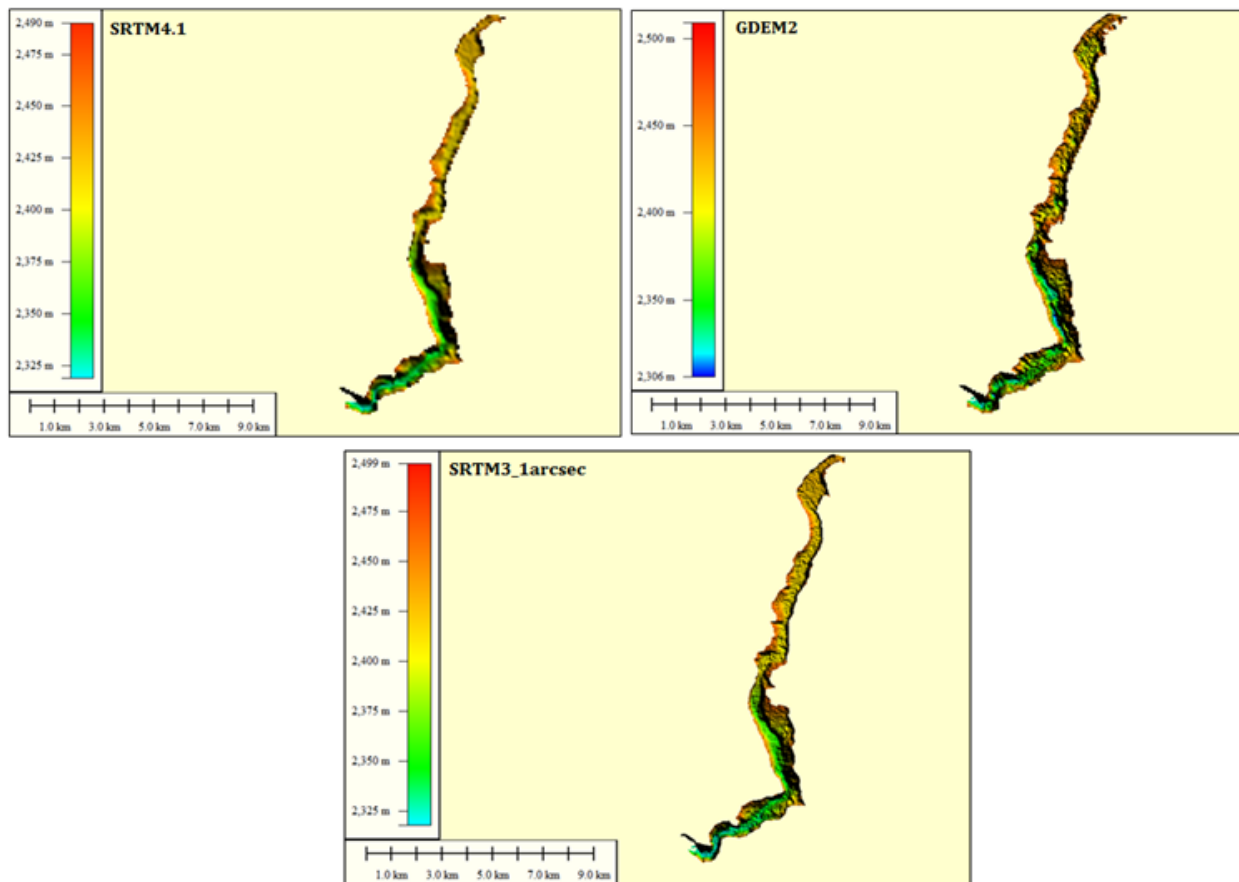


Figure 5.7: Shaded Relief map of SRTM4.1, GDEM2 and SRTM3_1arcsec representing Attabad Lake, clearly demonstrates the 3D effect of DEMs, also providing proper visualization of terrain features

5.4.2 Profile Comparison

A second visual technique is to generate the topographic profiles from each of the DEMs and lay over one another (figure below). This reveals the comparative relationships of these DEMs; in our case the ASTER GDEM inclines below than the other DEMs but the SRTM4.1 is higher than the others, signifying a possible horizontal shift of the points (ASTER GDEM Validation Team, 2009) fixed these errors in Japan.

By superimposing the topographic profiles from each of the DEMs, we can visualize them properly. This displays the comparative relationships among various DEMs. In our case the ASTER GDEM2 lies below the others, and in the left diagram the SRTM4.1 is higher than the others, signifying a probable horizontal shift of the points (ASTER GDEM Validation Team, 2009, rectified that kind of problems in Japan).while SRTM3_1arcsec (diagram in the center) exist in between SRTM4.1 and ASTER GDEM2.

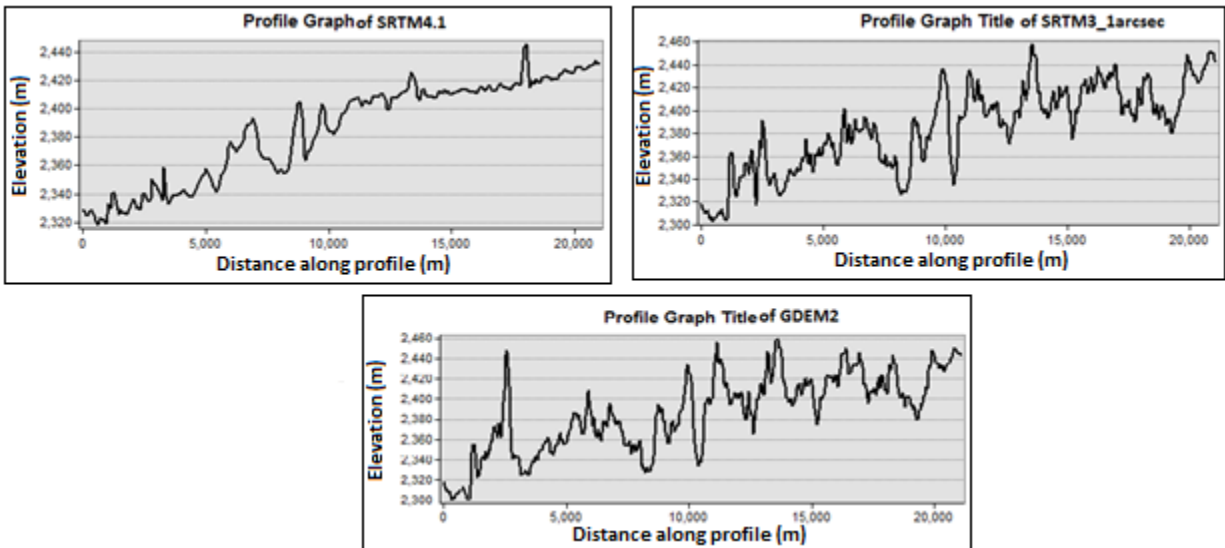


Figure 5.8: Topographic Profile Comparison of SRTM4.1, GDEM2, and SRTM3_1arcsec

5.5 Implications of the Results

Researcher can implement these relations of volume to area for conducting further research.

RVA (Ratio of Volume to Area) is the ratio of 3D volume (V) of a lake to its 2D planimetric area (A). It is found after you have calculated the volume of a Lake or sometimes called to be Minimum Eroded Volume or Lake Basin Volume. The purpose of this index to compare groups of watersheds in different phases of development.

RVA is helpful in comparing the relative effects of denudation and uplift in a tectonically steady mountain range versus one actively uplifting. We recorded RVA value up to two decimal places for each DEM.

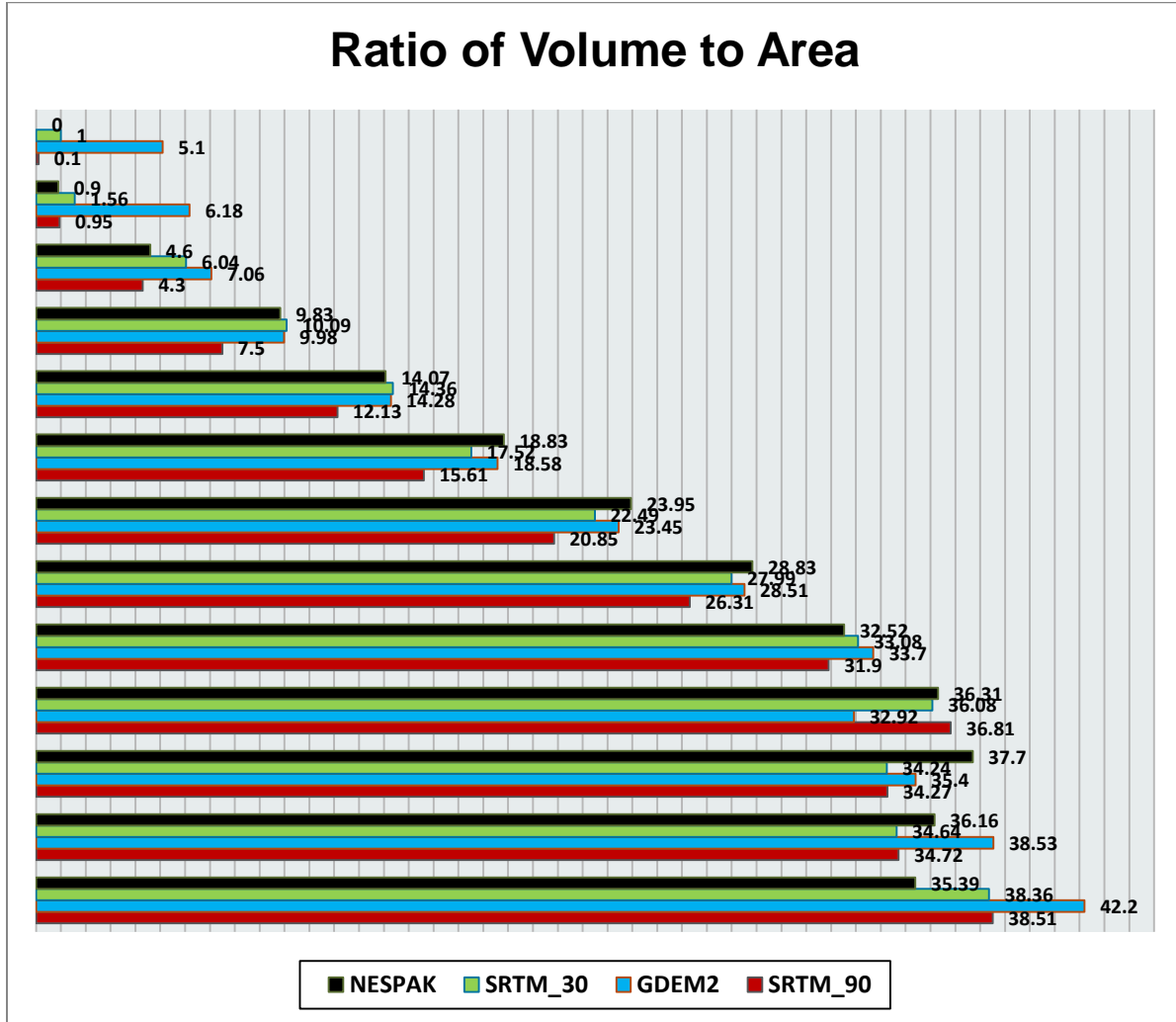


Figure 5.9: Ratio of volume (V) to area (A) determined from volume and area calculations extracted from SRTM4.1, GDEM2, and SRTM3_1arcsec

The bar graph presented above depicting the Ratio of Volume to area by using the data inferred from contour interpolation of SRTM4.1, ASTER GDEM2, and SRTM3_1arcsec.

6 Discussion

We are going to interpret our results and observations on the basis of strong arguments provided by many researchers as follows:

6.1 Interpretations related to Accuracy Assessment

Despite of the facts stated above, a "good" correlation coefficient (approaching 1.0) in this regression method is not only sufficient to guarantee a meaningful or well-performed function. Assessment about a result's correctness is more a matter of decision than mathematics, (P.Lutus, 2013) also agrees with this argument.

6.2 Interpretation of Statistical Results

As far as statistical observations are concerned the large number of counts in GDEM2 demonstrates the effect of missing/including islands (Chricco, September 2004) and artifacts that inherently associated with it due to this facts it overestimates the areas of impoundments and its associated volumes while SRTM3_1arcsec includes less number of pixels compared to GDEM2 but more than SRTM4.1 (because of resolution difference). On the other hand, SRTM4.1 in cooperates less number of pixels because of its coarser resolution ~90 m as well as problem of resembling and averaging.

With reference to table 5.3, it is obvious that GDEM2 attained highest standard deviation than others that reflects the large number of artifacts associated with them. According to (Rumsey, 2014), it is also clear that similar to the mean outliers disturb the standard deviation greatly because the formula for standard deviation contains the mean. As number of artifacts increases standard deviation becomes larger for that data.

6.3 Trustworthiness of Visual Comparisons

According to (Guth, 2010), these kind of visual comparisons are significant in a way that DEMs provide a valuable base map. However, quantitative measures should back up the qualitative visual assessments. This study focuses on both aspects. The quality of a Digital Elevation Model itself chiefly rely on the accurateness of the elevation values, and the number of anomalies and

the number of voids (anomalies) as dictated by **(Suwandana E. , Kawamura, Sakuno, Y., & Raharjo, 2012)** in his research.

6.4 Validation Summary of the Results

(Abrams, Bailey, B., & Hato, 2010) detected and observed a number of anomalies such as clouds, "bumps" "pits", and or "mole runs" in GDEM2, and on local scale GDEM2 also encompasses large height errors. Thus GDEM2 should be taken as "experimental" or "research grade". Our study also agrees with this suggestion because during geometric calculations GDEM2 sometimes overestimates volume because of the reason described above.

By keeping in view that DEMs can never be perfect so that their estimated volumes cannot be as much accurate as field based data but can give results closer to actual data as mentioned in our investigation because **(Flood & Gutelius, 1997)** clearly reveal in their study that DEMs are produced by adopting different procedures with varying degree of precision and cost. Regardless of the method adopted, created DEMs are inexorably exposed to errors, mostly due to the methodology followed or the numerous post-processing steps the models have to undergo (i.e. interpolation). It is, however, imperative that errors must be reckoned so to offer users with firsthand information on the DEM consistency as **(Piacentini, Ben, & Gerald, 2012)** reveled in his investigation.

7 CONCLUSION

Following conclusions are drawn on the basis of analysis and results of this study:

- ❖ Volume predictions of proposed Lake are made possible by means of digital topographic data and spatial analyst extension within the Arc Map[®] toolbox.
- ❖ All global DEMs (SRTM4.1, ASTER GDEM, and SRTM3_1arcsec) are suitable for the geometric calculations (area-volume) of Attabad Lake.
- ❖ High quality SRTM3_1arcsec is preferred over ASTER GDEM2 because it uses radar systems for DEM acquisition which has advantages over optical systems due their penetration capability from clouds and their independency from optical contrast. The relatively smooth geometry of Lakes and the low optical contrast of water or also the presence of clouds over mountainous regions (during peak rainy seasons) also favor radar systems.
- ❖ SRTM3_1arcsec provides good estimation of volumes at all elevations although some artifacts associated with it during interpolation but GDEM2 consistently overestimates the volumes and this difference becomes larger for higher Lake Elevations while the volumes derived from SRTM4.1 are closer to the field observed data but at lower altitudes discrepancy in results arises due to the resampling problem of it from the original resolution.
- ❖ As SRTM4.1 is the coarser resolution DEM that increases minimum and reduces the maximum elevation but despite of this it did good quantification of Lake as compare to high resolution ASTER GDEM2.
- ❖ GDEM2 incorporates more number of pixels (COUNTS) than SRTM3_1arcsec to represent the lake at specific dates which is the indication of inherent anomalies associated with it or might reflect the effect of missing/including islands whereas SRTM4.1 includes less number of pixels because of its coarser resolution.

- ❖ In addition to artifacts, the difference in volume calculations derived from all DEMs may occur due to different acquisition dates and techniques (radar, optical) as well as resolution.
- ❖ Remote sensing imagery give us the exact extend of lake at specific dates and then integration of it with elevation data make the volumetric calculations more accurate or close to the actual results as depicted in our study.
- ❖ The accuracy of the elevation values, the number of anomalies, and the number of voids (artifacts) dictates the quality of DEM (**Suwandana E. , Kawamura, Sakuno, Y., & Raharjo, 2012**).

This study is conducted for the sake of volumetric comparison of Attabad Lake between two elevations data sets available free of cost at the internet. DEM analysis and Remote sensing imagery were integrated for the quantification of Attabad Lake at its different stages of filling, stable overtopping and partial draining , also recent surface hydrological changes of Attabad lake was observed. It is strongly recommended that measures must be carried out to take advantages of these water resources prior to lose entirely with evaporation. In addition to this, geo-environmental problems may possibly arise from the concentration of salts after the lakes dried (**Bastawesy, Arfat, & Khalaf, 2007**). Up to now, DEM handlers would frequently use the DEM as a truth surface instead of a model, but it is not assured to consider this decision without a thorough assessment.

In association to this study user can conclude how ambiguity in the DEM will affect the geometric calculations of Attabad Lake. Our studies exhibited that the void filled SRTM for the analyzed area (Attabad Lake) is satisfactory to accomplish multifaceted calculations of morphometric as compared to ASTER GDEM2. The study has revealed that void filled SRTM-3 is “closer” to the actual volume determined from field survey- than ASTER GDEM2, even though both available free products have an excellent replacement for local hypsographic data and are very appropriate for geographic researches and analysis at a global scale. LIDAR and airborne InSAR based new technologies are rapidly adopting GIS practitioners and land managers concerning with very high resolution DEMs. Lastly we expect that these technologies will be accessible in open source to offer the opportunity for the Pakistani researchers to conduct

and evaluate these systems for geometric calculation and terrain modeling in the Pakistan territory for future studies (Dr.Jean A., 2013-2014).

7.1 Limitation

There are several limitations encountered during this analysis related to the data quality and suppositions made in advance for analysis which restricts the validity of the results. Although these results are precise, rely on the information supplied but they should only be regarded as approximations.

Problem of High Resolution DEMs

- ❖ The SRTM3_1arcsec and GDEM2 are not perfect because they encompass the highest pixel resolution for elevation in this region. The pixel elevation values are only the mean for every pixel area, and possibly will under and overestimate the actual neighboring values.

Unavailability of High Quality DEM

- ❖ LiDAR DEM data would have been ideal in generating a more accurate DEM that would be able to produce results nearer to the actual volume. The long term unavailability of information about Lake Data is another limitation since any deviation in Lake Elevation can significantly influence the results.

Overestimations of Volume

- ❖ ASTER GDEM2 sometimes overestimate the results due to incapability of it to consider the river bed elevation, alluvium, and reservoir retention elevation so these limitation also associated with this.

Predictable Errors of Global DEMs

- ❖ The primary reason of the presence of unavoidable errors in global elevation datasets mainly due to the fact of methodology adopted for the extraction of elevation data and the many processing steps like interpolation that the models have to suffer. Logical

and widespread assessment of these datasets is not quite easy due to insufficiency of extensive ground truthing.

Unavailability of High Resolution Topographic Map

- ❖ No good quality topographic data were present to us so that determination of the potential lake storage volume might become problematic.

Lack of Bathymetric Maps

- ❖ The water volumes of lakes are usually estimated using accurate bathymetry along with the data of lake surface elevations and coastline topographic data. Moreover, coast topography maps and bathymetry data are difficult to gain because high costs are required for equipment and labor.

Release from Artifacts

- ❖ Recently release SRTM3_1arcsec (global) is actually not free from artifacts either, but GRASS GIS or GDAL provides a fantastic "mdnoise" module/utility which does a great job of removing noise while preserving sharp features like valleys and ridge lines.

System Requirements

- ❖ Extensive hardware storage is necessary for the accomplishment of Arc GIS tasks because sometimes substantial processing is required.

Works Cited

- ASTER GDEM Validation Team. (2009). Retrieved September 6, 2014, from ASTER global DEM Validation: <https://lpdaac.usgs.gov/lpdaac/content/download/4009/20069/version/3/file/ASTER+GDEM+Validation+Summary+Report.pdf>
- Abrams, M., Bailey, B., B., T. H., & Hato. (2010). The ASTER global DEM. *The Photogrametric Engineering & Remote Sensing*, 4, 344-348.
- Abuckley, A. (2008, May 23). *ArcGIS Online blog*. Retrieved June 11, 2015, from ArcGIS Resources: <http://blogs.esri.com/esri/arcgis/2008/05/23/aspect-slope-map/>
- Ahmet İRVEM. (2010, November 24). Application of GIS to Determine Storage Volume and Surface Area of Reservoirs: The Case Study of Buyuk Karacay Dam. *International Journal of Natural and Engineering Sciences*(23 July 2010).
- Ahmet İRVEM. (2011). Application of GIS to Determine Storage Volume and Surface Area of Reservoirs: The Case Study of Buyuk Karacay Dam. *International Journal of Natural and Engineering Sciences*, 5(24November2010), 39-43.
- Athmania, D., & Achour, H. (2014). External Validation of the ASTER GDEM2, GMTED2010 and CGIAR-CSI- SRTM v4.1 Free Access Digital Elevation Models (DEMs) in Tunisia and Algeria. *Remote Sensing*, 6(21 May 2014), 1-21.
- Bastawesy, M. A., Khalaf, F. I., & Arafat, S. M. (2008). The Use of Remote Sensing and GIS for the Estimation of Water Loss from Tushka Lakes, Southwestern Desert, Egypt. *Journal of African Earth Sciences*, 52: 73–80.
- Bastawesy, M., Arfat, S., & Khalaf, F. (2007). Estimation of water loss from Toshka Lakes using remote sensing and GIS. *10th AGILE International Conference on Geographic Information Science* (pp. 1-9). Aalborg University, Denmark: National Authority for Remote Sensing and Space Science (NARSS).
- Becek, K. (2008). Investigating error structure of shuttle radar topography mission elevation data product. *Geophysical Research Letters*, 35-39.
- Bolten, A., & Waldhoff, G. (2010). Error estimation of ASTER GDEM for regional applications – comparison to ASTER DEM and ALS elevation models. *3rd ISDE Digital Earth Summit*. Nessebar, Bulgaria.
- Brooks, R. T., & Hayashi, M. (2002). “Depth-Area-Volume and Hydroperiod Relationships of Ephemeral (Vernal) Forest Pools in Southern New England. *Taylor French*, 247-255.
- Butt, M., Umar, M., & Qamar, R. (2013). Landslide dam and subsequent dam-break flood estimation using HEC-RAS model in Northern Pakistan. *Natural Hazards. Wiley Online*, 241 – 254.

- Carreiro, H. (March 16, 2010). *Update: Pakistan's Karakoram Highway blocked by major landslide. Matador Trips.*
- Chen, R.-F., Chang, K.-J., Angelier, J., Chan, Y.-C., Deffontaines, B., Lee, C.-T., et al. (2006). Topographical changes revealed by high-resolution airborne LiDAR data: the 1999 Tsaoling landslide induced by the Chi-Chi earthquake. *Engineering Geology*, 88, 160-172.
- Chricco, P. G. (September 2004). AN EVALUATION OF SRTM, ASTER, AND CONTOUR-BASED DEMS IN THE CARIBBEAN REGION. In E. S. USGS (Ed.), *URISA Caribbean GIS Conference* (p. 17). Caribben: U.S. Department of the Interior; U.S. Geological Survey.
- Christensen, G. V., & Bergman, L. A. (2005). *Hydrologic Conditions and Lake-Level Fluctuations at Long Lost Lake, 1939–2004, White Earth Indian Reservation, Clearwater County, Minnesota*. Prepared in cooperation with the White Earth Band of Chippewa Indians.
- Clause, V. (2014). *Using ArcMap to Streamline Reservoir Volume Computation: Susitna-Watana Reservoir Volume and Surface Area Calculations*. Australia: Science Direct.
- Cook, N., & Butz, D. (2013). The Atta Abad landslide and everyday mobility in Gojal, northern Pakistan. *International Mountain Society*, 33, 372 – 380.
- Cosat, J. E., & Schuster, R. L. (1988). The formation and failure of natural dams. *Geological Society of America Bulletin*, 100.
- CSI, C. (n.d.). Retrieved from <http://srtm.csi.cgiar.org/>
- Czubski, K., Kozak, J., & Kolecka, N. (2013). Accuracy of SRTM-X and ASTER Elevation Data and its influence on Topographical and Hydrological Modeling: Case study of the Pieniny Mts. in Poland. *International Journal of Geoinformatics*, 9 No.2, 8.
- Delaney, K. B. (2014). Characterisation and Analysis of Catastrophic Landslides and Related Processes using Digital Cartographic Techniques. *Earth Science*, 248: 54-192.
- Delaney, K. B., & Evans, S. G. (2011). Rockslide dams in the northwestern Himalayas (Pakistan, India) and adjacent Pamir Mountains (Afghanistan, Tajikistan), Central Asia. In: Evans, S.G., Hermanns, R.L., Strom, A.L., and Scarascia-Mugnozza, G. (Eds), *Natural and Artificial Rockslide Dams. Lecture Notes in the Earth Sciences*, 133, 205 - 242.
- Disqus. (2015, May 3). *GraphPad Statistics Guide: Interpreting Results Skewness and Kurtosis*. Retrieved June 6, 2015, from © 1995-2015 GraphPad Software, Inc.: http://www.graphpad.com/guides/prism/6/statistics/index.htm?stat_skewness_and_kurtosis.htm

- Dong, J. -J., Lai, P.-J., Chang, C.P., et al. (2014). Deriving landslide dam geometry from remote sensing images for the rapid assessment of critical parameters related to dam-breach hazards. *Landslides*, (11), 93-105.
- Dr. Jean A., D. (2013-2014). Comparison of SRTM DEM and ASTER GDEM Derived Digital Elevation Models with elevation points over the Lebanese territory. *HANNON, Lebanese journal of Geography*, 27, 7-28.
- Duan, Z., & Bastiaanssen, W. M. (2013). Estimating water volume variations in lakes and reservoirs from four operational satellite altimetry databases and satellite imagery data. *Remote Sensing of the Environment*, 134, 403 – 416.
- Ekström, G., & Stark, C. P. (2013). Simple scaling of catastrophic landslide dynamics. *Science*, 339.
- Evans, S., & Clague, J. J. (1988). *Catastrophic rock avalanches in glacial environments*. In: Bonnard, C. (ed) *Proceedings of the 5th International Symposium on Landslides, Lausanne, 2*, 1153–1158.
- Evans, S., Bishop, N., Fidel, S., L., V., P., D., K., B., et al. (2009a). A re-examination of the mechanism and human impact of catastrophic mass flows originating on Nevado Huascarán, Cordillera Blanca, Peru in 1962 and 1970. *Engineering Geology*, 108: 96 – 118.
- Evans, S., Bishop, N., Fiedel, S. L., Valderrama, M. P., Delaney, K. B., & Oliver, S. A. (2009a). A re-examination of the mechanism and human impact of catastrophic mass flows originating on Nevado Huascarán, Cordillera Blanca, Peru in 1962 and 1970. *Engineering Geology*, 108, 96 – 118.
- Evans, S., Delaney, K., Hermanns, R., Storm, A., & Scarascia-Mugnozza, G. (2011). The Formation and behaviour of natural and artificial rockslide dams; implications for engineering performance and hazard management. In: Evans SG, Hermanns RL, Strom A, Scarascia Mugnozza G (eds), *Natural and artificial rockslide dams*. Springer, 133: 1-76.
- Evans, S., Fiedal, S., & Zegarra, L. (2007). Los Movimientos en Masa de 1962 y 1970 en el Nevado de Huascarán, Valle del rio Santa, Cordillera Blanca, Perú. Anexo B4. In: *Movimientos en Masa en la Región Andina: Una guía para la evaluación de amenazas*. *Publicacion Geologica Multinacional*, 4, 386-404.
- Evans, S., Fiedal, S., Zegarra, L., Los Movimientos en Masa de 1962 y 1970 en el, Nevado de Huascarán,, Valle del rio Santa, et al. (2007). *Proyecto Multinacional Andino Geociencias para las Comunidades Andians*. *Publicacion Geologica Multinacional*, 4, 386-404.
- Evans, S., Roberts, N., Ischuk, A., Delaney, K.B., Morozova, G., et al. (2009b). Landslides triggered by the 1949 Khait earthquake, Tajikistan, and associated loss of life. *Engineering Geology*, 109: 195 – 212.

- Evans, S., Tutubalina, O. T., Drobyshev, V. N., Chernomorets, S. S., McDougall, S., Petrakov, D. A., et al. (2009c). Catastrophic detachment and high-velocity long-runout flow of Kolka Glacier, Caucasus Mountains, Russia in 2002. *Geomorphology*, 105:314 – 321.
- Fan, X. v., C.J., Xu, Q., Gorum, T., & Dai, F. (2012). Analysis of landslide dams induced by the 2008 Wenchuan earthquake. *Journal of Asian Earth Sciences*, 57, 25-37.
- Farr, T. G., & Kobrick, M. (2000). Shuttle Radar Topography Mission produces a wealth of data. 583-585.
- Farr, T.G., Rosen, P.A., Caro, E., C., et al. (2007). The shuttle radar topography mission. *Reviews of Geophysics*. (2004), 1-45.
- Feng, L., Hu, C., Chen, X., Li, R., Tian, L., & Much, B. (2011). MODIS Observations of the Bottom Topography and Its Inter-Annual Variability of Poyang Lake. *Remote Sensing of Environment*, 115: 2729-2741.
- Flencer, C., Lotsari, E., Alho, P., & Kaayhko, J. (2012). Comparison of Empirical and Theoretical Remote Sensing Based Bathymetry Models in River Environments. *River Research and Application*, 28: 118-113.
- Flood, M., & Gutelius, B. (1997). Commercial Implications to Topographic Terrain Mapping Using Scanning Airborne Laser Radar. *Photogrammetric Engineering and Remote Sensing*, 327.
- Frost, J. (2014, January 23). *A Minitab blog: Copyright ©2015 Minitab Inc. All rights Reserved*. Retrieved August 20, 2015, from Minitab.com: <http://blog.minitab.com/blog/adventures-in-statistics/regression-analysis-how-to-interpret-s-the-standard-error-of-the-regression>
- Fujita, K., Suzuki, R., Nuimura, T., & Sakai, A. (2008). Performance of ASTER and SRTM DEMs, and their potential for assessing glacial lakes in the Lunana region, Bhutan Himalaya. *Journal of Glaciology*, 54, 220-228.
- Furnans, J., & B., A. (2008). Hydrographic Survey Methods for Determining Reservoir Volume. *Environmental Modeling and Software*, 23: 139-146.
- FWO. (2010). <http://fwo.com.pk/new/index.php/news-info/attabad-lake>. Pakistan: Frontier Works Organization Copyright © 2015. Designed & Develoepd by IT Dept FWO.
- FWO. (2012, May 15). *Frontier Works Organization*. Retrieved from , <http://fwo.com.pk/new/index.php/news-info/attabad-lake> Copyright © 2015.
- Gamble, D. E., Grody, J. U., Micacchion, M., & Mack, J. J. (2007). *An Ecological and Functional Assessment of Urban Wetlands in Central Ontario* (Vol. 2). Columbus: Ohio EPA Technical Protection Agency.

- Gauri, K. A. (2015, February 02). Attabad Lake Level Report. (B. Amin, Interviewer) Lahor: International Sedimentation Research Institute of Pakistan, Pakistan Water and Power Development Authority (ISRIP-WAPDA).
- Gleason, R. A., M.K., L., B.A., T., K.E., K., & J.N.H., E. (2007). *Estimating Water Storage Capacity of Existing and Potentially Restorable Wetland Depressions in a Subbasin of the Red River of the North*. Reston VA: U.S. Geological Survey Open file Report.
- Guth, P. L. (2010). Geomorphic Comparison of ASTER GDEM AND SRTM. *Department of Oceanography, US Naval Academy, Annapolis MD 21402 USA, Commission IV, WG IV/7 - pguth@usna.edu* (pp. 1-10). Orlando, Florida: ISPRS.
- Harp, E., Keefer, D., Sato, H., & Yagi, H. (2011). Landslide inventories: the essential part of seismic landslide hazard analyses. *Engineering Geology. Engineering Geology*, 9-21.
- Hayashi, M., & van der Kamp, G. (2000). Simple Equations to Represent the Volume-Area-Depth Relations of Shallow Wetlands in Small Topographic Depressions. *Journal of Hydrology*, 74-85.
- Hengl, T., & Evans, I. S. (2009). Mathematical and Digital models of the Land Surface. (H. T., & I. H., Eds.) *In Geomorphometry*, 31-63.
- Hewitt, K. (1968). *Records of natural damming and related events in the upper Indus basin. Indus Journal of Water Power Development Authority*, 10, 11–19.
- Hewitt, K. (1982). *Natural dams and outburst floods of the Karakoram Himalaya. IAHS Publication*, 138, 259-269.
- Hewitt, K. (1998). *Catastrophic landslides and their effects on the upper Indus streams Karakoram Himalaya, northern Pakistan Geomorphology*, 26, 47–80.
- <http://gdem.ersdac.jspacesystems.or.jp/>. (n.d.). *ASTER GDEM2 datasets*. Retrieved from Japan Space System.
- <http://srtm.csi.cgiar.org/>. (n.d.). Retrieved from http://e4ftl01.cr.usgs.gov/ASTT/AST_L1B.003/2000.03.10/
- <http://worldaerodata.com/>. (n.d.). *World Official Aeronautical Database* . Retrieved March 18, 2015
- <http://www.wapda.gov.pk>. (n.d.). *Water*.
- <http://www.wapda.gov.pk>. (n.d.). *Water and Power Development Authority of Pakistan*. Retrieved February 29, 2015
- <http://www.wapda.gov.pk>. (n.d.). *Water and Power Development Authority of Pakistan*. Retrieved February 29, 2015

- <http://www.wapda.gov.pk>. (n.d.). Retrieved February 29, 2015, from Water and Power Development Authority of Pakistan.
- <http://www2.jpl.nasa.gov/srtm/>. (n.d.). *NASA Jet Propulsion Laboratory California Institute of Technology*. Retrieved January 26, 2015
- <https://lta.cr.usgs.gov/SRTM1Arc>. (n.d.). *Shuttle Radar Topography Mission (SRTM) 1 Arc-Second Global*. Retrieved September 2014
- Huggel, C., Schneider, D., M., J., D., & H. and Kääh. (2008). Evaluation of ASTER and SRTM DEM data for lahar modeling: a case study on lahars from Popocatépetl Volcano. *Journal of Volcanology and Geothermal Research*, 170, 99-110.
- Hussain, S. H., & Awan, A. A. (2009). *Report for National Disaster Management Authority on Causative Mechanisms of Terrain Movement in Hunza Vallley*. Pakistan: Issued by Dr.Imran Khan, Director General, Geological Survey of Pakistan.
- Iqbal, M., Shah, F., Chaudhary, A., & Baig, M. (2014). Impacts of Attabad lake (Pakistan) and its future outlook. *European Scientific Journal*(10), 107 – 120.
- James. (2015, Jan 1). *Percentage Difference, Percentage Error, and Percentage Change*. Retrieved August 30, 2015, from Copyright © 2014 MathsIsFun.com: <http://www.mathsisfun.com/numbers/percentage-error.html>
- Jing, C., Shortridge, A., Lins, S., & Wu, J. (2013). Comparison and validation of SRTM and ASTER GDEM for a subtropical landscape in southeastern China. *International Journal of Digital Earth*.
- Kalla, S. (2011, January 20). *Quartile*. Retrieved September 21, 2015, from Explorable.com - Copyright © 2008-2015. All Rights Reserved: <https://explorable.com/quartile>
- Kargel, J., Leonard, G., Crippen, R., Delaney, K., Evans, S., & Schneider, J. (2010). Satellite monitoring of Pakistan's rockslide-dammed Lake Gojal. *EOS*, 91, 394-395.
- Khan, A., Richards, K. S., Parker, C. T., McRobie, A., & Mukhopadhyay, B. (2013). How large is the Upper Indus Basin? The pitfalls of auto-delineation using DEMs. *Journal of Hydrology*, 442–453.
- king, R., & Julstorm, B. (1982). *Applied Statistics Using the Computer*. U.K.: Sherman Oaks,CA: Alfred Pub. Co.
- Korup, O., Montgomery, D. R., & Hewitt, K. (2010). Glacier and landslide feedbacks to topographic relief in the Himalayan syntaxes. *Proceedings of the National Academy of Sciences*, 107.
- Lane, C. R., & D'Amico, E. (2010). Calculating the Ecosystem Service of Water Storage in Isolated Wetlands Using LiDAR in North Central Florida, USA. *Wetlands*, 30: 967-977.

- Le Fort, P., Michard, A., Sonet, J., & Zimmermann, J. L. (1983). Petrography, geochemistry and geochronology of some samples from the Karakorum Axial Batholith, Pakistan. (F. A. Shams, Ed.) 277 – 387.
- Leblanc, M., Favreau, G., Maley, J., Nazoumou, Y., Leduc, C., Stagnitti, F., et al. (2006, January 8). Reconstruction of Megalake Chad using Shuttle Radar Topographic. [www.elsevier.com/locate/palaeo\(2005\)](http://www.elsevier.com/locate/palaeo(2005)), 16-27.
- Li, P., Shi, C., Li, Z., M., J.-P., Drumender, J., et al. (2012). Evaluation of ASTER GDEM VER2 using GPS measurements and SRTM VER4.1 in China. *ISPRS Annals of the Photogrammetry, Remote Sensing and Spatial Information Sciences*, 1- 4, 181-186.
- Lipovsky, P., Evans, S., Clague, J., Hopkison, C. C., Bobrowsky, P., Ekström, G., et al. (2008). The July 2007 rock and ice avalanches at Mount Steele, St. Elias Mountains, Yukon, Canada. *Landslides. Science Direct*, 5, 445-455.
- Lu, S., Ouyang, N., Wu, B., Wei, Y., & Tesemma, Z. (2013, July 6). Lake water volume calculation with time series remote sensing images. *International Journal of Remote Sensing*, 34(2012), 7962-7973.
- Lu, S., Shen, X., Zou, L., Li, C., Mao, Y., Zhang, G., et al. (2008). An Integrated Classification Method for Thematic Mapper Imagery of Plain and Highland Terrains. *Journal of Zhejiang University Science*, A 9: 858–866.
- Lu, S., Wu, B., Wang, H., & Yan, N. (2011). Water Body Mapping Method with HJ-1A/B Satellite Imagery. *International Journal of Applied Earth Observation and Geoinformation*, 13: 428-434.
- Mashimbye, Z., de Clercq, W., Van Niekerk, & A.V. (2014). An evaluation of digital elevation models (DEMs) for delineating land components. *Geoderma*, 213, 312-319.
- McFeeters, S. K. (1996). The Use of Normalized Difference Water Index (NDWI) in the Delineation of Open Water Features. *International Journal of Remote Sensing*, 17: 1425–1432.
- Medina, C. E., Gomez, E., Alonso, J. J., & Villares, P. (2010). Water Volume Variations in Lake Izabal (Guatemala) from In Situ Measurements and ENVISAT Radar Altimeter (RA-2) and Advanced Synthetic Aperture Radar (ASAR) Data Products. *Journal of Hydrology*, 34-48.
- Meyer, D., Tachikawa, T., Kaku, M., Kaku, M., Iwasaki, A., Gesch, D., et al. (2011). ASTER global digital elevation model verison 2 – summary of validation results. 27.
- Minke, A. (2009). Estimating Water Storage of Prairie Pothole Wetlands, University of Saskatchewan, Saskatoon.
- NASA. (2004). *ASTER instrument subsystems*. Retrieved January 2, 2015, from <http://ast905erweb.jpl.nasa.gov/instrument.asp>

- NESPAK. (May 2014.). *Hydrology, sedimentation and flood routing study report for Attabad landslide lake*. Lahore: National Engineering Services of Pakistan (NESPAK).
- Ouimet, W. B., Whipple, K. X., Royden, L. H., Sun, Z., & Chen, Z. (2007). The influence of large landslides on river incision in a transient landscape: Eastern margin of the Tiberan Plateau. *GSA Bulletin*, 119.
- Ouma, Y. O., & Tateishi, R. (2006). A Water Index for Rapid Mapping of Shoreline Changes of Five East African Rift Valley Lakes: An Empirical Analysis Using Landsat TM and ETM+ Data. *International Journal of Remote Sensing*, 27: 3153–3181.
- P.Lutus. (2013, 20 07). *Polynomial Regression Data Fit*. Retrieved 04 25, 2015, from Java script version of polysolve: <http://www.arachnoid.com/polysolve>
- Pan, F., Liao, J., Li, X., & Guo, H. (2013). Application of the inundation area – lake level rating curves constructed from the SRTM DEM to retrieving lake levels from satellite measured inundation areas. *Computers and Geoscience*, 52, 168 – 176.
- Petley, D. (2010). *The Attabad landslide crisis in Hunza, Pakistan – lessons for the management of valley blocking landslides*.
- Petley, D. (2011). London: Damming events at Attabad. International Water and Power.<http://www.waterpowermagazine.com/features/featuredamming-events-at-attabad->/Oxford Press.
- Petley, D. (August 24, 2010). New satellite images of the Attabad landslide site. The Landslide Blog.
- Petley, D. (July 6, 2010). Attabad—No substantial changes in the lake level. Dave’s Landslide Blog.
- Petley, D. (June 1, 2010). Attabad: Continued retrogression. Close to the next stage? Dave’s Landslide Blog.
- Petley, D. (June 26, 2010). Attabad—Situation Report Dave’s Landslide Blog.
- Petley, D. (March 11, 2010). *Attabad. Dave’s Landslide Blog*.
- Petley, D. (n.d.). *May 10, 2010*. Accelerating rate of filling at the Attabad landslide in Hunza, Pakistan. Dave’s Landslide Blog.
- Petley, D. (May 27, 2010). Attabad: The freeboard is now reportedly about 1.3 meters. Dave’s Landslide Blog.
- Petley, D. (May 8, 2010). Inflow to the landslide lake at Attabad. Dave’s Landslide Blog.
- Petley, D. (May 9, 2010). The landslide at Attabad – new videos of the spillways and the drowning land upstream. Dave’s Landslide Blog.

- Petley, D. (September 1, 2010). The latest NASA image of Attabad Dave's Landslide Blog.
- Petley, D., Rosser, N. J., Karim, D., Wali, S., Ali, N., Nasab, N., et al. (2010). Non-seismic landslide hazards along the Himalayan arc. 143–154.
- Piacentini, D. T., Ben, M., & Gerald, F. (2012). *Comparison of SRTM and ASTER Derived Digital Elevation Models over Two Regions in Ghana – Implications for Hydrological and Environmental Modeling*. 1Ghana, 2The Netherlands: www.intechopen.com.
- Reuter, H. I., Nelson, A., J., & A., N. (2007). An evaluation of void filling interpolation methods for SRTM data . *International Journal of Geographic Information Science*, 9-21.
- Rodriguez, E., Morris, C. S., & Belz, J. E. (2006). A global assessment of the SRTM performance. *Photogrammetric Engineering and Remote Sensing*, 72, 249 – 260.
- Rogers, A. S., & Kearney, M. S. (2004). Reducing Signature Variability in Unmixing Coastal Marsh Thematic Mapper Scenes Using Spectral Indices. *International Journal of Remote Sensing*, 25: 2317–2335.
- Rumsey, D. J. (2014, March 23). *How to Interpret Standard Deviation in a Statistical Data Set: Statistics For Dummies*. (J. W. sons, Ed.) Retrieved June 15, 2015, from For Dummies a wiley brand making every thing easy. Copyright © 2015 & Trademark by John Wiley & Sons, Inc. All rights reserved: <http://www.dummies.com/how-to/content/how-to-interpret-standard-deviation-in-a-statistic.html>
- Schneider, D., Huggel, C., Cochachin, A., Guillén, S., & Garcia, J. (2014). Mapping hazards from glacier lake outburst floods based on modeling of process cascades at Lake. *Advances in Geosciences*(35), 145-155.
- Searle, M. P. (1991). Geology and tectonics of the Karakoram Mountains. *John Wiley and Sons Ltd.*, 358.
- Shah, F. H., Ali, A., & Baig, M. N. (2013). Taming the monster – Attabad landslide dam. *Journal of Environmental Treatment Techniques*, 1, 46 - 55.
- Shanlong, L., Ninglei, O., Bingfang, W., Yongping, W., & Zelalem, T. (2015). Lake water volume calculation with time series remote-sensing images. *International Journal of Remote Sensing*, 34-22.
- Shaw, G., & Wheeler, D. (1985). *Statistical Techniques in Geographical Analysis*. Chichester: Wiley.
- Sheikh. (2010, July 2). Hunza Landslide Relief Support.
- Sivanpillai, R., & Miller, S. N. (2010). Improvements in Mapping Water Bodies Using ASTER Data. *Ecological Informatics*, 5: 73–78.

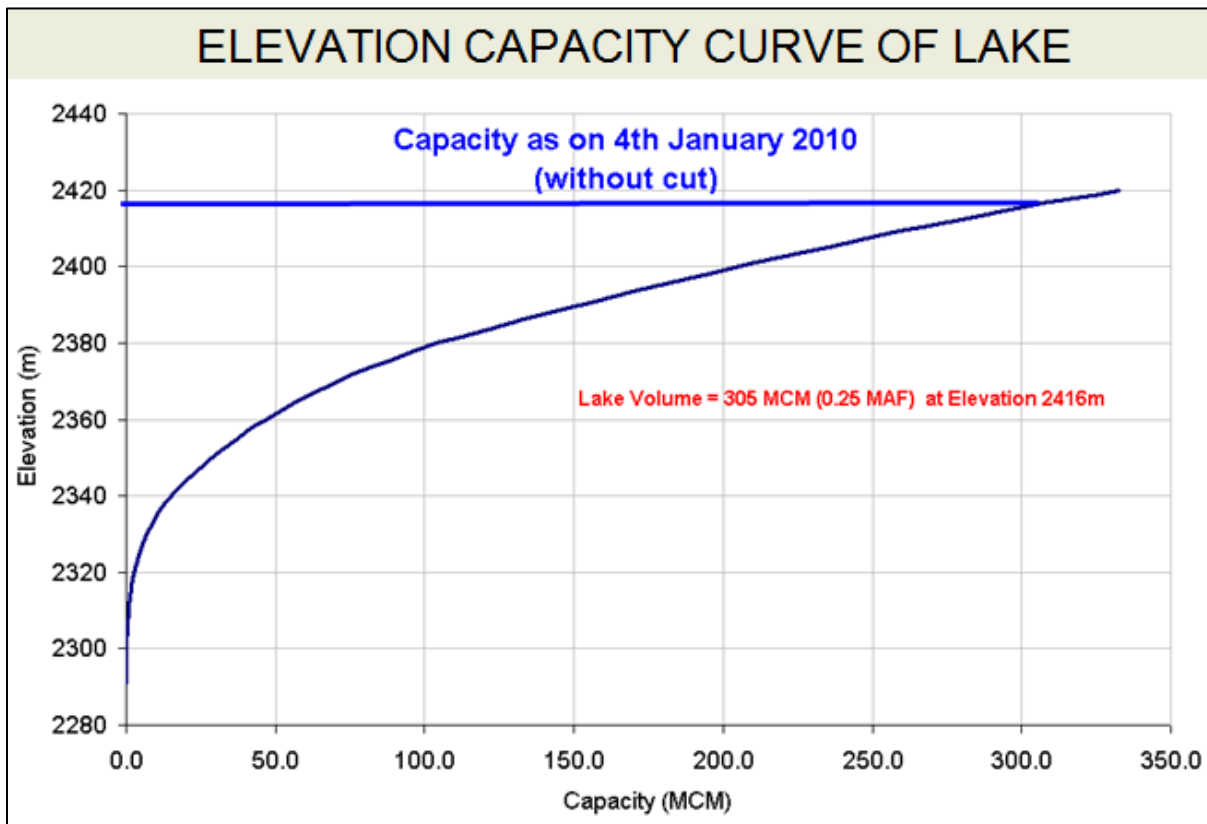
- Smith, L. C., & Pavelsky, T. M. (2009). Remote sensing of volumetric storage changes in lakes. *Earth Surface Processes and Landforms*, 34.
- Suwandana, E. (n.d.). Evaluation of ASTER GDEM2 in Comparison with GDEM1, SRTM DEM and Topographic-Map-Derived DEM Using Inundation Area Analysis and RTK-dGPS Data.
- Suwandana, E., Kawamura, K., Sakuno, Y., K. E., & Raharjo, B. (2012). Evaluation of ASTER GDEM2 in comparison with GDEM1, SRTM DEM and topographic-map-derived DEM using inundation area analysis and RTK-dGPS data. *Remote Sensing*, 4, 2419 – 2431.
- Suwandana, E., Kawamura, K., Sakuno, Y., Kustiyanto, E., & Raharjo, B. (2012). *Evaluation of ASTER GDEM2 in Comparison with GDEM1, SRTM DEM and Topographic-Map-Derived DEM Using Inundation Area Analysis and RTK-dGPS Data*. *Remote Sensing*(15 August 2012), 1-13.
- Suwandana, E., Kawamura, K., Sakuno, Y., Kustiyanto, E., & Raharjo, B. (2012, June 20). Evaluation of ASTER GDEM2 in Comparison with GDEM1, SRTM DEM and Topographic-Map-Derived DEM Using Inundation Area Analysis and RTK-dGPS Data. *Remote Sensing:www.mdpi.com/journal/remotesensing*, 4(15August2012), 2419-2431.
- Taylor, A. (June 4, 2010). Landslide lake in Pakistan. Boston.com: The Big Picture.
- Taylor, C. (2015, April 12). *about education*. Retrieved August 23, 2015, from © 2015 About.com — All rights reserved: <http://statistics.about.com/od/Descriptive-Statistics/a/What-Are-The-First-And-Third-Quartiles.htm>
- USGS. (2011). *Earth observing 1 (EO-1)*. Retrieved January 31, 2015, from <http://eo1.usgs.gov/sensors/ali>
- USGS. (2013). Retrieved 28 January, from http://landsat.usgs.gov/about_ldcm.php
- Wale, A. (2010, June 11). Lake Tana Flood Zone Mapping. (B. D. Bahir Dar University, Ed.) *Regional Training Course in Integrated Flood Management (IFM)*, pp. 1-50.
- Wallace, R. (2010, 05 16). *Lab Write Resources: Graphing with Excel*. Retrieved 06 17, 15, from A NC STATE UNIVERSITY Website : Sponsored and funded by National Science Foundation: <https://www.ncsu.edu/labwrite/res/gt/gt-reg-home.html>
- Wang, W., Yang, X., & Yao, T. (2011). Evaluation of ASTER GDEM and SRTM and their suitability in hydraulic modeling of a glacial lake outburst flood in southeast Tibet, *Hydrological Processes*. 213 – 225.
- Wang, X., Chen, Y., Song, L., Chen, X., Xie, H., & Liu, L. (2013). Analysis of lengths, waterareas and volumes of the Three Gorges Reservoir at different water levels using Landsat images and SRTM DEM data. *Quaternary International*, 304, 115 – 125.

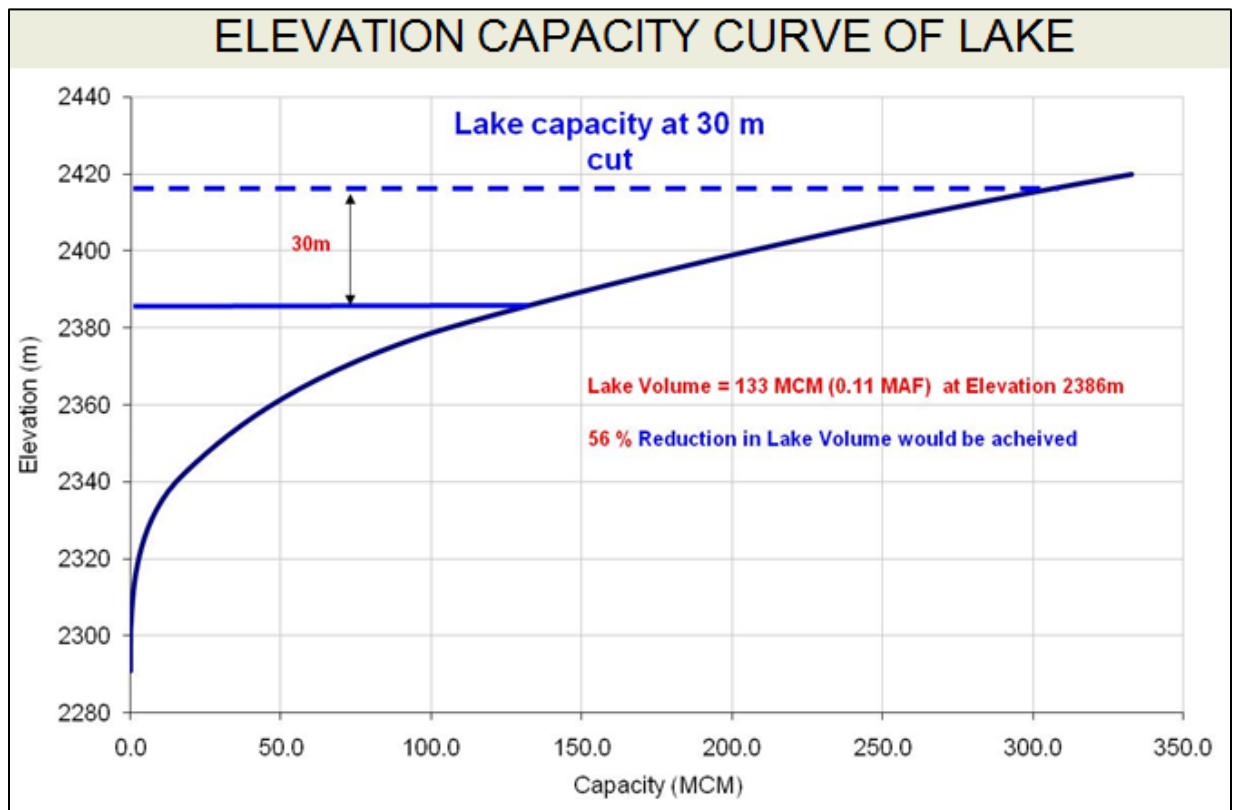
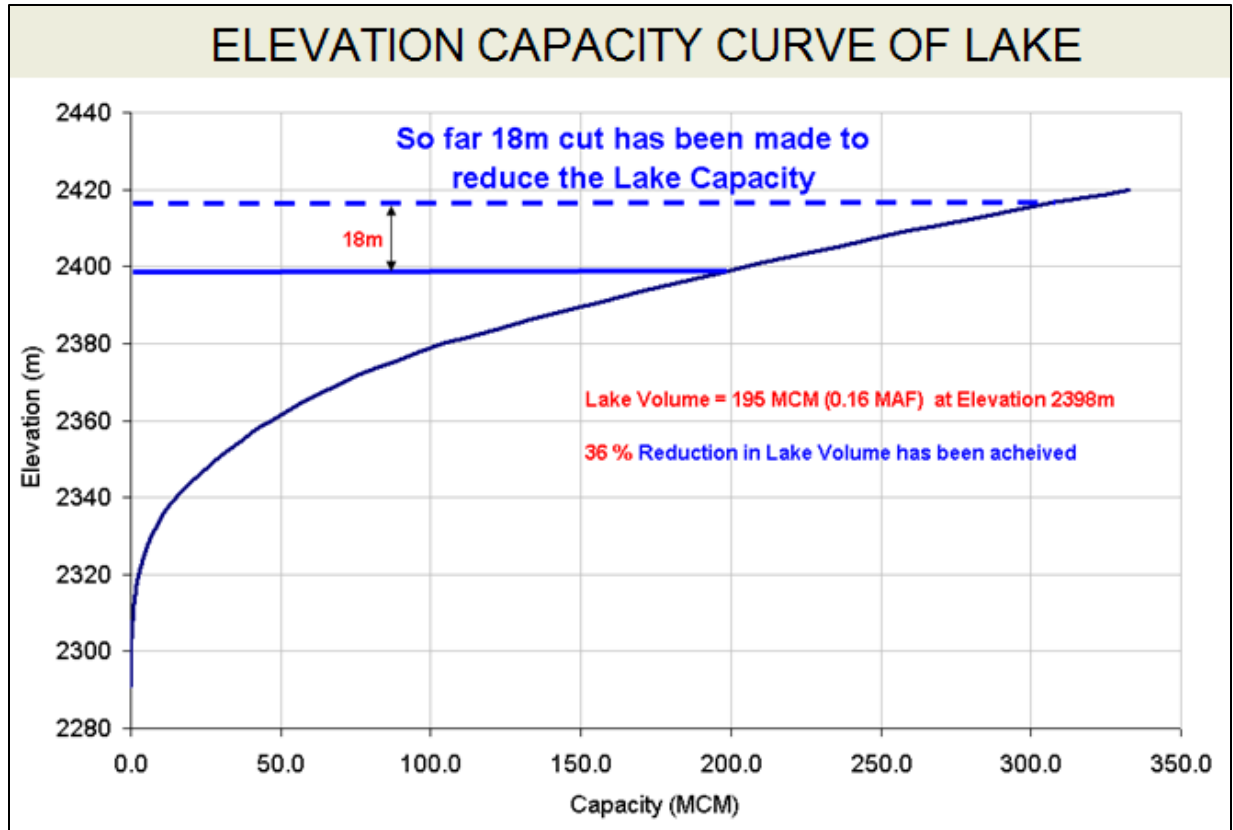
- Wang, Y., Liao, M., Sun, G., & Gong, J. (2005). Analysis of the water volume, length, total area and inundated area of the Three Gorges Reservoir, China using the SRTM DEM data. *International Journal of Remote Sensing*, 26.
- Wang, Z., & Lu, J. (2002). Satellite monitoring of the Yigong landslide in Tibet, China. *Proceedings SPIE*, 4814, 34.
- Wilcox, C., & M., L. H. (2005). A Simple, Rapid Method for Mapping Bathymetry of Small Wetland Basins. *Journal of Hydrology*, 301: 29-36.
- Xiao, X., Boles, S., Liu, J., Zhuang, D., Froking, S., Li, C., et al. (2005). Mapping Paddy Rice Agriculture in Southern China Using Multi-Temporal MODIS Images.”. *Remote Sensing of Environment*, 95: 480–492.
- Xu, H. (2006). Modification of Normalized Difference Water Index (NDWI) to Enhance Open Water Features in Remotely Sensed Imagery. 27: 3025–3033. *International Journal of Remote Sensing*, 27: 3025–3033.
- Zhang, B., Wu, Y., Zhu, L., Wang, J., Li, & Chen, D. (2011). Estimation and Trend Detection of Water Storage at Nam Co Lake, Central Tibetan Plateau. *Journal of Hydrology*, 405: 161–170.

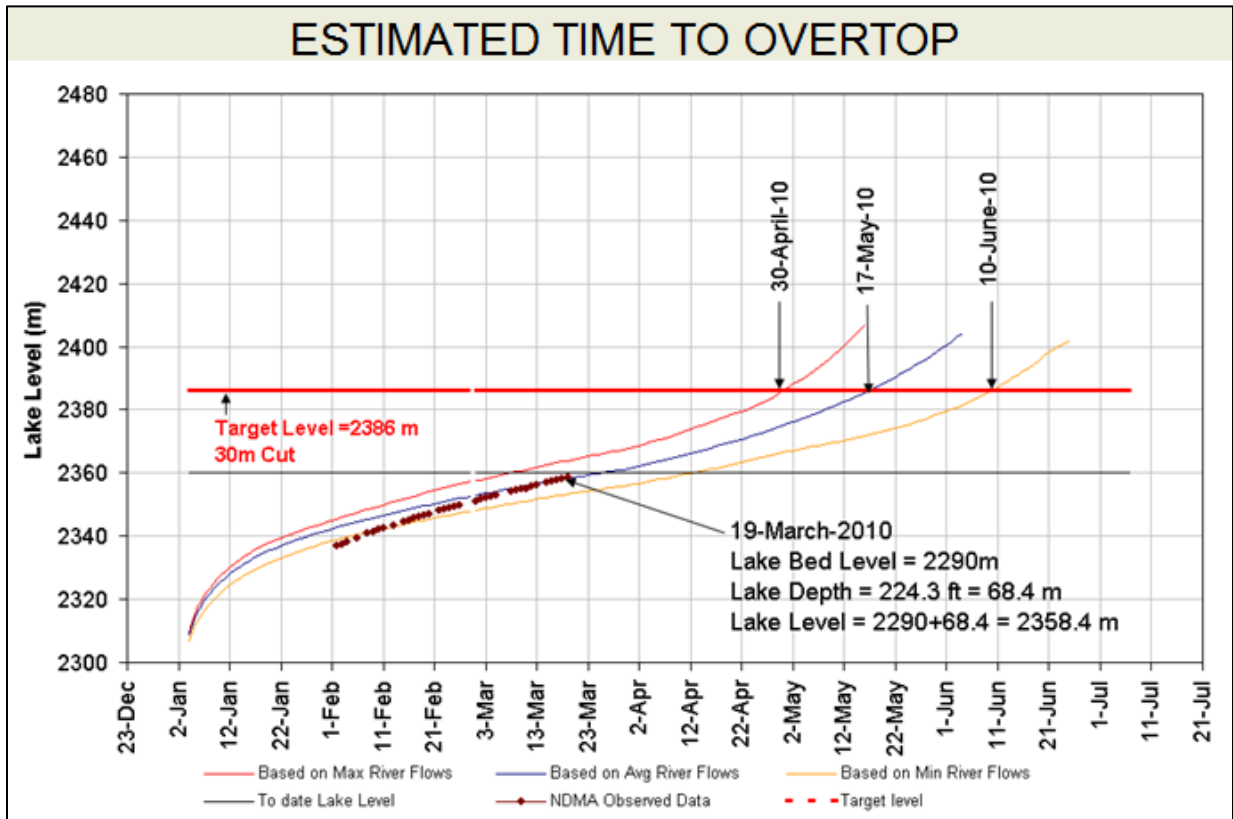
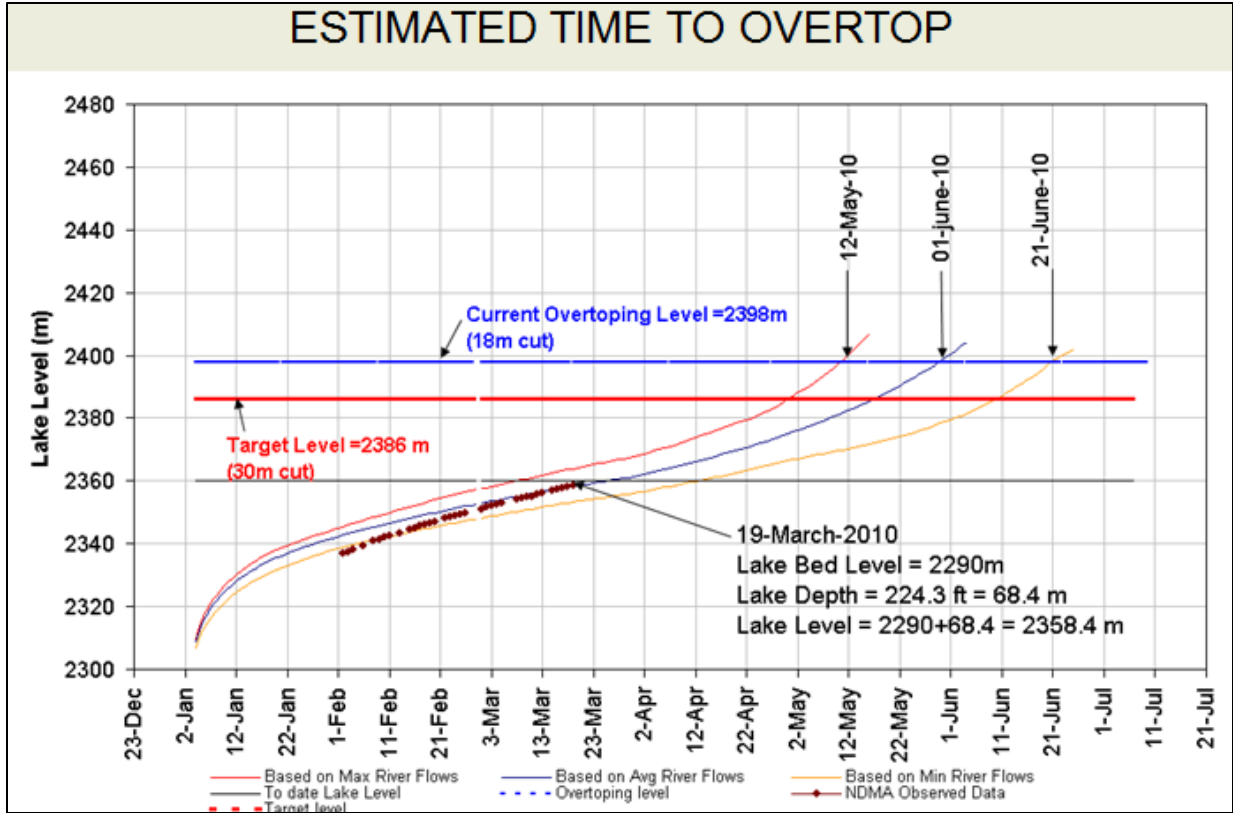
APPENDICES

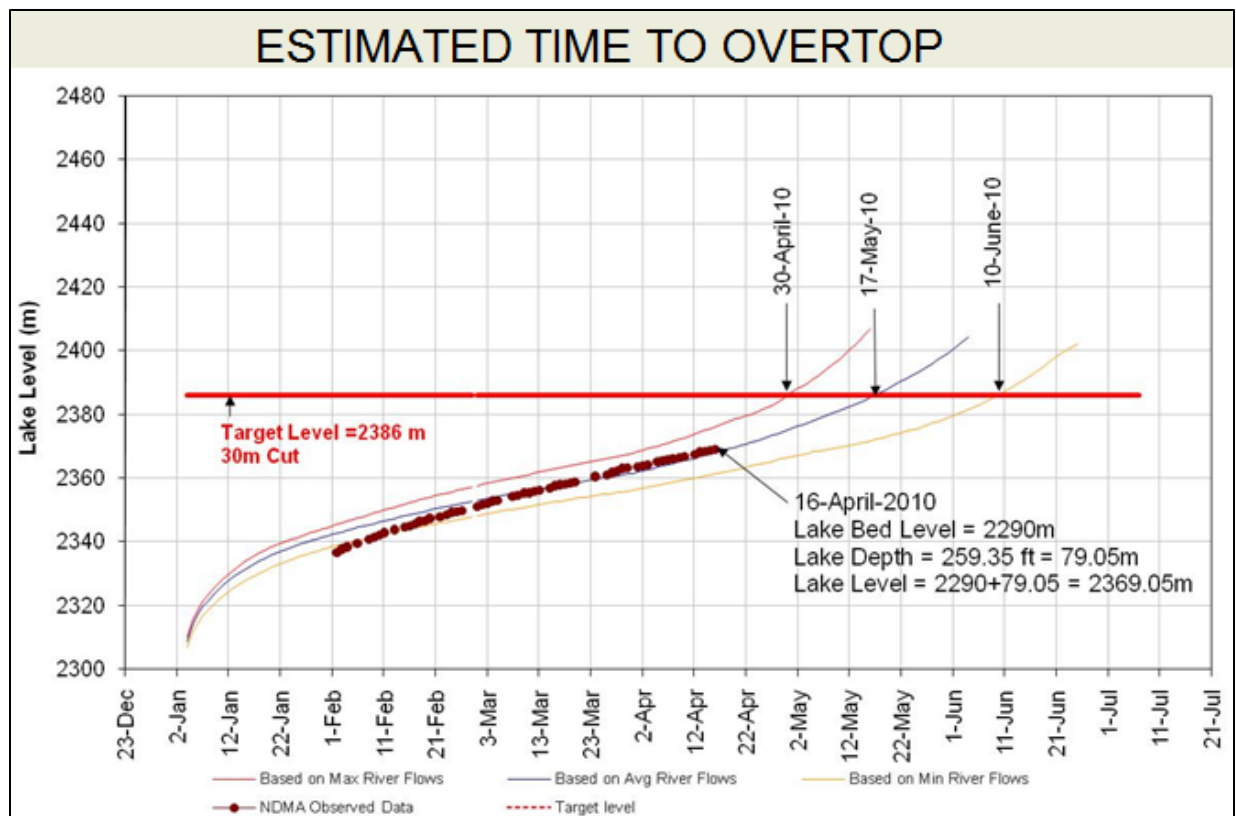
Appendix-A: Elevation Capacity Curves of Attabad Lake

- ◆ Here Capacity dictates the Volumes of Attabad Lake which are obtained from the field observation data conducted by NESPAK.
- ◆ In the succeeding figures NDMA depths are added to the river bed elevation i.e. 22290 m in order to obtain the volume at particular pool (Lake) elevation.
- ◆ How much %age reduction in Attabad Lake volumes were achieved at specific date, time and particular pool elevation clearly depicted as from figures below:









Appendix-B: Descriptions About Attabad Lake Level Reduction

On 20th January, Government of Pakistan and FWO assigned the task which was completed in 18th May 2010. They handled the situation and constructed a 24m spillway immediately to curtail further storage of water into the lake, thus lessening the overall damage by 50%.

Planning commission awarded the *contract* of lowering the water level by 30 m to FWO, on October 2010. By May 2011, the water level was reduced by 4 m.

Cut Depth	18 m	30 m
Overtopping Level	2398 m	2386 m
Dam Height	108 m	96 m
Lake Volume	195 MCM	133 MCM

During the low flow season from October 2011 to May 2012, FWO was successful in lowering the lake water by 16 m much faster than the estimated time going to Planning Division.

Appendix C: Local GIS Data For Attabad Lake

Attabad Hunza landslide relief support information is obtained from <http://www.local.com.pk/hunza/>. All rights reserved by © ALI REHMAT MUSOAF.

These GIS data represented in figures by different symbols. For example figure below showing is represented by the red circles with dot at center,.

Below GIS data are displayed on the Google earth, showing the names of villages, roads, and bridges too that are inundated as a result of overtopping of the lake till early July 2010.

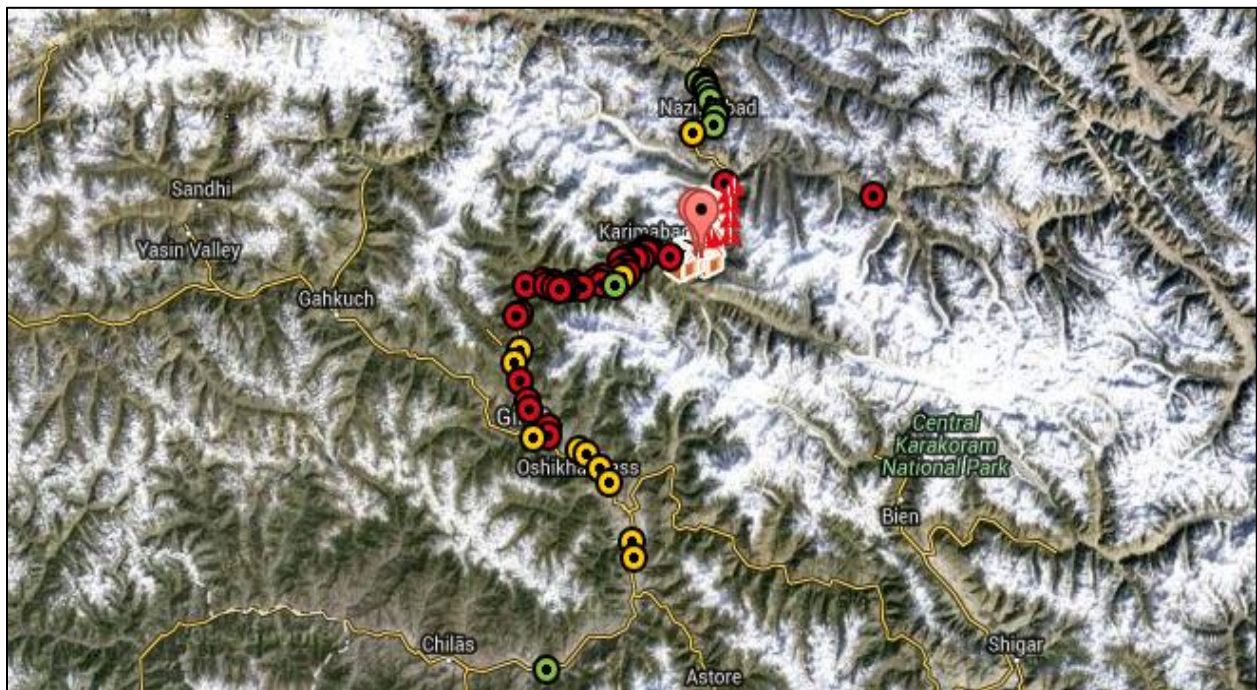
LOSS OF PROPERTY



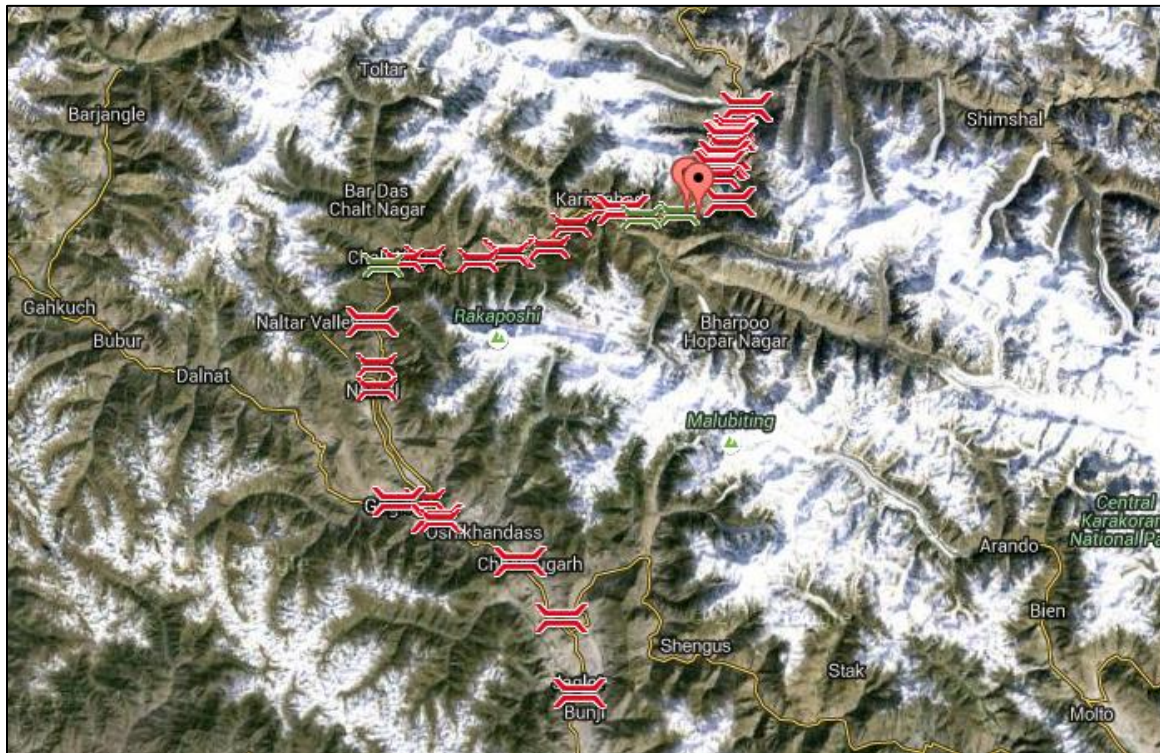
IDP RELIEF CAMP



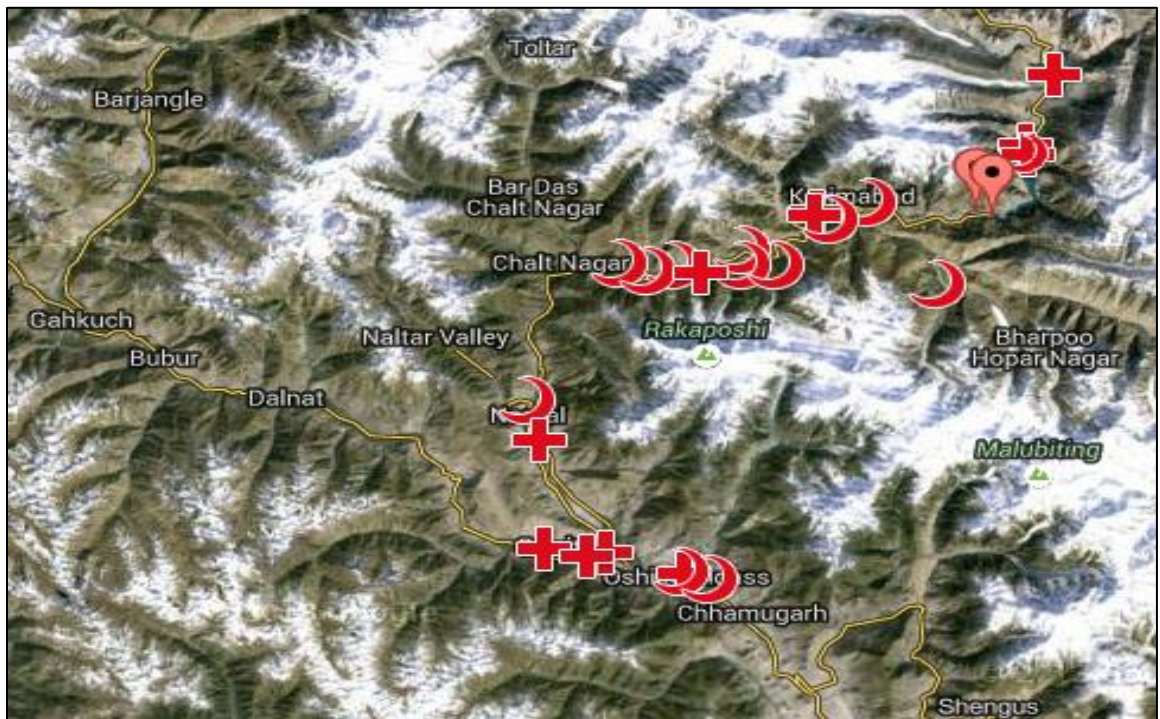
FLOODED VILLAGES



INUNDATED BRIDGES



MEDICAL CAMPS



Appendix-D: Hunza Landslide Relief

This information provided by ©UNOSAT and UNitar.

HUNZA RIVER POST FLOOD FLOW



HUNZA RIVER POST FLOOD FLOW



Appendix E: Detail Description of ASTGDEM2_0N36E074

Table below contained information that is retrieved from <http://earthexplorer.usgs.gov/>.

Entity ID	ASTGDEM2_0N36E074
Agency	NASA/METI
Acquisition Date	2011/10/17
Vendor	NASA/METI
Map Projection	GEOGRAPHIC
Sensor	ASTER
Resolution	1 ARC-SECOND
File Size	25051164
Sensor Type	GDEM
Ellipsoid	WGS84
Units	DEGREES
Version	2.0
Product Format	GEOTIFF
Check Sum Value	2237607861
License ID	17
License Uplift Update	
Date Entered	16-NOV-11
Date Updated	01-FEB-12
Center Latitude	36°30'00.00"N
Center Longitude	74°30'00.00"E
NW Corner Lat.	37°00'00.50"N
NW Corner Long	73°59'59.50"E
NE Corner Lat.	37°00'00.50"N
NE Corner Long	75°00'00.50"E
SE Corner Lat.	35°59'59.50"N
SE Corner Long	75°00'00.50"E
SW Corner Lat.	35°59'59.50"N
SW Corner Long	73°59'59.50"E
Center Latitude dec.	36.5
Center Longitude dec	74.5
NW Corner Lat dec	37.0001389
NW Corner Long dec	73.9998611
NE Corner Lat dec	37.0001389
NE Corner Long dec	75.0001389
SE Corner Lat dec	35.9998611
SE Corner Long dec	75.0001389
SW Corner Lat dec	35.9998611
SW Corner Long dec	73.9998611